TECHNISCHE UNIVERSITÄT MÜNCHEN

Lehrstuhl für Phytopathologie

Molecular analysis of the function of BAX INHIBITOR-1 (BI-1), BI-1-interacting, and BI-1-like proteins in plant response to biotic and abiotic stress

Corina Weis

Vollständiger Abdruck der von der Fakultät Wissenschaftszentrum Weihenstephan für Ernährung, Landnutzung und Umwelt der Technischen Universität München zur Erlangung des akademischen Grades eines

Doktors der Naturwissenschaften

genehmigten Dissertation.

Vorsitzender:　　　　　Univ.-Prof. Dr. B. Küster

Prüfer der Dissertation:　1. Univ.-Prof. Dr. R. Hückelhoven
　　　　　　　　　　　　　2. Univ.-Prof. Dr. J. Durner

Die Dissertation wurde am 14.03.2012 bei der Technischen Universität München eingereicht und durch die Fakultät Wissenschaftszentrum Weihenstephan für Ernährung, Landnutzung und Umwelt am 28.04.2012 angenommen.

AAL	*Alternaria alternata* f.sp. lycopersici
AGT	appressorial germ tube
AHA	PLASMA MEMBRANE PROTON ATPASE
APP	appressorium
At	*Arabidopsis thaliana*
Avr	avirulence
BAK1	BRASSINOSTEROID INSENSITIVE 1-ASSOCIATED KINASE 1
Bgh	*Blumeria graminis* f.sp*. hordei*
BI-1	BAX INHIBITOR-1
BR	brassinosteroid
CaM	CALMODULIN
Col-0	Columbia 0
CWA	cell wall apposition
CYP83A1	CYTOCHROME P450 83A1
dab	days after bombardment
dai	days after inoculation
EH	elongated hyphae
ER	endoplasmic reticulum
ESH	elongated secondary hyphae
ETI	effector triggered immunity
ETS	effector-triggered susceptibility
f.sp./ff.spp	*forma specialis/formae speciales*
GFP	green fluorescing protein
GPI	GLYCOSYLPHOSPHATIDYL INOSITOL TRANSAMIDASE SUBUNIT PIG-U
H_2O_2	hydrogen peroxide
hab	hours after bombardment
hai	hours after inoculation
HAP6	HAPLESS 6
HAU	haustorium
HR	hypersensitive reaction
Hv	*Hordeum vulgare*
LFG	LIFEGUARD
LRR-RLK	leucin-rich repeat receptor-like kinase
MLA	MILDEW LOCUS A
MLO	MILDEW LOCUS O

MYHC	MYOSIN HEAVY CHAIN-RELATED
NPR	NADPH-dependent cytochrome P450 reductase
PAMP	pathogen-associated molecular pattern
PCD	programmed cell death
PE	penetration efficiency
PGT	primary germ tube
PHB	PROHIBITIN
PM	plasma membrane
PP	penetration peg
PR	PATHOGENESIS-RELATED
PRR	pattern-recognition receptors
PTI	pathogen-triggered immunity
pv.	pathovar
R	RESISTANCE
REF2	REDUCED EPIDERMAL FLUORESCENCE 2
RFP	red fluorescing protein
RNAi	RNA interference
ROS	reactive oxygen species
SA	salicylic acid
spp.	species pluralis
TIGS	transient-induced gene silencing
TRN1	TRANSPORTIN 1
VHA-A	VACUOLAR H^+-ATPASES SYNTHASE SUBUNIT A

1 Introduction

Plant innate immunity is a complex and efficient defense system against the majority of pathogens. However, several pathogens can overcome plant immunity due to their specialized adaptation to certain host plants. In a changing environment and due to ongoing evolutionary processes, plants as well as pathogens are continuously evolving sophisticated strategies to succeed (JONES and DANGL 2006). In the last decade, fundamental research provided deeper insights into plant - pathogen interactions on the molecular level, for instance revealing that many pathogenic bacteria deliver effector molecules into plant host cells to suppress defense mechanisms by manipulating host cell function and structure (GRANT et al. 2006). More and more evidences appear showing similar infection strategies for fungi. Several effectors of *Cladosporium fulvum*, *Fusarium oxysporum* f.sp. *lycopersici* and *Magnaporthe oryzae* are already identified (DE WIT et al. 2009). It is assumed that fungi induce susceptibility by the interference of distinct effectors with host proteins, which then function as so-called susceptibility or compatibility factors. However, little is known about the molecular/cellular mechanisms behind this (PANSTRUGA 2003). Fundamental research in phytopathology contributes to the elucidation of resistance as well as susceptibility mechanisms, which are the prerequisite for a forward-looking biotechnology-based improvement of crop disease resistance (GUST et al. 2010).

1.1 The plant immune system

Two general defense branches constitute plant immunity. In addition to physical and chemical barriers, the first line of defense bases on the recognition of conserved non-self pathogen-associated molecular patterns (PAMPs) or modified-self danger/damage-associated molecular patterns (DAMPs) by surface-localized pattern-recognition receptors (PRRs) resulting in defense responses referred to as PAMP-triggered immunity (PTI, CHISHOLM et al. 2006, BOLLER and FELIX 2009). However, specialized pathogens release effector proteins into host cells to overcome defense mechanisms and to establish effector-triggered susceptibility (ETS). In turn, plants evolved RESISTANCE (R) proteins to specifically recognize given effector proteins, which are then also called avirulence (Avr) factors. Hence, the second layer of defense, also called effector-triggered immunity (ETI), is taking effect. In contrast

to PTI, ETI is an intensified, prolonged immune response typically ending up in the hypersensitive cell death response (HR) to restrict the pathogen's growth (DODDS and RATHJEN 2010). Due to continuous co-evolutionary processes, plants and pathogens evolve new R proteins and effectors, respectively, in a currently ongoing move-countermove situation, as described in the so-called 'zigzag model' (JONES and DANGL 2006).

1.1.1   PAMP-triggered immunity

PTI bases on the perception of PAMPs, described as conserved molecular features, which are characteristic and vital for whole classes of pathogens. Therefore, PTI is effective against a broad spectrum of potential invaders and is also referred to as basal resistance (BOLLER and FELIX 2009). In *Arabidopsis*, the best-studied examples for bacteria-mediated PTI depend on the specific binding of flg22 (derived from flagellin) and elf18 (derived from elongation factor Tu (EF-Tu)) to FLAGELLIN-SENSING 2 (FLS2) and EF-TU RECEPTOR (EFR), respectively (CHINCHILLA et al. 2006, ZIPFEL et al. 2006). FLS and EFR, both leucine-rich repeat receptor-like protein kinases (LRR-RLKs), form heterocomplexes with several members of the SOMATIC-EMBRYOGENESIS RECEPTOR-LIKE KINASE (SERK) family, such as BRASSINOSTEROID INSENSITIVE 1-ASSOCIATED KINASE 1 (BAK1) and BAK1-LIKE 1 (BKK1) in response to elicitation (CHINCHILLA et al. 2007, HEESE et al. 2007, ROUX et al. 2011). BAK1 and BKK1 are both required for full flg22- and elf18-mediated signaling (CHINCHILLA et al. 2007, ROUX et al. 2011).

In 2006, YAMAGUCHI and co-workers identified the first DAMP/PRR couple, *Arabidopsis* PEPTIDE 1 (AtPEP1)/AtPEP1 RECEPTOR 1 (AtPEPR1). AtPEP1 derives from the precursor protein PROPEP1 that is upregulated upon diverse stimuli, and binds at least to one additional LRR-RLK receptor, namely the AtPEP1 homologue AtPEP2 (YAMAGUCHI et al. 2010, KROL et al. 2010). As described for flg22- and elf18-triggered immune responses, BAK1 and BKK1 are also crucial regulators of AtPEP1-dependend signaling, indicating BAK1 and BKK1 as common coreceptors in PTI (HEESE et al. 2007, ROUX et al. 2011).

Chitin, a polymer of β-1,4-linked N-acetyl-glucosamine, constitutes the major component of fungal cell walls and is a potent PAMP. Perception of chitin occurs through binding to lysin motif (LysM)-containing cell surface receptors, which are conserved in monocots and dicots (KOMBRINK et al. 2011). In rice, fungal chitin

oligosaccharides bind to CHITIN ELICITOR-BINDING PROTEIN (CEBiP), lacking an intracellular domain, which in turn constitutes a complex with CHITIN ELICITOR RECEPTOR KINASE 1 (OsCERK1), essential for chitin-induced signaling (KAKU et al. 2006, SHIMIZU et al. 2010). Since HvCEBiP, the barley receptor homolog, is involved in mediating basal resistance to *Magnaporthe oryzae*, a similar role in PTI is expected in *Triticeae* (TANAKA et al. 2010). In *Arabidopsis*, chitin binds to CERK1, a plasma membrane protein with three LysM domains and an intracellular serine/threonine (Ser/Thr) kinase domain (MIYA et al. 2007). CERK1 is phosphorylated upon chitin-binding, initiating chitin-induced immune responses (PETUTSCHNIG et al. 2010).

In general, PTI is associated with mitogen-activated protein kinase (MAPK) signaling, resulting in early defense gene transcription controlled by WRKY and other transcription factors, activation of calcium-dependent protein kinases, reactive oxygen species (ROS) production, synthesis and release of antimicrobial compounds, and callose deposition at sites of infection (NÜRNBERGER et al. 2004, AUSUBEL et al. 2005, HE et al. 2007, BOUDSOCQ et al. 2010).

1.1.2   Effector-triggered susceptibility and immunity

With the purpose to overcome immunity, pathogens deliver effector proteins into their host cells to establish susceptibility (JONES and DANGL 2006, BLOCK et al. 2008). Therefore, effectors are significantly involved in mediating virulence. The best-characterized effectors derive from phytopathogenic gram-negative bacteria, such as *Pseudomonas syringae* or *Xanthomonas* spp., which use the type III secretion system to inject a strain-specific set of 15-30 effectors directly into the host cytoplasm (GRANT et al. 2006, JONES and DANGL 2006). Effector proteins interfere with diverse events of defense signaling and are capable of reprogramming plant physiology, partially by operating redundantly. For instance, *P. syringae* pv. *tomato* (*Pto*) strain DC3000 effectors AvrPto and AvrPtoB inhibit the FLS-BAK1 complex to disrupt flg22-induced immune responses (SHAN et al. 2008). Besides, AvrPtoB, additionally carrying an E3 ubiquitin ligase domain, targets, ubiquitinates and promotes the degradation of FENTHION SENSITIVITY (FEN), a tomato kinase and part of an ancient ETI pathway (ROSEBROCK et al. 2007).

Another effector of *P. syringae*, HopAI1, interferes with PAMP-induced MAPK-dependent signaling by irreversibly dephosphorylating phosphothreonine residues of

MAPKs (ZHANG et al. 2007). In contrast, transcriptional activator-like (TAL) effectors of *Xanthomonas* spp. directly induce the expression of host genes by binding to specific promoter sequences dependent on the tandem repeat domain of the effector (BOCH et al. 2009, BOGDANOVE et al. 2010). In such a way, *X. campestris* pv. *vesicatoria* race 1 effector AvrBs3 targets the *upa20* promoter in susceptible host plants, likely for reprogramming host cell size development towards hypertrophy, resulting in ETS (KAY et al. 2007).

Upon effector recognition in the presence of corresponding R proteins, mostly encoding cytoplasmic nucleotide-binding (NB) and LRR domain-containing receptors, the plant's second defense layer (ETI) is initiated, resulting in HR-mediated host resistance. Since PTI and ETI share many molecular events, JONES and DANGL (2006) suggested the quantitative output of ETI to be crucial for the induction of HR. The interaction of bacterial effectors with NB-LRR proteins is supposed to occur indirectly rather than directly (GRANT et al. 2006). In the current 'bait and switch' model, COLLIER and MOFFETT (2009) postulate an activation of autoinhibited NB-LRR receptors by cofactors, here also referred to as baits, due to their interaction with respective effectors. In such a way, tomato NB-LRR protein PFR (PSEUDOMONAS RESISTANCE AND FENTHION SENSITIVITY) is activated through the physical interaction of AvrPto or AvrPtoB with Pto, a Ser/Thr kinase, which confers defense signaling (MUCYN et al. 2006). Besides, effector-mediated modifications of cofactors, such as the cleavage of AvrPphB SUSCEPTIBLE 1 (PBS1) by AvrPphB, can also induce NB-LRR activation, e.g. the activation of RESISTANCE AGAINST PSEUDOMONAS SYRINGAE 5 (RPS5, SHAO et al. 2003, ADE et al. 2007). However, a direct physical interaction is assumed for *Ralstonia solanacearum* type III effector PopP2 with the *Arabidopsis* R protein RESISTANT TO RALSTONIA SOLANACEARUM 1-R (RRS1-R), composed of a Toll-interleukin 1 receptor (TIR) homology region-NB-LRR domain and a WRKY motif, in the nucleus (DESLANDES et al. 2003). BERNOUX and co-workers (2008) showed a PopP2-dependent relocalization of *Arabidopsis* cysteine protease RESPONSIVE TO DEHYDRATION 19 (RD19) to the nucleus, where both proteins interact, which is supposed to be crucial for RRS1-R-mediated immune signaling.

Over recent years, the knowledge about oomycete and fungal effectors expanded enormously. In contrast to bacteria, fungi and oomycetes likely use the endomembrane system to deliver their effectors into the apoplast or into the

cytoplasm of host cells. However, until now, translocation mechanisms are not understood in detail (STERGIOPOULOS and WIT 2009, DE JONGE et al. 2011). Apoplastic effectors, such as cell-wall-degrading enzymes, necrosis and ethylene-inducing protein-like proteins and small cysteine-rich secreted proteins, are involved in early steps of pathogenesis (DE JONGE et al. 2011). Examples for cysteine-rich proteins are secreted effectors of *Cladosporium fulvum* such as Avr2, which suppresses basal defense by inhibiting extracellular host proteases, or Avr4 and EXTRACELLULAR PROTEIN 6 (Ecp6), preventing chitin-triggered signaling (VAN ESSE et al. 2008, SHABAB et al. 2008, SONG et al. 2009, VAN DEN BURG et al. 2006, DE JONGE et al. 2010). Moreover, at least Avr4 and Ecp2, another *C. fulvum* effector, are assumed to be core effectors, since functional orthologs are identified in other pathogenic Dothideomycetes, such as *Mycosphaerella fijiensis*, as well (STERGIOPOULOS et al. 2010). However, in resistant tomato plants, corresponding extracellular R proteins perceive distinct effectors, as shown for C. FULVUM-2 (Cf-2), a receptor-like protein (RLP), which recognizes the Avr2-REQUIRED FOR *CLADOSPORIUM* RESISTANCE 3 (RCR3) complex, resulting in HR (ROONEY et al. 2005, THOMMA et al. 2005).

Oomycete effectors characteristically contain an N-terminal RxLR translocation motif, of which effectors of fungal pathogens contain functional variants (WHISSON et al. 2007, KALE et al. 2010). RxLR motifs enable effectors to bind to outer plasma membrane surface phosphatidylinositol-3-phosphate (PI3P), which is supposed to be crucial for their subsequent transfer into the host cell cytoplasm via vesicle-mediated endocytosis (KALE et al. 2010). Effector candidates of biotrophic powdery mildew and rust fungi, predominantly expressed in haustoria, share a Y/F/WxC motif that possibly mediates their transfer across the extrahaustorial membrane (EHM, GODFREY et al. 2010). Based on biochemical, genetic, and bioinformatic approaches, hundreds of putative effector candidates were identified in diverse oomycete and fungal species, like *Phytophthora infestans*, *M. oryzae* or *Blumeria graminis* f.sp. *hordei* (*Bgh*, DEAN et al. 2005, KAMOUN 2006, JIANG et al. 2008, SPANU et al. 2010). Currently, little is known about their functions. However, recent findings give rise to the assumption that plant transport and metabolism pathways are potential fungal effector targets. CHEN et al. (2010) observed enhanced expression of plant 'SWEET' sugar efflux transporters during infections with several pathogens, including powdery mildew fungi, probably to enhance their nutritional gain. Moreover, *Ustilago maydis CMU1*

encodes a chorismate mutase, which functions as virulence factor by changing the metabolic status, amongst others towards a reduced salicylic acid (SA) level, through metabolic priming (DJAMEI et al. 2011).

In contrast, interactions of diverse cytoplasmic effectors with corresponding R proteins have been identified in a couple of incompatible plant - fungus interactions. *M. oryzae* effector Avr-Pita, for instance, directly interacts with the LRR domain of the corresponding NB-LRR receptor Pi-ta in rice (JIA et al. 2000). And diverse haustorially secreted effectors of the flax rust fungus (*Melampsora lini)* elicit defense responses initiated by binding TIR-NB-LRR proteins (DODDS et al. 2004, CATANZARITI et al. 2006, DODDS et al. 2006, CATANZARITI et al. 2010). Two barley powdery mildew effector proteins Avr_{k1} and Avr_{a10}, both lacking an N-terminal signal sequence, are recognized by MLK1 and MLA10 proteins, respectively (RIDOUT et al. 2006, chapter 1.2.3). Interestingly, MLA10 interferes with WRKY transcription factors in an Avr_{a10}-dependent manner, resulting in defense signaling (SHEN et al. 2007).

1.1.3 The hypersensitive response (HR)

In 1915, STAKMAN adopted the term 'hypersensitiveness' to describe his observation of a rapidly occurring cell death reaction upon *Puccinia graminis* infection, which correlated with the dimension of disease resistance in wheat. To date, HR is a well-established concept, defining a type of programmed cell death (PCD) that is restricted to one or a few cells at the site of pathogen attack as a typical consequence of R protein-mediated defense reactions (KOGA et al. 1990, HEATH 2000a,b, MUR et al. 2008). HR is sufficient in preventing the development of biotrophic pathogens, such as powdery mildew fungi, whereby certain features are overlapping with necrotrophic pathogen-induced cell death reactions (HÜCKELHOVEN et al. 1999, GORVIN and LEVINE 2000). HR also shares some characteristics with mammalian cell death programs, like cytoplasmic shrinkage, cytochrome *c* release, or loss in mitochondrial membrane potential. However, there is still a large gap of knowledge concerning this distinct form of cell death (MUR et al. 2008).

The HR resistance mechanism is suggested to involve an oxidative burst, i.e. the production of ROS, primarily hydrogen peroxide (H_2O_2) and superoxide, SA, and cytosolic Ca^{2+} influx (LAMB and DIXON 1997). The following reactions include disruption of membranes, decompartmentalization, transient activation of protein kinases, production of phytoalexins and transcriptional reprogramming (HAHLBROCK

et al. 2003). In 2005, L IU et al. demonstrated a role of autophagy in restricting HR to the site of attempted penetration, maybe by eliminating death-eliciting signals emerging from the HR lesion.

1.2 Powdery mildew fungi

Powdery mildew fungi are ascomycetes infecting all aerial parts of almost 10,000 species of angiosperms (B RAUN 2002). As obligate biotrophic ecto-parasites powdery mildew fungi grow epiphytically on their host. Only their feeding organs, called haustoria, are accommodated in host epidermal cells for nutrient uptake (H ALL and W ILLIAMS 2000). Taxonomically, powdery mildew fungi belong to the order of *Erysiphales* with only one family, named *Erysiphaceae*, which subdivides into five major tribes: *Erysipheae*, *Golovinomycetinae*, *Cystotheceae*, *Phyllactinieae*, and *Blumeriea* (B RAUN 2002).

Powdery mildew fungi infecting *Poaceae* belong to *Blumeria*, the single genus within the tribe *Blumerieae*, with *B. graminis* (DC.) Speer as the only species. The different *formae speciales* (*ff.spp.*) are specialized to only one cereal species, respectively, such as *Blumeria graminis* f.sp. *hordei* (*Bgh*) to barley (*Hordeum vulgare* L., I NUMA et al. 2007). Mainly for animal feed production and malting, barley is cultivated worldwide on about 64.1 million hectares with a yield average of 2.34 t/ha. The potential yield loss due to fungal pathogens, especially *Pyrenophora teres*, *Rhynchosporium secalis*, *Puccinia hordei*, *Bgh*, and *Cochliobolus sativus*, is estimated to 15% of the achievable yield. The actual losses to fungal pathogens range between 5% in northwest Europe and 15% in southeast Asia depending on the crop protection practices (O ERKE and D EHNE 2004). At least the three powdery mildew species *Golovinomyces* (syn. *Erysiphe*) *cichoracearum*, *G. orontii*, and *Erysiphe cruciferarum* can infect *Arabidopsis thaliana* (V OGEL and S OMERVILLE 2002, M ICALI et al. 2008).

The interactions of the monocot barley and the dicot *Arabidopsis thaliana* with powdery mildew fungi constitute model systems for understanding host defense mechanisms and infection strategies of biotrophic pathogens. Recently, the genome of *Bgh* has been sequenced by S PANU et al. (2010, http://blugen.org). As disadvantages for research purposes, powdery mildew fungi need to be maintained on their living host and are not yet transformable (G LAWE 2008).

1.2.1   Infection cycle of powdery mildew fungi

Here, exemplarily the infection cycle of *B. graminis* (DC Speer) should depict the life cycle of powdery mildew fungi, which can be described as follows: A compatible interaction of *B. graminis* with a corresponding host starts with the landing of an ascospore or a conidium on the leaf surface. Shortly thereafter, the spore releases an exiguous portion of non-specific esterase-, cutinase-, and lipase-activity exhibiting extracellular material, fastening the spore to its host (CARVER et al. 1999, WRIGHT et al 2002a,b, FENG et al. 2009). As a further adhesion tool, within the next 30-90 min a primary germ tube (PGT) begins to generate close to the contact site, which is unique among powdery mildew fungi (KUNOH et al. 1979). Moreover, the PGT is assumed to be involved in water uptake and in perception of host surface features, both required for further differentiation (GREEN et al. 2002). Presumably, for attaching to the host, this PGT in turn shapes a cuticular peg to break through the cuticle whereas the cell wall remains unaffected (EDWARDS 2002). Within 8-10 hours after inoculation (hai) a second germ tube, also referred to as appressorial germ tube (AGT), develops and becomes septate. In about the next 2 hours, the apex of the AGT differentiates by swelling to a hooked appressorium (APP) followed by the generation of a penetration peg (PP, GREEN et al. 2002).
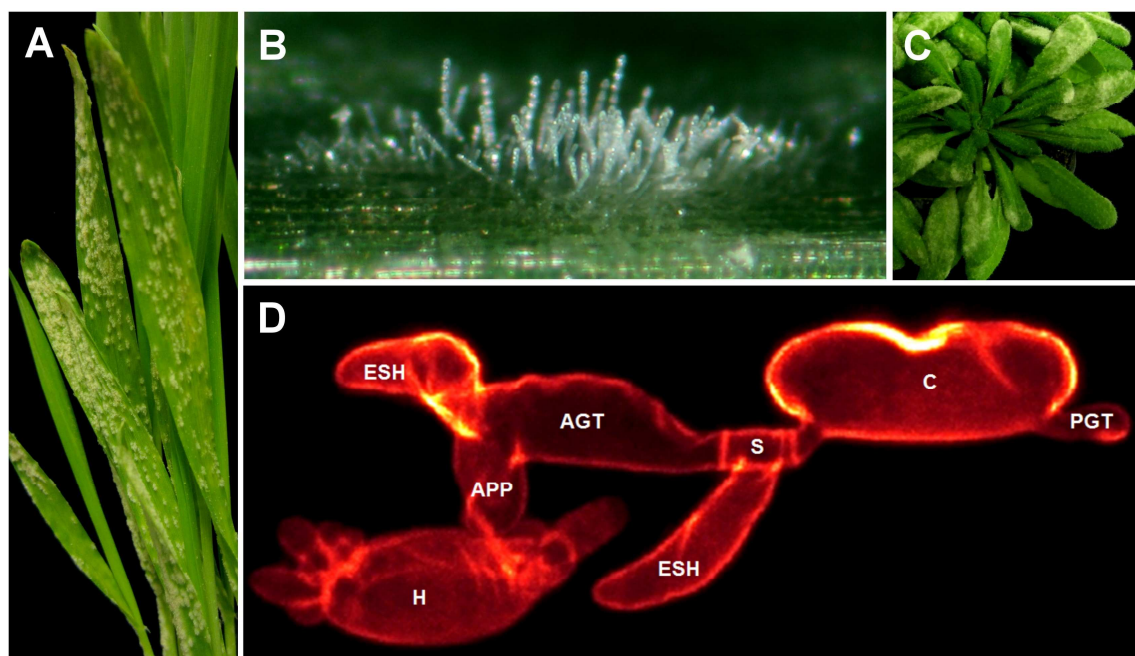
Fig. 1.1: Powdery mildew symptoms and development. Macroscopic symptoms **A** of *Bgh* on barley and **C** of *E. cruciferarum* on *Arabidopsis thaliana*. **B** Conidiophores of *Bgh* colonies on barley. **D** Microscopic picture of wheat germ agglutinin-tetramethylrhodamin (WGA-TMR)-stained *Bgh* structures 24 hai. Conidia (C), primary germ tube (PGT), septe (S), appressorial germ tube (AGT), appressorium (APP), haustorium (H), and elongated secondary hyphae (ESH) are labeled.

By means of turgor pressure and enzymatic activity, the fungus breaches the cuticle, the epidermal cell wall, as well as the underlying papilla, formed as a host response to fungal attack (PRYCE-JONES et al. 1999, ZEYEN et al. 2002). The PP enlarges within the epidermal cell to generate a digitate haustorium (15-18 hai). The fungus invaginates the host plasma membrane, resulting in a highly modified extrahaustorial membrane (EHM), which tethers to the neck of the haustorium. The interfacial matrix in between the haustorial cell wall and the EHM is called extra-haustorial matrix (EHMx, GREEN et al. 2002, PERFECT and GREEN 2008). The haustorium, the EHMx and the EHM constitute the haustorial complex (HC, GIL and GAY 1977). Successful accommodation of a haustorium results in the generation of epiphytic elongated secondary hyphae (ESH) at about 24 hai. Fig. 1.1D displays a successful *Bgh* penetration, approximately at this point of time. ESH develop secondary appressoria and haustoria (48 hai), ending up in the formation of aerial conidiophores, macroscopically visible as white velvety pustules 5-10 dai (fig 1.1A,B,C). Newly produced conidia are released to start another infection cycle. These asexual spores are responsible for epidemic spread (GREEN et al. 2002). To over-winter and to survive extreme environmental conditions, sexual spores develop after mating within Cleistothecia (GLAWE 2008).

However, even on susceptible host plants, not every germinated spore succeeds in penetration, since the interactions are determined on the single-cell level. Fungal virulence, its ability to suppress host defense, and the physiological status of the attacked cell are factors that determine penetration success (LYNGKJÆR and CARVER 2000, GJETTING et al. 2004).

1.2.2 Early events in plant - powdery mildew interactions

Plant defense responses against powdery mildew fungi occur in different sequential steps (HÜCKELHOVEN 2005). Successful penetration of the first epidermal cell seems to be most crucial for powdery mildew pathogenesis. Vice versa, early defense responses at the pre-penetration stage are essential regarding the resistance of the host plant (HÜCKELHOVEN and PANSTRUGA 2011).

1.2.2.1 Cell wall appositions and cytoskeleton reorganization
As an early pre-invasive defense response against powdery mildew fungi, host cells generate cell wall appositions (CWA), also known as papillae, within a few hours at

the site of attempted penetration. CWA, composed of cross-linked cell wall material like callose (β-1,3-glucan), other polysaccharides, phenolic compounds, H_2O_2, and antimicrobial proteins, are thought to constitute an effective physical and chemical barrier against fungal penetration (ZEYEN et al. 2002). Delayed CWA formation correlates with enhanced fungal infection, showing the importance of fast defense responses (ASSAAD et al. 2004). On the one hand, papilla material, such as antimicrobial compounds or H_2O_2, is delivered by secretory vesicles, which fuse to the plasma membrane to deposit the compounds onto the inner cell wall surface. On the other hand, cell wall-resident enzymes directly synthesize papilla compounds at the site of fungal attack (ZEYEN et al. 2002, HÜCKELHOVEN et al. 2007a,b). However, in compatible interactions, the fungus penetrates cell wall appositions. Only in non-penetrated papillae H_2O_2 accumulates, suggesting an importance of H_2O_2 enrichment in penetration resistance, maybe through the involvement of H_2O_2 in protein cross-linking and lignification (THORDAL-CHRISTENSEN et al. 1997, HÜCKELHOVEN et al. 1999).

Depositions of cell wall material as well as dynamic mobilization of the nucleus and the endoplasmic reticulum (ER) towards the site of attempted penetration accompany reorganization of the actin cytoskeleton. Interestingly, the barley ROP (RHO OF PLANTS, syn. to plant RAC) small G-protein RACB, a susceptibility (syn. compatibility) factor to *Bgh*, regulates cell polarization as well as actin reorganization in the pre-penetration stage (SCHULTHEISS et al. 2002, SCHULTHEISS et al. 2003, OPALSKI et al. 2005). Strong actin filament polarization within the host cell correlates with penetration resistance to *Bgh*, whereas only a weak actin polarization is detectable in successfully penetrated cells (OPALSKI et al. 2005). As shown for RACB, a ROP-INTERACTIVE CRIB MOTIF CONTAINING PROTEIN of 171 amino acids (RIC171) supports fungal ingress when overexpressed. The interaction of RIC171 with RACB directly at the site of attempted penetration gives rise to the assumption that local activity of ROPs supports *Bgh* haustoria accommodation in epidermal cells of barley (SCHULTHEISS et al. 2008). Recently, MICROTUBULE-ASSOCIATED ROP-GTPASE ACTIVATING PROTEIN 1 (MAGAP1) was identified as further RACB-interacting partner. HÖFLE and co-workers (2011) showed a role of MAGAP1 in penetration resistance and microtubule organization, indicating MAGAP1 and RACB as antagonistic components in cytoskeleton organization during plant - powdery mildew interactions.

1.2.2.2 Role of MILDEW LOCUS O (MLO) and PENETRATION (PEN) proteins at the pre-invasive stage

Plant specific plasma membrane-resident MILDEW LOCUS O (MLO) proteins, possessing seven transmembrane domains, confer susceptibility to powdery mildew fungi in barley, *Arabidopsis*, tomato, and pea (BÜSCHGES et al. 1997, CONSONNI et al. 2006, BAI et al. 2008, HUMPHRY et al. 2011). Powdery mildew fungi somehow use MLO proteins as entry portals to invade their host cells (SCHULZE-LEFERT 2004, LIPKA et al. 2008). However, an evidence of MLO as effector target is missing (PANSTRUGA 2005). The lack of the functional MLO protein leads to complete resistance of barley against all known barley powdery mildew isolates by arresting the fungus at the pre-penetration stage, assigning MLO as major susceptibility factor (JØRGENSEN 1992, BÜSCHGES et al. 1997, ECKARDT 2002). Thus, recessively inherited *mlo*-mediated resistance, which is associated with papillae formation and H_2O_2 production, has been established in breeding of spring-barley since more than 20 years (STOLZENBURG et al. 1984, HÜCKELHOVEN et al. 1999, PANSTRUGA 2005).

For *mlo*-mediated nonhost resistance in *Arabidopsis* and penetration resistance in barley, the plasma membrane-resident SOLUBLE N-ETHYLMALEIMIDE-SENSITIVE FACTOR ATTACHMENT PROTEIN RECEPTOR (SNARE) protein PENETRATION 1 (PEN1) and its barley ortholog ROR2 (REQUIRED FOR MLO RESISTANCE 2) are required, respectively (COLLINS et al. 2003, ASSAAD et al. 2004). Both orthologs form ternary SNARE complexes with VAMP721/722 (VESICLE-ASSOCIATED MEMBRANE PROTEIN 721/722) and SNAP33/34 (SOLUBLE N-ETHYLMALEIMIDE-SENSITIVE FUSION PROTEIN ATTACHMENT PROTEIN 33/34) directly beneath fungal entry sites (DOUCHKOV et al. 2005, PAJONK et al. 2008, KWAAITAAL et al. 2010). Since a yeast two-hybrid assay demonstrated an interaction of SNAP33 with EXO70B2, a subunit of the exocyst complex that mediates vesicle tethering to the plasma membrane before fusion, it has been speculated whether EXO70 proteins are also required for penetration resistance to powdery mildew fungi (PEČENKOVÁ et al. 2011, HÜCKELHOVEN and PANSTRUGA 2011).

In *Arabidopsis*, *mlo2*-mediated resistance to powdery mildew fungi additionally depends on the operation of PEN3, a membrane-localized ATP-binding cassette (ABC) transporter, and on the atypical myrosinase PEN2 (CONSONNI et al. 2006). While PEN2 seems to be involved in the synthesis of indole glucosinolate-derived toxic secondary metabolites, PEN3 is suggested to mediate the transport of these

compounds to the apoplast (STEIN et al. 2006, BEDNAREK et al. 2009). Therefore, in compatible interactions, MLO proteins might influence SNARE protein-dependent and vesicle transport-associated processes. However, the actual biochemical function of MLO in plant - powdery mildew interactions needs to be elucidated (DEVOTO et al. 1999).

In barley, *mlo*-mediated resistance can be compromised by the overexpression of B-cell leukemia/lymphoma-2 gene (Bcl-2) associated X protein (BAX) INHIBITOR-1 (BI-1), an ancient cell death suppressor protein, suggested to be a susceptibility factor in the barley - powdery mildew interaction as well (HÜCKELHOVEN et al. 2003, EICHMANN et al. 2004, 2006b, BABAEIZAD et al. 2009, see below).

1.2.3   Post-penetration resistance in plant - powdery mildew interactions

As the name suggests, post-penetration defense mechanisms affect powdery mildew fungi that already initiated haustorium formation. More than 85 dominant or semi-dominant *MILDEW R* genes (*Ml*) conferring resistance to barley powdery mildew fungi have been identified. Among them, about 30 highly homologous genes map to the *MILDEW LOCUS A* (*MLA*) of barley chromosome 5 (JENSEN et al. 1980, JØRGENSEN 1994). All cloned *MLA* genes, namely *MLA1*, *MLA6*, *MLA7*, *MLA10*, *MLA12*, and *MLA13*, encode intracellular NB-LRR receptor proteins with N-terminal coiled-coil regions (WEI et al. 1999, SHEN et al. 2003). Recognition of isolate-specific *Bgh* effectors conferring race-specific resistance, is predicted to be determined by sequence diversity within the LRR region (SHEN et al. 2007). As mentioned in chapter 1.1.2, MLA10 confers resistance to *Bgh* through recognizing AVR_{A10} (RIDOUT et al. 2006). Partly, *MLA*-mediated defense signaling depends on additional downstream signaling components (HALTERMAN et al. 2001, SHEN et al. 2003, HALTERMAN and WISE 2004). For instance, MLA6-, MLA10-, MLA12-, and MLA13-mediated resistance to *Bgh* is RAR1 (REQUIRED FOR MLA12 RESISTANCE 1)-dependent, while MLA7 and MLA1 confer RAR1-independent defense responses (HALTERMAN et al. 2001, HALTERMAN and WISE 2004). To some extent, MLA proteins, as MLA6, additionally require SUPPRESSOR OF G-TWO ALLELE OF SKP 1 (SGT1), which physically interacts with RAR1 (AZEVEDO et al. 2002, SHEN et al. 2003, SHIRASU and SCHULZE-LEFERT 2003). Since HR is a hallmark for race-specific resistance, MLA-mediated

defense goes along with this feature (BUSHNELL 1981). Thereby, depending on the MLA protein, HR can occur in the attacked epidermal cell but also in the underlying mesophyll cells (KOGA et al. 1990, BOYD et al. 1995, HÜCKELHOVEN et al. 1999).

In contrast to the barley - *Bgh* pathosystem, no true race-specific *R* genes against powdery mildew fungi have been identified in *Arabidopsis* (GÖLLNER et al. 2008). In fact, resistance to powdery mildew in *Arabidopsis* is based on polygenetic origin and on the two atypical *R* genes *RESISTANCE TO POWDERY MILDEW 8* (*RPW8*), *RPW8.1* and *RPW8.2*, or on a combination of both (GÖLLNER et al. 2008, MICALI et al. 2008). RPW8.1 and RPW8.2 contain a coiled-coil (CC) domain and an N-terminal transmembrane helix. Both confer resistance to a broad range of powdery mildew fungi in *Arabidopsis* (XIAO et al. 2001, WANG et al. 2007). Upon powdery mildew ingress, RPW8.2 specifically localize to the EHM, which is dependent on actin cytoskeleton function. RPW8.2-mediated defense responses, such as haustoria encasement, accumulation of H_2O_2 in the HC, and *PATHOGENESIS-RELATED* (*PR*) gene expression, are SA signaling-dependent and end in HR (XIAO et al. 2001, 2005, WANG et al. 2009). However, since RPW8 confers resistance to *Hyaloperonospora parasitica* and cauliflower mosaic virus as well, RPW8 might be part of a general basal defense pathway against biotrophic pathogens rather than a specific powdery mildew R protein (WANG et al. 2007).

In *Arabidopsis*, defense mechanisms against powdery mildew fungi are often associated with SA-dependent pathways ending up in HR (GLAZEBROOK 2001, HAMMOND-KOSACK and PARKER 2003). Several SA signaling proteins, as ENHANCED DISEASE SUSCEPTIBILITY 1 (EDS1), PHYTOALEXIN DEFICIENT 4 (PAD4), NON-EXPRESSOR OF PATHOGENESIS-RELATED GENES 1 (NPR1), or SGT1b, identified in *Arabidopsis* mutant screenings, are involved in mediating basal resistance to powdery mildew fungi (GLAZBROOK 2005). Moreover, an EDS1-PAD4-SENESCENCE ASSOCIATED GENE 101 (SAG101) complex was shown to confer efficient post-penetration resistance to non-adapted powdery mildew fungi (LIPKA et al. 2005).

1.3 BAX INHIBITOR-1 (BI-1), an ancient cell death regulator involved in plant - pathogen interactions

BI-1 was first mentioned in 1994 as testis enhanced gene transcript (TEGT) in mammals (WALTER et al.). In 1998, the protein occured in a functional screening for cDNA clones, rescuing yeast cells from BAX-induced cell death (XU and REED 1998), giving the protein his current name.

In mammals, BAX-induced apoptosis-like PCD starts with the activation of BAX by Bcl-2 homology 3-only proteins (CORY and ADAMS 2002, WALENSKY and GAVATHIOTIS 2011). In turn, BAX translocates from the cytosol to the mitochondria, possibly regulated through ER-released Ca^{2+} (MORALES et al. 2011). In the outer mitochondrial membrane, BAX proteins are predicted to form homo-oligomeric pores, by which cytochrome *c* and other apoptogenic factors are released. Subsequently, a caspase-cascade is initiated, leading to the execution of cell death (BRECKENRIDGE and XUE 2004, KULIKOV et al. 2011). As cell death suppressor, BI-1 seems to function downstream or in parallel to BAX by regulating ER-releasable Ca^{2+} (CHAE et al. 2004, WESTPHALEN et al. 2005, XU et al. 2008).

In 1999, the first plant BI-1 homologs were isolated from rice and *Arabidopsis* by KAWAI and co-workers. Although the entire Bcl-2 family of pro- and antiapoptotic proteins as well as BAX it self is apparently not present in plants, overexpression of plant *BI-1* suppresses BAX-induced PCD in yeast and *Arabidopsis* (KAWAI et al. 1999, SANCHEZ et al. 2000, HÜCKELHOVEN 2004). *BI-1* overexpression also inhibits cell death induced by application of H_2O_2 or SA in tobacco BY-2 cells (KAWAI-YAMADA et al. 2004). Moreover, WATANABE and LAM (2006) showed accelerated cell death reactions in two *atbi-1* knock-out mutants upon treatment with the fungal toxin fumonisin B1 (FB1) or heat stress. Therefore, a highly conserved function of BI-1 proteins as cell death suppressors has been proposed (KAWAI et al. 1999, KAWAI-YAMADA et al. 2001, 2004, HÜCKELHOVEN 2004).

BI-1 proteins are ER-resident and predicted to possess six to seven transmembrane domains (XU and REED 1998, KAWAI et al. 1999, BOLDUC et al 2003, EICHMANN et al. 2004). Via *in silico* analyse, a coiled-coil structure was predicted for the C-terminal part of AtBI-1 that is suggested to be required for cell death inhibition and presumably reaches into the cytosol (BOLDUC et al. 2003, KAWAI-YAMADA et al. 2004). In 2007, IHARA-OHORI and co-workers could demonstrate the interaction of CaM with the C-terminal region of AtBI-1. This interaction turned out to be crucial for the

suppression of *Pseudomonas syringae*-induced HR-associated cell death (KAWAI-YAMADA et al. 2009).

Besides their role as cell death inhibitors, BI-1 proteins are involved in plant development and in responses to biotic and abiotic stress. During wounding and pathogen stress, the expression level of *BI-1* is up-regulated (SANCHEZ et al. 2000, HÜCKELHOVEN et al. 2001, EICHMANN et al. 2004). In carrots, *HvBI-1* overexpression results in partial resistance against the necrotrophic fungus *Botrytis cinerea* (IMANI et al. 2006), and barley plants expressing a green fluorescing protein (GFP)-HvBI-1 fusion protein resist infection against the necrotrophic fungus *Fusarium graminearum* (BABAEIZAD et al. 2009). The root endophytic fungus *Piriformospora indica* requires host cell death for proliferation during mutalistic symbiosis with barley. Some days after inoculation, expression of *HvBI-1* is suppressed, and consistently, overexpression of *GFP-HvBI-1* in barley results in inhibition of fungal proliferation. Therefore, DESHMUKH et al. (2006) suggested that the fungus interferes with a host cell death program to establish symbiosis.

By transiently expressing a GFP-HvBI-1 fusion protein in barley cells, accumulation of BI-1 can be detected after *Bgh* inoculation at the site of attempted penetration, beneath the appressorial germ tube (EICHMANN et al. 2006b). Overexpression of *HvBI-1* leads to reduced oxidative defense and enhanced susceptibility against *Bgh* (HÜCKELHOVEN et al. 2003). Vice versa, knock-down of *HvBI-1* results in enhanced resistance to *Bgh* defining HvBI-1 as susceptibility factor (EICHMANN et al. 2010). Moreover, overexpression of HvBI-1 also supports haustoria accommodation in race-non-specifically resistant barley *mlo*-mutants and in race-specifically resistant MLA12-barley cells (HÜCKELHOVEN et al. 2003, EICHMANN et al. 2006b). Penetration resistance of barley cells against the non-adapted *B. graminis* f.sp*. tritici* is also suppressed by *HvBI-1* overexpression, which links penetration resistance with cell death regulation (EICHMANN et al. 2004). Thus, BI-1 seems to be involved in susceptibility to biotrophic pathogens, as powdery mildew fungi or *U. maydis*, and in resistance to necrotrophic pathogens, as *F. graminearum* (EICHMANN and HÜCKELHOVEN 2008, BABAEIZAD et al. 2009, VAN DER LINDE et al. 2011). However, it is still questionable whether BI-1-controlled defense and cell death pathways are independent or common (HÜCKELHOVEN 2004).

1.4 LIFEGUARD (LFG) proteins

LIFEGUARD (LFG) proteins are proteins structurally related to BI-1, and named after the mammalian paralogue with the best-annotated function. The evolutionarily conserved LFG protein family consists of five subfamilies, LFG1 through LFG5 (HU et al. 2009). Table 1.1 is modified after HU et al. 2009 and lists the five subfamilies, including protein names known in literature.

Table 1.1: The mammalian LIFEGUARD family (HU et al. 2009, modified)

LFG subfamily	known in literature	
	symbol	full name
LFG1	GBP	Glutamate binding protein
	Grina	Glutamate receptor, ionotropic N-Methyl-D-Aspartate associated (NMDA) protein
	NMDARP-71	71 kDa NMDA receptor protein
	OTMP	Oligodendrocyte transmembrane protein
	PM02	Putative MAPK-activating protein
	Tmbim3	Transmembrane Bax Inhibitor Motif-containing 3
LFG2	Faim2	Fas apoptotic inhibitory molecule 2
	LFG	Lifeguard
	NMP35	35 kDa Neural membrane protein
	Tmbim2	Transmembrane BAX Inhibitor Motif-containing 2
LFG3	RECS1	Responsive to centrifugal force and shear
	Tmbim1	Transmembrane BAX Inhibitor Motif-containing 1
LFG4	GAAP	Golgi anti-apoptotic protein
	h-GAAP	Human GAAP
	Tmbim4	Transmembrane BAX Inhibitor Motif-containing 4
	v-GAAP	Viral GAAP
LFG5	Tmbim1b	Sequence similarity to Tmbim1
	4930511M11Rik	RIKEN cDNA 4930511M11 gene

As BI-1 proteins, LFG proteins contain the PFAM *Bax1-I* motif (PF01027, formerly UPF0005) and are predicted to possess seven transmembrane domains (REIMERS et al. 2006, HU et al. 2009). Moreover, as demonstrated for BI-1, several members of the mammalian LFG family seem to share conserved functions in the regulation of apoptosis (HU et al. 2009). SOMIA et al. (1999) showed that LFG/LFG subfamily 2 protects cells from fetal alcohol syndrome (Fas)/Fas ligand-mediated apoptosis by physical interaction, giving the protein its name. For instance, in breast cancer cells, the expression of LFG/LFG2 correlates with tumor grades (BUCAN et al. 2010). A neuroprotective role in cerebellar granule neurons, mediated by the prevention of

Fas-induced cell death through interfering with caspase 8 activation, has been attributed to LFG/LFG2 as well (FERNÁNDEZ et al. 2007, DE MENDOZA et al. 2011). Furthermore, LFG/LFG2 co-immunoprecipitated with BAX (FERNÁNDEZ et al. 2007). High levels of RECS1/LFG3 can also prevent Fas/Fas ligand-induced apoptosis, most likely by interrupting Fas trafficking to the cell membrane (SHUKLA et al. 2010). Moreover, h-GAAP/LFG4 is involved in the regulation of intrinsic and extrinsic cell death pathways in mammalian cells (GUBSER et al. 2007, DE MATTIA et al. 2009). Phylogenetic analysis indicates that plant LFG proteins are all LFG4 derived (HU et al. 2009). *Arabidopsis* and barley possess five homologues, respectively, listed in table 1.2 (YAMAGAMI et al. 2009, R. Eichmann, TUM, personal communication).

Table 1.2: The *Arabidopsis* and barley LIFEGUARD family

Arabidopsis homologs		Barley homologs	
symbol	AGI code	symbol	TIGR plant transcript assembly
AtLFG1	At4g14730	HvLFG1	TA49291_4513
AtLFG2	At3g63310	HvLFG2	TA42670_4513
AtLFG3	At1g03070	HvLFG3	TA38842_4513
AtLFG4	At4g02690	HvLFG4	TA39011_4513
AtLFG5	At4g15470	HvLFG5	TA32154_4513

According to R. Eichmann (TUM, personal communication)

Until now, nearly nothing is known about the function of LFG proteins in plants, particularly during plant - pathogen interactions.

1.5 Objectives

The elucidation of cellular signal transduction pathways constitutes a main part of fundamental research in phytopathology. The interactions of the monocot barley and the dicot *Arabidopsis thaliana* with powdery mildew fungi are model systems for understanding host defence mechanisms as well as infection strategies of biotrophic pathogens. Until now, many studies aided to extend the understanding of plant resistance mechanisms and powdery mildew infection strategies. However several aspects remain still unclear.

The conserved cell death suppressor protein BI-1 is a susceptibility factor in the interaction of barley with the biotrophic barley powdery mildew fungus *Bgh* (HÜCKELHOVEN et al. 2003, EICHMANN et al. 2004, 2006b, 2010). Besides BI-1 proteins themselves, there are structurally related BI-1-like proteins, namely LFG proteins. Like BI-1, LFG proteins are described as evolutionarily conserved cell-death suppressor proteins with seven transmembrane domains (REIMERS et al. 2006). Since LFG proteins might therefore share functional properties with BI-1, I analyzed LFG proteins concerning their role in plant - powdery mildew interactions and plant cell death reactions.

A further aim of this thesis was to shed light on the mode of action of BI-1 in modulating basal defense reactions during plant - powdery mildew interactions and in the regulation of cell death reactions. I therefore investigated the impact of potential BI-1-linked signaling components, namely MLO and CALMODULIN (CaM), during compatible barley - powdery mildew interactions.

Moreover, in order to identify new BI-1-interacting proteins, I conducted a co-immunoprecipitation assay using AtBI-1-GFP overexpressing mutants. Out of the identified putative AtBI-1-interacting proteins, several selected candidate proteins should be investigated concerning their impact in BI-1-assosiated processes. Therefore, I analyzed a set of *Arabidopsis* mutants, deficient in the expression of respective AtBI-1-interacting candidate proteins, in the interaction with adapted *E. cruciferarum* and upon cell death inducing treatments. Moreover, barley homologs of putative AtBI-1-interacting proteins were analyzed in the interaction with *Bgh* to investigate conserved functions in monocots.

The investigations of BI-1, BI-1-like, and BI-1-interacting candidate proteins should contribute to the understanding of mechanisms involved in resistance or susceptibility to powdery mildew fungi and in the regulation of cell death reactions.

2 Material and methods

2.1 Investigation on the role of BI-1-like LFG proteins during biotic stress

2.1.1 Plants, pathogens and inoculation

Barley (*Hordeum vulgare* L.) cv. Ingrid was used. Plants were cultivated in a growth chamber at 18°C, a photoperiod of 16 h, and a relative humidity of 65%. *Blumeria graminis* (DC) Speer f.sp. *hordei* race A6 was maintained on barley cv. Golden Promise under the same conditions. Transiently transformed barley leaf segments were inoculated with a density of 150 conidia per mm^2 for subsequent functional analysis, and with a density of about 50 conidia per mm^2 for pathogen-dependent protein localization studies.

Arabidopsis thaliana ecotype Columbia 0 (Col-0) was purchased from Lehle Seeds (Round Rock, USA), and *LFG* SALK-lines (listed in table 2.1) were ordered from the Nottingham Arabidopsis Stock Centre (NASC, Nottingham, UK). All seeds were stratified for 2 days at 4°C before placement in a growth chamber (22°C, photoperiod of 10 h, 64% relative humidity).

Table 2.1: *AtLFG* SALK-lines

gene description	AGI code	NASC stock number	T-DNA position	internal name
AtLFG1	At4g14730	SALK_147263C	promoter	*Atlfg1-1*
AtLFG1	At4g14730	SALK_111590	promoter	*Atlfg1-2*
AtLFG2	At3g63310	SALK_052507C	3' UTR	*Atlfg2*

Gene description according to R. Eichmann (TUM, personal communication), AGI code, NASC stock number, and T-DNA position according to The Arabidopsis Information Resource-database (TAIR, http://arabidopsis.org/).

Erysiphe cruciferarum was maintained on Col-0, to obtain constant aggressiveness, and on more susceptible phytoalexin-deficient *pad4* mutants for strong conidia production (REUBER et al. 1998). Conditions were the same as mentioned above. For inoculation, *Arabidopsis* plants were placed under an inoculation box, covered with a polyamide net (0.2 mm^2). Plants used for microscopic analysis were inoculated with a density of 3-5 conidia per mm^2 by brushing conidia off of *pad4* plants through the net, and were further cultivated under the conditions described above. Hyphae per spore

were counted 4 dai, conidiophores per colony 5 dai, and macroscopic evaluations took place 8-13 dai.

2.1.2   Staining methods

For counting of conidiophores per colony, leaves were discolored, stored in 50% glycerol and stained with acetic ink, as previously described for staining epiphytical structures of *Bgh* (HÜCKELHOVEN and KOGEL 1998).

2.1.3   AAL toxin treatment of *Atlfg* mutants

For cell death induction, 10 µl of a 100 µM *Alternaria alternata* f.sp. lycopersici (AAL) toxin (A8331, Sigma-Aldrich Chemie GmbH, Munich, Germany) solution were dropped on leaves of 5-weeks-old *Arabidopsis* Col-0 and *Atlfg* mutants (table 2.1). Distilled water served as control. Plants were cultivated under normal growth conditions until leaves were harvested and photographed for evaluation 9 days after treatment. A minimum of ten leaves per line and individual experiment was evaluated, respectively.

2.1.4   Cloning of *LFG* cDNAs

2.1.4.1 Constructs for functional assessment of *LFG* genes

The coding sequences of *HvLFG1* (TA49291_4513), *AtLFG1* (At4g14730) and *AtLFG2* (At3g63310) were subcloned into the expression vector pGY-1 (SCHWEIZER et al. 1999). The coding sequence of *HvLFG1* was amplified by PCR using the primers 5'-<u>GGATCC</u>ACGCCGACGACGATGTAT'-3 and 5'-GGACAGGAGGAGGGGCTA-3', the one of *AtLFG1* by using the primers 5'-<u>GGATCC</u>GCGATTTCAACAACAAA-3' and 5'-CGATAAATCTATGTCTGGAA-3', and *AtLFG2* by using the primers 5'-<u>GGATCC</u>CACCGGCGTTGACAAA-3' and 5'-TGGCACAGTCTTAAGAGCAA-3'. PCR fragments were cloned into the pGEM-T vector (Promega GmbH, Mannheim, Germany) and subcloned into the expression vector pGY-1, after sequence confirmation.

For transient-induced gene silencing (TIGS) by RNA interference (RNAi), a 976 bp *HvLFG1* fragment was amplified by PCR using the primers 5'-<u>GGATCC</u>GAAGAACGCCGACGAC-3' and 5'- <u>GTCGAC</u>GAGGGGCTACGCTACG-3',

which contained a 138 bp-long intron 270 bp downstream of the start codon. The blunt-ended fragment was ligated into the Gateway® pENTR vector pIPKTA38 in anti-sense orientation and subcloned into the final RNAi Gateway® destination vector pIPKTA30N by standard lambda-based site-specific recombination (LR) reaction (DOUCHKOV et al. 2005). The final pIPKTA30N-HvLFG1 construct contained the *HvLFG1* fragment as inverted repeats under the control of the CaMV 35S promoter, separated by the second intron of the wheat *RGA2* gene.

2.1.4.2 GFP-LFG fusion constructs for localization studies

To archive a GFP-HvLFG1 fusion construct, the *HvLFG1* coding sequence was cut out of pGY-1-HvLFG1 (chapter 2.1.4) using *Bam*HI, blunted and inserted in frame into pGY-1-GFP, lacking the stop codon (provided by H. Schultheiss, JLU, Giessen), by using the internal *Xba*I site behind *GFP*, resulting in pGY-1-GFP-HvLFG1. For the N-terminal fusion of AtLFG1 with GFP, *GFP* was amplified by PCR using the primers 5'-GGATCCATGGTGAGCAAGGGCGAG-3' and 5'-CTTGTACAGCTCGTCCAT-3', which eliminated the stop codon, and inserted in frame into pGY-1-AtLFG1 (chapter 2.1.4) using the *Not*I site in front of *AtLFG1* by blunt-end ligation. A GFP-AtLFG2 fusion construct was obtained by *Bam*HI digestion of pGY-1-GFP (see above) and subsequent insertion of the resulting *GFP* fragment into the internal *Bam*HI site of pGY-1-AtLFG2 (chapter 2.1.4).

2.1.5 Transient transformation of barley cells and evaluation of the penetration efficiency

For gene function analysis and protein localization studies, single epidermal cells of 7-days-old barley cv. Ingrid leaf segments were transiently transformed via ballistic delivery of expression vectors, based on a protocol originally developed for wheat (SCHWEIZER et al 1999). For transient overexpression and TIGS experiments, the expression vector pGY-1 and the GATEWAY® destination vector pIPKTA30N were employed, respectively (SCHWEIZER et al. 1999, DOUCHKOV et al. 2005). Per shot, 236 µg 1 µm gold particles or 312 µg 1.1 µm tungsten particles were coated with pGY-1-GFP (GFP under control of CaMV 35S promoter) as transformation marker together with the respective test plasmid, which contained the gene of interest, or with the corresponding empty vector. Gold particles coated with plasmids were delivered

using a PDS-1000/He particle gun with hepta-adapter (Bio-Rad Laboratories GmbH, Munich, Germany), as described previously (DOUCHKOV et al. 2005), while plasmid-coated tungsten particles were delivered using a Particle Inflow Gun as described by FINER et al. (1992). After ballistic delivery of coated particles, the leaf segments were subsequently inoculated with a density of about 150 *Bgh* spores per mm^2 to obtain fungal attacks on approximately 50% of the transformed cells (HÜCKELHOVEN et al. 2003). Table 2.2 lists all transient overexpression and TIGS experiments with *LFG* genes and reveals information about the appropriate plasmid amounts, particles used, and the time point of inoculation after ballistic transformation, respectively.

For localization studies, tungsten particles were coated with 1 µg of pGY-1-GFP-HvLFG1, pGY-1-GFP-AtLFG1 or pGY-1-GFP-AtLFG2 construct together with either 0.8 µg pGY-1-RFP (red fluorescing protein under control of CaMV 35S promoter, R. Eichmann, TUM, Freising) or 1 µg of the Golgi marker GmMan1-RFP (YANG et al. 2005). To analyze pathogen-dependent localization of the GFP-HvLFG1 fusion protein, transiently transformed barley cv. Ingrid leaf segments were inoculated 1 day after bombardment with approximately 50 conidia per mm^2. To investigate GFP-AtLFG1 and GFP-AtLFG2 localization, Col-0 epidermal cells were transformed in the same manner.

Table 2.2: Transient overexpression and TIGS of *LFG* genes

test plasmid	plasmid/shot	pGY-1-GFP/shot	coated particles	time point of inoculation
pGY-1-HvLFG1	1 µg	1 µg	gold	1 dab
pGY-1-GFP-HvLFG	1 µg	1 µg	gold	1 dab
pGY-1-AtLFG1	0.8 µg	0.5 µg	tungsten	4 hab
pGY-1-AtLFG2	1 µg	1 µg	gold	1 dab
pIPKTA30N-HvLFG1	1 µg	0.8 µg	tungsten	1 dab

hab/dab = hours/days after bombardment

The penetration success of *Bgh* on transiently transformed epidermal cells was evaluated 2 days after inoculation by fluorescence and light microscopy as described previously (SCHULTHEISS et al. 2002, HÜCKELHOVEN et al. 2003).

At least three independent experiments were conducted per overexpression or RNAi construct, whereby for each individual experiment, a minimum of 60 interactions were evaluated. Penetration efficiency (PE) was calculated as the quotient of the number of penetrated cells and the number of attacked (non-penetrated and penetrated) cells

multiplied by 100, as measure of resistance of transformed cells. Absolute values of PE were used for significance examination by two-sided paired Student's t test. The deviation of PE from the average control was calculated for data presentation.

2.1.6 Transient knock-down of *GFP-HvLFG1* expression

Tungsten particles were coated with 1 µg per shot of the RNAi construct pIPKTA30N-HvLFG1 or empty vector pIPKTA30N together with 1 µg of the pGY-1-GFP-HvLFG construct and delivered into single barley cv. Ingrid epidermal cells. As transformation marker, 0.8 µg per shot of pGY-1-RFP was co-transformed. By fluorescence microscopy, *RFP*-expressing cells were analyzed concerning a *GFP-HvLFG1* co-expression 2 dab. In three independent experiments, 100 cells per variant were observed, respectively. Statistical significance was calculated by means of two-sided unpaired Student's t test.

2.1.7 Confocal laser-scanning microscopy

The localization of a GFP-LFG fusion protein was detected by confocal laser-scanning microscopy (CLSM, Leica TCS SP2, Leica Microsystems, Bensheim, Germany) 24-72 hab.

GFP fusion proteins were excited by a 488 nm laser line and detected at 505-530 nm. RFP or GmMAN1-RFP were excited by a 561 nm laser line and detected at 580-650 nm.

2.1.8 Stable *A. tumefaciens*-mediated transformation of *Arabidopsis* plants

The expression cassettes of pGY-1-AtLFG1 and pGY-1-AtLFG2 (*Xho*I blunt/*Hind*III sticky, chapter 2.1.4.1) were subcloned into the binary vector pLH6000 (*BamH*I blunt/*Hind*III sticky). *Agrobacterium tumefaciens* strain AGL1 was transformed using the freeze-thaw method described by WEIGEL and GLAZEBROOK (2006). The floral-dip method based on the protocols of CLOUGH and BENT (1998) and ROSSO et al. (2003) was adopted to transform *Arabidopsis* Col-0 plants. Flower buds (5-10 cm-long) were submerged for 1 min into an overnight grown *A. tumefaciens* culture (OD_{600} = 1.5) mixed one to one with 10% sucrose solution containing 0.02% Silwet L-77 (Lehle

Seeds, Round Rock, USA). Transgenic *Arabidopsis* plants were selected on 0.003% hygromycin-containing ½ MS medium by additional light stress adaption, as described by HARRISON et al. (2006).

2.1.9 Characterization of *AtLFG* mutants

To investigate the expression level of target genes in the respective *AtLFG* SALK-lines (table 2.1) and *AtLFG* overexpressing mutants (chapter 2.1.8), semi-quantitative two-step reverse-transcription polymerase chain reaction (RT-PCR) was conducted. Total RNA was extracted from frozen plant material using the NucleoSpin® RNA II kit (Macherey-Nagel GmbH & Co. KG, Düren, Germany). cDNA synthesis was primed with oligo (dT) using RevertAid™ Reverse Transcriptase (Fermentas GmbH, St. Leon-Rot, Germany). Equal cDNA loading was confirmed by the amplification of *UBIQUITIN 5 (UBQ5,* At3g62250) using the primers 5'-CCAAGCCGAAGAAGATCAAG-3' and 5'-ACTCCTTCCTCAAACGCTGA-3'. *AtLFG1* expression was analyzed by using the primers 5'-GGATCCGCGATTTCAACAACAAA-3' and 5'-CGATAAATCTATGTCTGGAA-3', and *AtLFG2* expression using the primers 5'-GGATCCCACCGGCGTTGACAAA-3' and 5'-TGGCACAGTCTTAAGAGCAA-3'.

2.2 Investigation of putative components of BI-1-dependent signaling in susceptibility towards *Bgh*

2.2.1 Plants, pathogens and inoculation

Barley cv. Ingrid and the Pallas backcross line BCPallas-*mlo5* (P22, KØLSTER et al. 1986) were cultivated under controlled conditions (see chapter 2.1.1). Leaf segments were transiently transformed and inoculated with a density of 150 *Bgh* conidia per mm^2 (see chapter 2.1.1).

2.2.2 Transient overexpression of *MLO* and simultaneous knock-down of *BI-1*

Tungsten particles, coated with 0.5 µg per shot of pGY-1-MLO (MLO under control of CaMV 35S promoter, EICHMANN et al. 2004) together with 1 µg of a *BI-1* TIGS construct (obtained from Patrick Schweizer, IPK, Gatersleben, Germany, EICHMANN et al. 2010) or 1 µg empty TIGS vector pIPKTA30N were delivered into barley backcross line BCPallas-*mlo5* cells by using a Particle Inflow Gun (FINER et al. 1992, chapter 2.1.5). Control cells were co-transformed with 0.5 µg per shot empty pGY-1 vector and 1 µg pIPKTA30N-BI-1. As reporter gene, 0.5 µg per shot pGY-1-GFP was co-bombarded. 2 days after ballistic transformation, leaf segments were inoculated. PE (chapter 2.1.5) was assessed 2 days after inoculation, whereby a minimum of 80 interaction sites were evaluated per variant, respectively. Three independent experiments were performed.

2.2.3 Transient knock-down of *GFP-BI-1* expression

The ability of the pIPKTA30N-BI-1 construct to knock-down *GFP-BI-1* expression was analyzed. Barley cv. Ingrid cells were transformed with 1 µg per shot of pIPKTA30N-BI-1 or empty RNAi vector pIPKTA30N together with 1 µg pGY-1-GFP-BI-1 (EICHMANN et al. 2004). As transformation marker, 0.5 µg per shot of pGY-1-DsRED (DsRED under control of CaMV 35S promoter, DIETRICH and MAISS 2002) was co-delivered. Two days after bombardment, *GFP-BI-1* and *DsRED* co-expressing cells and only *DsRED* expressing cells were counted. I conducted this experiment three times, whereby 100 cells per variant were evaluated, respectively.

Statistical significance was calculated by means of two-sided unpaired Student's *t* test.

2.2.4 Transient overexpression of *BI-1* and simultaneous knock-down of *CaM* expression

For transient overexpression of *BI-1* with simultaneous knock-down of *CaM* expression, barley cv. Ingrid cells were co-transformed with 1 µg per shot of pGY-1-BI-1 (BI-1 under control of CaMV 35S promoter, HÜCKELHOVEN et al. 2003) and TIGS construct pIPKTA30N-CaM or empty pIPKTA30N vector. The 496 bp-long ORF of *CaM* (P62162) was amplified with primers 5'-<u>CCCGGG</u>CCTCCGTCGGTCCAC-3' and 5'-<u>CCCGGG</u>TTTGGCCATCATGACCTT-3'. Analogous to *HvLFG1* (chapter 2.1.4.1), *CaM* was cloned into pIPKTA38 and subcloned into the RNAi destination vector pIPKTA30N as inverted repeats. Tungsten particles coated with 1 µg per shot empty plant expression vector pGY-1 together with 1 µg empty pIPKTA30N were co-delivered into control cells. As transformation marker, 0.8 µg per shot pGY-1-GFP was co-transformed, respectively. I inoculated the leaf segments 1 day after bombardment with 150 *Bgh* conidia per mm^2, and calculated the PE (chapter 2.1.5) 2 days after inoculation. In total, three independent experiments were conducted, whereby for each individual experiment, a minimum of 70 interaction sites were evaluated, respectively.

2.3 AtBI-1-GFP co-immunoprecipitation

2.3.1 Plant material and protein extraction

As starting material 4-weeks-old *AtBI-1-GFP* overexpressing *Arabidopsis* mutants as well as control plants, carrying the empty over-expression vector pBin19 were used (KAWAI-YAMADA et al. 2001). Half of the plants of each line were inoculated with approximately 80 conidia per mm^2 of *Bgh* and 30 conidia per mm^2 of *E. cruciferarum.* Plants were harvested 12 hai. See chapter 2.1.1 for plant cultivation conditions, pathogen strains, and inoculation details.

Protein was extracted from 10 g frozen plant material using 10 ml extraction buffer A (see below). After 15 min incubation on ice, the protein extract was diluted 1:1 with extraction buffer B (see below) and centrifuged for 10 min at 4,000 rpm. The

precipitate was discarded and the supernatant was extruded through a 0.45 µm nylon filter. Protein concentration was calculated via Bradford test (KRUGER 1994).

Extraction buffer A

Tris-HCl	50 mM
NaCl	150 mM
PhosStop® (Roche Deutschland Holding GmbH, Grenzach-Wyhlen, Germany)	1 tablet/10 ml
Protease Inhibitor Cocktail (Sigma-Aldrich Chemie GmbH, Munich, Germany)	1%
Leupeptin	0.005%
Sodium orthovate	100 µM
TritonX-100	0.5%

Extraction buffer B

Extraction buffer A without TritonX-100	

2.3.2 Co-immunopreciptation assay

At first, 100 µl GFP-Trap A® (ChromoTek, Munich, Germany, ROTHBAUER et al. 2008) and 2 x 100 µl Protein A sepharose (Sigma-Aldrich Chemie GmbH, Munich, Germany) were washed with 5 ml washing buffer A (see below). Upon centrifugation (2,000 rpm, 20 sec), the buffer was removed.

About 40 mg protein extract (3 µg/µl) were incubated with 100 µl washed Protein A sepharose for 30 min on a rotor at 4°C to minimize subsequent unspecific protein binding to GFP-Trap A® coupled Protein A sepharose. After centrifugation (2,000 rpm, 20 sec), the protein extract was transferred to the second batch of Protein A sepharose. After a further centrifugation step (2,000 rpm, 20 sec), the extract was removed to previously washed GFP-Trap A®, and incubated on a rotor for 1 h at 4°C. Centrifugation (2,000 rpm, 20 sec) precipitated AtBI-1-GFP bound to GFP-Trap A® together with putative interaction partners, while unbound proteins remained in the supernatant and were removed. Unspecific low-bonded proteins were washed off the beads by adding 12 ml washing buffer A. Solution was spun down for 20 sec at 2,000 rpm. I eliminated the supernatant and repeated the washing step. A further washing step followed by adding 12 ml washing buffer B (see below). Thereafter, 1 ml washing buffer B helped to transfer the precipitate in a 1.5 ml tube. Samples were

centrifuged again for 20 sec at 2,000 rpm, and the supernatant was replaced by 30 µl NuPAGE® LDS Sample Buffer (4x, Invitrogen GmbH, Karlsruhe, Germany) together with 30 µl 100 mM DTT. Incubation at 50℃ for 15 mi n reduced disulfide bonds.

Washing buffer A

Tris-HCl	50 mM
NaCl	100 mM
TritonX-100	0.05%

Washing buffer B

Washing buffer A without TritonX-100

Centrifugation (3,000 rpm, 30 sec) of samples on MicroSpin™ columns (GE healthcare, Buckinghamshire, UK) allowed the separation of beads and precipitated proteins. For alkylation, 1/10 jodacetamid (1 M) was added and samples were incubated for 30 min in the dark at RT.

2.3.3 Protein identification by liquid chromatography and tandem mass spectrometry (LC-MS/MS)

Via liquid chromatography and tandem mass spectrometry (LC-MS/MS), putative AtBI-1-interacting proteins were identified in cooperation with the chair of Proteomics and Bioanalytics (Prof. B. Küster, H. Hahne/F. Pachl, TUM).

Nanoflow LC-MS/MS of tryptic peptides was performed on an amaZon ETD mass spectrometer (Bruker Daltronik, Bremen, Germany) coupled to an easy-nLC (Proxeon, Denmark). Peptides were separated on a self packed 0.075x20 cm reversed-phase column (Reposil, Dr. Maisch, Ammerbuch, Germany) using a 110 minutes gradient from 10% to 35% of buffer B (0.1% FA in acetonitrile) at a flowrate of 300 nL/min. Intact masses of eluting peptides were determined in enhanced scan mode and the five most intense peaks were selected for further fragmentation by collision-induced dissociation (CID) and acquisition of fragment spectra in ultra scan mode. Singly charged ions as well as ions with unknown charge state were rejected. Dynamic exclusion was enabled and dynamic exclusion duration was set to 10 seconds. Peaklist files were generated with DataAnalysis 4.0 (Bruker Daltonik, Bremen, Germany) and database searches were performed using the Mascot search

engine version 2.3.01 (Matrix Science, London, UK) with a tolerance of 0.3 Da for peptide and 0.6 Da for fragment ions against the NCBI (National Center for Biotechnology Information, http://.ncbi.nlm.nih.gov/) database (nr_20070216, 4,626,804 entries, state February 16, 2007) and the viridiplantae-subset of the NCBI database (339,709 entries, state February 16, 2007) considering oxidation of methionine (+15.99 Da), carbamidomethylation of cystein residues (+57.01 Da) and pyro-glutamic acid from Q or E (-18.01 Da) as variable modifications. The Mascot search result files were analyzed using Scaffold version 2.6.2 (Proteome Software Inc., Portland, USA). Threshold parameters were set as follows: protein probability, 80 %; minimum number of peptides, 1; peptide probability, 80 %, yielding a false-discovery rate of 8.8% on protein level and 7.0% on peptide-spectrum match level.

2.3.4　SDS page, silver staining, and Western blot analysis

Standard discontinuous SDS gel electrophoresis (LAEMMLI 1970, AMES 1974) was performed using the Mini-PROTEAN® Tetra Cell system (Bio-Rad Laboratories GmbH, Munich, Germany). Acrylamide gels (4% acrylamide in 0.125 M Tris-HCl, pH 6.8, with 0.1% SDS for the stacking gel and 12% acrylamide in 375 mM Tris-HCl, pH 8.8, with 0.1% SDS for the separating gel) of 1 mm thickness were prepared. Electrophoresis was carried out at 100 V for approximately 2.5 h using 25 mM Tris (pH 8.3) with 192 mM glycine, and 0.1% SDS as electrode buffer. Silver staining was performed using a protocol developed by BLUM et al. (1987). When the staining was sufficient the reaction was stopped by a 1.9% EDTA solution. For Western blot analysis, proteins were electrophoretically transferred (Fastblot B43, Biometra, Göttingen, Germany) onto a 0.2 µm pore Protran™ nitrocellulose membrane (Whatman, Springfield Mill, UK) at 112 mA per gel for 1.15 h. The transfer buffer consists of 25 mM Tris (pH 8.3) with 200 mM glycine, and 10% methanol. Protein transfer and equal protein loading was confirmed by reversible Ponceau S staining (0.2% Ponceau S in 3% trichloroacetic acid). The membrane was incubated in 5% fat-free milk powder in TBS (25 mM Tris-HCl, pH 7.5; 150 mM NaCl) for 1 h to block nonspecific binding sites. Anti-GFP rabbit polyclonal serum (A6455, Invitrogen GmbH, Karlsruhe, Germany) was diluted 1:2,000 in the saturating agent and applied over night. Second antibody (anti-rabbit IgG peroxidise conjugate, A9169, Sigma-Aldrich Chemie GmbH, Munich, Germany) was diluted 1:80,000 and applied for 1 h. TBS was used as washing buffer throughout between each step. Detection was

realized by chemoluminescence using SuperSignal® West Femto Maximum Sensitivity Substrate (Pierce, Rockford, USA).

2.4 Analysis of putative BI-1-interacting candidate proteins

2.4.1 Plants, pathogens and inoculation

Barley cv. Ingrid and the adapted powdery mildew fungus *Bgh* was used. See chapter 2.1.1 for cultivation and inoculation procedure.

Arabidopsis ecotype Col-0 was purchased from Lehle Seeds (Round Rock, USA). SALK-lines, listed in table 2.3, were ordered from NASC.

The *atbi1-2* mutant, which is identical to line 117B05 from the GABI-Kat collection (Bielefeld, Germany), was provided by N. Watanabe (The State University of New Jersey, New Brunswick, USA) and was indicated as being a *atbi-1* null-mutant (WATANABE and LAM 2006). The *CYP83A1* mutant *ref2-1* (HEMM et al. 2003) was provided by C. Chapple (Purdue University, West Lafayette, USA).

For *A. tumefaciens*-mediated transient transformation of tobacco leaf-segments *Nicotiana tabacum* cv. Samsun was used, cultivated under the same conditions as barley (chapter 2.1.1).

Table 2.3: SALK-lines to investigate putative AtBI-1-interacting proteins

gene description	AGI code	NASC stock number	T-DNA position	internal name
HAPLESS 6 (HAP6)	At4g21150	SALK_019955C	intron	*hap6-1*
		SALK_017994C	promoter	*hap6-2*
VACUOLAR H+-ATPASES SYNTHASE SUBUNIT A (VHA-A)	At1g78900	SALK_081473C	exon	-
		SALK_089595C	exon	-
PLASMA MEMBRANE PROTON ATPASE 1 (AHA1)	At2g18960	SALK_065288C	exon	-
PROHIBITIN 2 (PHB2)	At1g03860	SALK_004663C	promotor	*phb2-1*
		SALK_061282C	intron	*phb2-2*
CYTOCHROME P450 83A1 (CYP83A1)	At4g13770	SALK_123405C	intron	*cyp83a1*

Gene description, AGI code, and T-DNA position according to TAIR.

The adapted powdery mildew fungus *E. cruciferarum* was used to investigate *Arabidopsis* - powdery mildew interactions. Plants, used for macroscopic and microscopic analysis, were inoculated with a density of 3-5 conidia per mm^2. Detailed information about cultivation and inoculation practices is given in chapter 2.1.1.

The *Botrytis cinerea* strain B05.10, provided by B. Tudzynski (Westfälische-Wilhelms-Universität, Münster), was cultivated on potato-dextrose-agar (PDA, see below) plates under UV-light at RT. The used infection assay based on a protocol of SCHULZE GRONOVER et al. (2001). Conida were washed off of 7-10-days-old PDA plates with Gamborgs B5 medium (see below), and adjusted to a concentration of 800,000 conidia per ml using B5 medium containing 10 mM KH_2PO_4 (pH 6.4).

Upon pre-germination (for 1 h at RT), 20 µl of the suspension were dropped on leaves of about 5-weeks-old *Arabidopsis* plants. Plants were further cultivated under normal growth conditions, covered with a plastic cap. *B. cinerea* symptoms were evaluated 4 dai.

PDA medium		Gamborgs B5-medium	
PDA	19.5 g	Gamborgs B5	0.16 g
instant mashed potatoes	6.25 g	glucose (2%):	1 g
ad H_2O dest. 500 ml		ad H_2O dest. 50 ml	

2.4.2   Characterization of *PHB2*, *HAP6*, and *CYP83A1* mutants

To investigate the expression level of target genes in the respective SALK-lines (table 2.3), semi-quantitative two-step RT-PCR was conducted. Total RNA was extracted from frozen plant material using the NucleoSpin® RNA II kit (Macherey-Nagel GmbH & Co. KG, Düren, Germany). cDNA synthesis was primed with oligo (dT) using RevertAid™ Reverse Transcriptase (Fermentas GmbH, St. Leon-Rot, Germany). Equal cDNA loading was confirmed by the amplification of *18S* rRNA using the primers 5'-CTTCACCGGATCATTCAATCGG-3' and 5'-CGCGCGCTACACTGATGTATT-3'. *PHB2* expression was analyzed by using the primers 5'-GGATCCAAATCCTACCATCGCC-3' and 5'-GTTGCTTCTTAGGCTCCA-3'. *HAP6* was amplified by PCR using the primers 5'-GGGATCCTCTTCGACTATACGGA-3' and 5'-CGAGCAGATTTCAACTT-3', and *CYP83A1* by using the primers 5'-ATTAAGGAGCTTTGCTG-3' and 5'-CAGAATACACTGGAGGA-3'.

2.4.3   Staining methods

To analyze the number of conidiophores per colony, leaves were discolored, stored in 50% glycerol, and stained with acetic ink, as previously described for staining epiphytical structures of *Bgh* (HÜCKELHOVEN and KOGEL 1998). Wheat germ agglutinin-tetramethylrhodamin (WGA-TMR, Invitrogen Molecular Probes GmbH Karlsruhe, Germany) was used to stain all fungal structures including haustoria. Discolored leaves were vacuum infiltrated with a staining solution, containing 10 µg WGA-TMR and 10 µg BSA per ml PBS, and were incubated over night in the staining solution at 4°C. Based on a protocol described by WOLTER et al. (1993), callose staining of WGA-TMR treated leaves was performed by using 0.05% (w/v) methyl blue in 0.067 M potassium phosphate buffer (pH 5.8). Vacuum was applied twice and leaves were stored in the staining solution over night at 4°C. Samples were observed via fluorescence-microscopy (Leica DM 1000). Red-fluorescence of WGA-TMR stained structures was detected with following filter settings: excitation filter BP 515-560, dichromatic mirror 580, and suppression filter LP 590. Methyl blue staining was detected using following filter settings: excitation filter BP450-490, dichromatic mirror 510, and suppression filter LP 515.

In order to assess cuticle permeability, calcofluor white staining was performed as described by BESSIRE et al. (2007). The incubation time was set to 30 sec. Calcofluor white was detected via fluorescence-microscopy using following filter settings: excitation filter BP450-490, dichromatic mirror 510, and suppression filter LP 515. To image cell walls, leaves were stained with mPS-PI, and detected via CLSM (TRUERNIT et al. 2008). DAB (3,3'-diaminobenzidine) staining was performed to visualize H_2O_2 accumulation (THORDAL-CHRISTENSEN et al. 1997).

2.4.4   AAL-toxin treatment

A cell death assay was performed by using AAL toxin as described above (chapter 2.1.3). Besides this drop application of AAL toxin, a further assay was performed, were 50 µl of a 100 µM AAL toxin solution were infiltrated into the lower leaf side of about 5-weeks-old *Arabidopsis* plants.

2.4.5 Co-localization of AtBI-1-GFP and PHB2-RFP in tobacco cells

Cloning of an AtBI-1-GFP fusion construct started with the amplification of the *AtBI-1* (At5g47120) coding sequence by PCR using the primers 5'-GGATCCATGGATGCGTTCTCTTCC-3' and 5'-GTTTCTCCTTTTCTTCTTC-3', which eliminated the stop codon, and subsequent cloning of the fragment into the internal *Sma*I site of pGY-1. ORF of *GFP* was amplified using the primers 5'-CCATGGTGAGCAAGGGCGAG-3' and 5'-TCATTTGTACAGCTCGTCCAT-3' and cloned in frame into pGY-1-AtBI-1 by using the internal *Pst*I site behind *AtBI-1* by blunt-end ligation, resulting in pGY-1-AtBI-1-GFP.

*PHB2 (*At1g03860) coding sequence was isolated by PCR using the primers 5'-GGATCCAAATCCTACCATCGCC-3' and 5'-GTTGCTTCTTAGGCTCCA-3', eliminating the stop codon, cloned into pGEM-T and subcloned into pGY-1 using the internal *BamH*I/*Sal*I site. *RFP* (AAS78495) amplification was performed using the primers 5'-CCCGGGGGATGGTGCGCTCCTCCA-3' and 5'-CCCGGGCTACAGGAACAGGT-3' and was inserted in frame into the *Spe*I site of pGY-1-PHB2 by blunt-end ligation.

AtBI-1-GFP, RFP, and PHB2-RFP expression cassettes were subcloned by *EcoR*I digestion of pGY-1 constructs into the internal *Hind*III site of the modified binary vector pBI101+ (PRÖLS and ROITSCH 2009), lacking the coding sequence of GUS.

A. tumefaciens strain LBA4404 was transformed using the freeze-thaw method described by WEIGEL and GLAZEBROOK (2006). Analogous to YANG et al. (2000), single transformed *A. tumefaciens* colonies were cultivated in induction medium over night until an OD_{600} of 1 was archived. *A. tumefaciens* were harvested, and leaf-segments of about 5-weeks-old tobacco plants were co-transformed with pBI101+-AtBI-1-GFP and pBI101+-RFP or pBI101+-PHB2-RFP by infiltration of respective *A. tumefaciens* cultures mixed 1:1 (YANG et al. 2000)*.

After agroinfiltration, tobacco plants were further cultivated in a growth chamber at 22°C and a photoperiod of 16 h for 5 days until sequential CLSM was conducted. AtBI-1-GFP was excited by a 488 nm laser line and detected at 505-530 nm. RFP and PHB2-RFP were excited by a 561 nm laser line and detected at 580-650 nm.

2.4.6 Co-localization of AtBI-1-GFP and CYP83A1-mCherry or HAP6-mCherry in *Arabidopsis* epidermal cells

The genomic sequence of *CYP83A1* (At4g13770) lacking the stop codon was isolated by PCR using the primers 5'-<u>GGGATCC</u>ATTAAGGAGCTTTGCTG-3' and 5'-TTAGCTGATACTTGTTCAC-3' and cloned into pGEM-T. Subcloning of *CYP83A1* into pGY-1 was performed by using the internal *BamH*I/*Sal*I site. *mCherry* was amplified by PCR using the primers 5'-AA<u>ACTAGT</u>TATGGTGAGCAAGGGCGAG-3' and 5'-AA<u>GCATGC</u>TCATTTGTACAGCTCGTCCAT-3', and cloned in frame behind *CYP83A1* into the internal *Spe*I/*Sph*I site of pGY-1-CYP83A1, resulting in pGY-1-CYP83A1-mCherry.

The ORF of *HAP6* (At4g21150) was isolated by PCR using the primers 5'-G<u>GGATCC</u>TCTTCGACTATACGGA-3' and 5'-CGAGCAGATTTCAACTT-3', eliminating the stop codon. The sequence was directly cloned into pGEM-T and subcloned into the *BamH*I/*Sal*I site of pGY-1, resulting in pGY-1-HAP6. By using the primers 5'-AA<u>GCGGCCGC</u>AATGGTGAGCAAGGGCGAG-3' and 5'-AA<u>GCATGC</u>TCATTTGTACAGCTCGTCCAT-3' *mCherry* was amplified and cloned into the internal *Not*I/*Sph*I site of pGY-1-HAP6, resulting in pGY-1-HAP6-mCherry.

Via particle bombardment, pGY-1-GFP or pGY-1-AtBI-1-GFP (chapter 2.4.5) was transiently transformed into *Arabidopsis* epidermal cells together with pGY-1-CYP83A1-mCherry or pGY-1-HAP6-mCherry, respectively. For this, tungsten particles were coated with 1 µg per shot of each appropriate plasmid, and delivered into *Arabidopsis* epidermal cells using a Particle Inflow Gun (FINER et al. 1992). 1 day after transient transformation, the localization of the fusion proteins was analyzed by CLSM using the sequential scanning modus to avoid channel cross-talk. GFP and AtBI-1-GFP were excited by a 488 nm laser line and detected at 505-530 nm. CYP83A1-mCherry and HAP6-mCherry were excited by a 561 nm laser line and detected in a spectral range between 580-650 nm.

2.4.7 Functional analysis of barley homologs of AtBI-1-interacting candidate proteins

To functionally analyze barley homologs of AtBI-1-interacting candidate proteins in the interaction of barley with *Bgh*, a transient transformation assay was conducted as

already described in chapter 2.1.5. For this, overexpression constructs as well as TIGS constructs were cloned.

For overexpression constructs, the ORF of *HvGPI* (BAK07917) was amplified by PCR using the primers 5'-<u>GGATCC</u>TTTGAGATCTGCCACTGA-3' and 5'-ACCCAAAATCACATGACG-3', the coding sequence of *HvVHA-A* (BAB18682) by using the primers 5'-<u>TCTAGA</u>CATGGCGCACGGCGACCG-3' and 5'-GGCCATACACAACGT-3', the ORF of *HvMYHC* (BAJ97759) with the primers 5'-<u>GGATCC</u>TTGGGTTACAGGAGGC-3' and 5'-TCTGCAACCCTAGATGG-3', and the coding sequence of *HvPHB2* (BAK00720) by using the primers 5'-<u>GGATCC</u>CGAGATGAACTTCAAGGG-3' and 5'-GCGTGACAGGAAACG-3'. Isolated sequences were cloned into pGEM-T and subcloned into pGY-1 using the *BamH*I/*Sal*I site, except for *HvVHA-A*, where the *Xba*I/*Sal*I site was used.

For TIGS, a 1,483 bp *HvHAP6* (BAJ85530) fragment was amplified by PCR using the primers 5'-<u>GGATCC</u>CGTCTATGATAGGAGTCG-3' and 5'-TCCTTCGCATCTTCAC-3', ligated into the Gateway® pENTR vector pIPKTA38 in anti-sense orientation and subcloned into the final RNAi Gateway® destination vector pIPKTA30N by standard LR reaction (DOUCHKOV et al. 2005). The same cloning procedure was used to clone the coding sequence of *HvPHB2* (see above) into pIPKTA30N. To create the RNAi construct pIPKTA30N-HvMYHC, pGY-1-HvMYHC was *Bgl*II digested, and the resulting *HvMYHC* fragment was cloned into pIPKTA30N as described for *HvHAP6*. The final TIGS constructs contained respective fragments as inverted repeats under the control of the CaMV *35S* promoter, separated by the second intron of the wheat *RGA2* gene (DOUCHKOV et al. 2005).

All cloned constructs were ballistically delivered into epidermal cells of barley cv. Ingrid leaf segments using a PDS-1000/He particle gun with hepta-adapter (see chapter 2.1.5). 236 µg 1 µm gold particles were coated with 1 µg per shot pGY-1-GFP as transformation marker together with 1 µg of the respective test plasmid, or corresponding empty vector plasmid. Leaf segments were inoculated with a density of about 150 *Bgh* conidia per mm^2 1 day after bombardment, and were microscopically analyzed after 2 further days. PE was calculated as described above (chapter 2.1.5).

3 Results

3.1 Investigations on the role of BI-1-like LFG proteins during biotic and abiotic stress

LFG proteins are predicted to possess seven transmembrane domains, as described for the ancient cell death inhibitor BI-1 (REIMERS et al. 2006, HU et al. 2009). Moreover, in mammals, several LFG proteins are involved in the prevention of apoptosis (HU et al. 2009). Due to this structural and functional similarity to BI-1, I studied LFG proteins concerning their impact during biotic stress, primarily in plant - powdery mildew interactions. In barley (*Hordeum vulgare*) and *Arabidopsis thaliana*, five LFG proteins exist according to *in silico* analysis (YAMAGAMI et al. 2009, R. Eichmann, TUM, personal communication). In this work, the function of HvLFG1 (TA49291_4513), AtLFG1 (At4g14730), and AtLFG2 (At3g63310) in biotic and abiotic stress responses was investigated.

3.1.1 Functional analysis indicate HvLFG1 as a potential susceptibility factor towards *Bgh*

HvLFG1 has high structural similarity to HvBI-1 (supplementary figure 1) and both proteins share the PFAM *Bax1-I* motif (PF01027), whereas the amino acid sequences have only 16% identity. To analyze weather HvLFG1 has an impact on the interaction of barley with *Bgh* as HvBI-1, *HvLFG1* was transiently overexpressed and silenced in susceptible barley cv. Ingrid epidermal cells. Leaf segments were inoculated with *Bgh* conidia 24 h after ballistic transformation and microscopically analyzed 2 days later.

In five independent experiments, the transient overexpression of *HvLFG1* resulted in a significantly enhanced penetration efficiency (PE) of *Bgh* compared to the empty vector control. The PE shifted from 37.6 ± 3.0% SE in control cells to 60.2 ± 7.9% SE in *HvLFG1* overexpressing cells. The relative deviation of PE from the average control was 60.1 ± 6.9% SE (fig. 3.1A). Vice versa, transient-induced gene silencing (TIGS, DOUCHKOV et al. 2005) of *HvLFG1* significantly reduced the penetration success of *Bgh* into barley epidermal cells from 37.2 ± 3.0% SE to 30.2 ± 3.3% SE. Hence, the relative deviation of PE from the average control was -18.8 ± 8.9% SE (fig. 3.1A). Data base on six independent experiments.

The efficiency of the *HvLFG1* RNAi construct to silence *HvLFG1* expression was proved by its ability to knock-down the expression of a co-transformed *GFP-HvLFG1* fusion construct in barley cv. Ingrid epidermal cells. In three independent experiments, control cells, co-bombarded with pGY-1-RFP, pGY-1-GFP-HvLFG1, and the empty RNAi vector pIPKTA30N showed 92.2 ± 4.6% SE co-expression of *GFP-HvLFG1* and *RFP*, which served as an independent transformation marker. In contrast, co-transformation with pIPKTA30N-HvLFG1 resulted in a significantly reduced co-expression of *GFP-HvLFG1* and *RFP* to 14.3 ± 2.3% SE (fig. 3.1B). This confirmed the functionality of the *HvLFG1* RNAi construct.
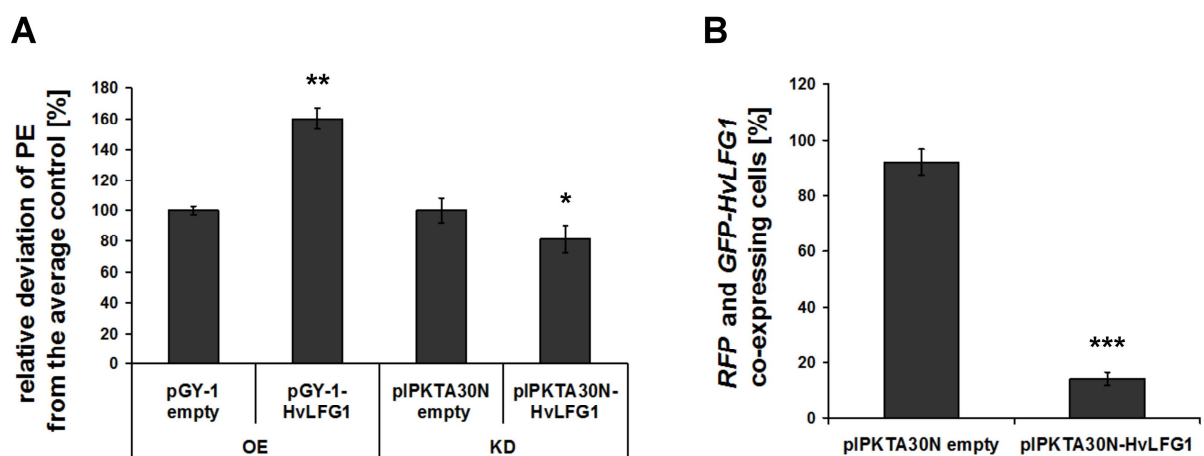
Fig. 3.1: Overexpression of *HvLFG1* induces supersusceptibility to *Bgh*, while the knock-down of *HvLFG1* expression reduces the penetration success of the fungus. A *HvLFG1* was transiently overexpressed (OE) or knocked-down (KD) in barley epidermal cells by particle bombardment. Respective empty vectors served as control. GFP was co-delivered as transformation marker. Leaf segments were inoculated with *Bgh* 1 day after bombardment (dab) and microscopically analyzed 1 dai. Columns belonging to the OE experiment represent means of five independent experiments, columns belonging to the KD experiment represent means of six independent experiments. The relative deviation of penetration efficiency (PE) from the average control is displayed, in which the control was set to 100%, respectively. **B** The functionality of the RNAi construct pIPKTA30N-HvLFG1 was evaluated in three independent experiments. Barley cv. Ingrid cells were co-bombarded with pGY-1-RFP, pGY-1-GFP-HvLFG1, and empty pIPKTA30N as control or pIPKTA30-HvLFG1. 2 dab, RFP expressing cells were analyzed concerning an additional presence of GFP-HvLFG1 expression. **A, B** Bars represent standard errors; *, **, and *** indicate significance at $P < 0.05$, 0.01, and 0.001 respectively, according to Student's *t* test.

HvBI-1 overexpression breaks *mlo*-mediated resistance to *Bgh* (HÜCKELHOVEN et al. 2003). To elucidate whether *HvLFG1* overexpression can also overcome *mlo*-mediated resistance to *Bgh*, *HvLFG1* was transiently overexpressed in BCPallas-*mlo5*. In contrast to *HvBI-1*, *HvLFG1* overexpression did not break *mlo*-mediated resistance to *Bgh* (data not shown).

Nevertheless, HvLFG1 seems to be functionally related to HvBI-1 since the transient overexpression enhanced the susceptibility to *Bgh*, while the knock-down reduced the penetration success of the fungus. This renders HvLFG1 a potential susceptibility factor towards *Bgh*.

3.1.2 Subcellular localization of a GFP-HvLFG1 fusion protein

HvLFG1 is predicted to be localized in the tonoplast, in the plasma membrane (PM), and/or in Golgi organelles, according to WoLF PSORT (http://wolfpsort.org/, Horton et al. 2007). To elucidate the actual subcellular localization of HvLFG1, I delivered a GFP-HvLFG1 fusion construct into barley cv. Ingrid epidermal cells via particle bombardment. GFP-HvLFG1 accumulated in the PM 2 days after bombardment (dab, fig. 3.2A), which could be confirmed by the initiation of plasmolysis by the application of 20% glycerol, resulting in readily identifiable Hechtian strands (fig. 3.2B). An additional localization in small dots and around the nucleus was visible. The number of the dots and the accumulation intensity around the nucleus varied. In fig. 3.2A a typical cell is displayed. To investigate whether these vesicle-like structures, which moved along the cytoplasmic strands, were Golgi-associated, barley cells were co-transformed with GFP-HvLFG1 and the cis-Golgi marker soybean α-1,2-MANNOSIDASE (GmMAN1)-RFP (Yang et al. 2005). No co-localization of the GFP-HvLFG1-labeled dots with Golgi organelles was visible (data not shown).

In order to examine the GFP-HvLFG1 accumulation in the barley-*Bgh* interaction, I inoculated transformed leaf segments 1 dab. An additional accumulation of GFP-HvLFG1 around small evolving haustoria appeared in successfully penetrated cells, 1 dai. 2 dai, GFP-HvLFG1 still accumulated around the full-developed haustoria, but additionally, big moving bubble- and tube-like structures appeared (fig. 3.2D), reminiscent of tonoplast-like localization (Reisen et al. 2005, Higaki et al. 2006). In incompatible interactions, GFP-HvLFG1 localization was predominant in the PM. An additional weak accumulation was observed at the site of non-successful attempted penetration (fig. 3.2E).

Furthermore, a functional analysis was conducted to confirm the capacity of *GFP-HvLFG1* overexpression to enhance the PE of *Bgh* in the interaction with barley epidermal cells as shown for *HvLFG1* overexpression (chapter 3.1.1).
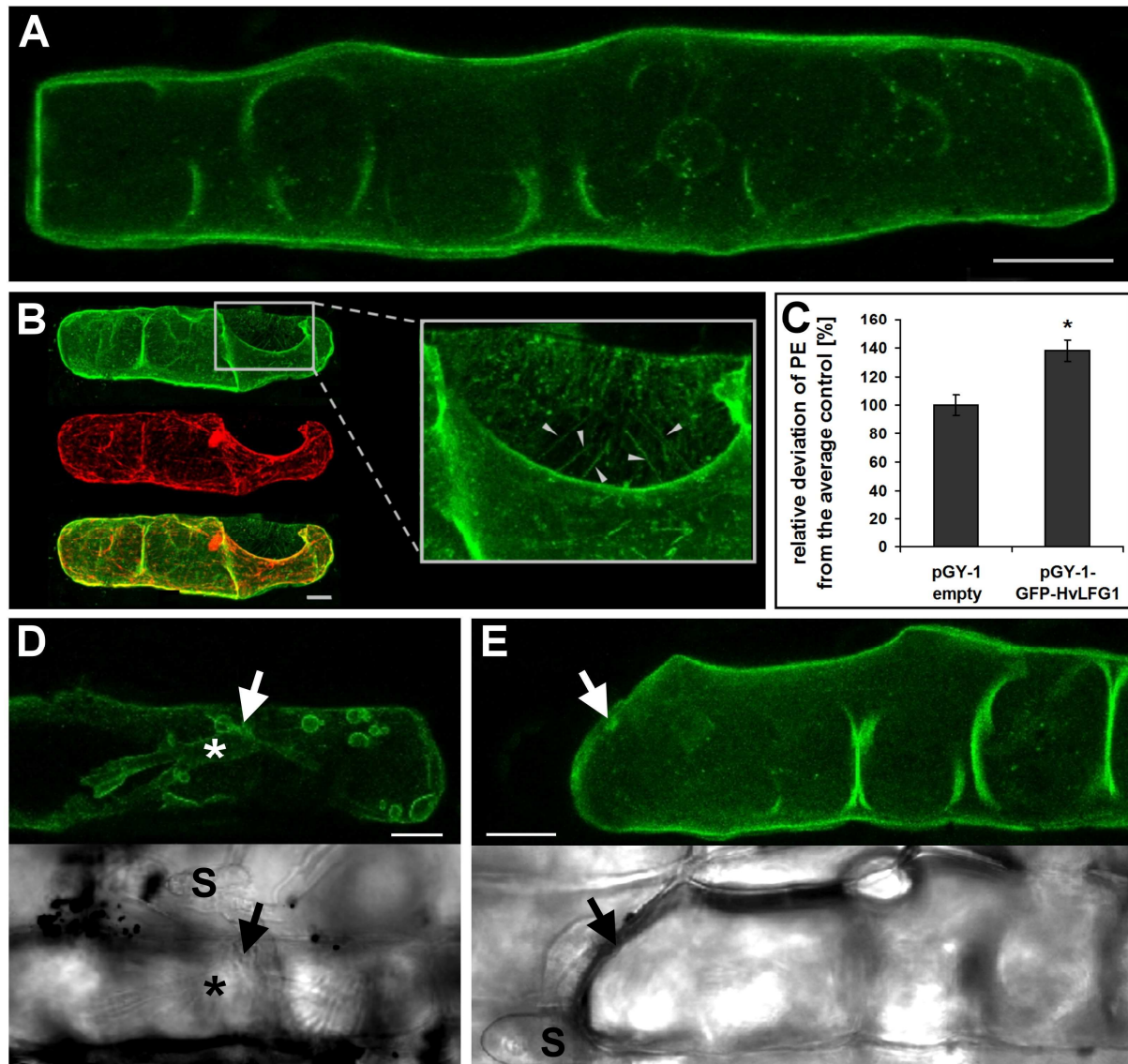
Fig. 3.2: Localization and functional analysis of a GFP-HvLFG1 fusion protein in barley epidermal cells. A, B, D, E A *GFP-HvLFG1* overexpression construct was transiently transformed into barley epidermal cells via particle bombardment and fluorescence was visualized by confocal laser scanning microscopy (CLSM). Scale bars = 20 µm. **A** Whole cell projections of a transformed cell illustrate typical patterns of GFP-HvLFG1 accumulation 24 hab. **B** Confirmation of PM localization of GFP-HvLFG1 by plasmolysis. Cytosolic and nucleoplasmic localization of RFP (in red) and the merge channel are illustrated as well. In the magnified detail, Hechtian strands are marked with arrowheads. **D, E** Localization of a GFP-HvLFG1 fusion protein in the barley - *Bgh* interaction. Lower panels illustrate the transmission channel, respectively, to visualize the fungal structures. Spores (S), sites of attempted penetration (arrows), and a haustorium (asterisk) are indicated. **D** Localization of GFP-HvLFG1 in a penetrated cell 2 dai with *Bgh*. **E** GFP-HvLFG1 accumulation in a non-penetrated cell 1 dai. **C** To investigate the functionality of the GFP-HvLFG1 construct in mediating supersusceptibility towards *Bgh*, barley cv. Ingrid leaf segments were co-bombarded with pGY-1-HvLFG1 or empty pGY-1 as control. RFP served as transformation marker. Leaf segments were inoculated 1 dab and microscopic analysis took place 2 dai. The relative deviation of PE from the average control, which was set to 100%, is represented. Mean values of three independent experiments are displayed. Bars represent standard errors; * indicates significance at $P < 0.05$ according to two-sided paired Student's *t* test.

Transient overexpression of *GFP-HvLFG1* in barley cv. Ingrid epidermal cells resulted in significantly enhanced PE of *Bgh.* From 43.7 ± 3.1% SE in control cells, which were transformed with the empty vector pGY-1, the PE of *Bgh* raised to 60.2 ± 3.2% SE in *GFP-HvLFG1* overexpressing cells, resulting in a relative deviation of PE from the average control of 37.8 ± 7.4% SE, indicating the functionality of the GFP-HvLFG1 construct in mediating supersusceptibility towards *Bgh* (fig. 3.2C).

3.1.3 The function of LFG proteins seems to be conserved in plant - powdery mildew interactions

3.1.3.1 Heterologous expression of *Arabidopsis LFG* genes in barley

To investigate the potential function of *Arabidopsis thaliana* homologs of LFG proteins in the interaction with powdery mildew fungi, I conducted a heterologous transient overexpression experiment in barley. *AtLFG1* or *AtLFG2* overexpression constructs were transiently delivered into barley cv. Ingrid epidermal cells by means of ballistic transformation. The overexpression of *AtLFG1* in barley epidermal cells did not significantly alter the PE of *Bgh* compared to empty vector control cells. The PE was slightly enhanced from 36.4 ± 3.4% SE in control cells to 40.4 ± 2.4% SE in *AtLFG1* overexpressing cells. The relative deviation of PE from the average control was 11 ± 6.7% SE (fig. 3.3A).

Fig. 3.3: Functional analysis of *AtLFG1* and *AtLFG2* in the interaction of barley with *Bgh*. Via ballistic transformation **A** *AtLFG1* and **B** *AtLFG2* were heterologously overexpressed in barley epidermal cells together with *GFP* as transformation marker. Leaf segments were inoculated 4 h and 1 dab, respectively. The relative deviation of PE from the average control was calculated 2 dai. Columns present means of five independent experiments, respectively. Bars represent standard errors; *** indicate significance at *P* < 0.001 according to two-sided paired Student's *t* test.
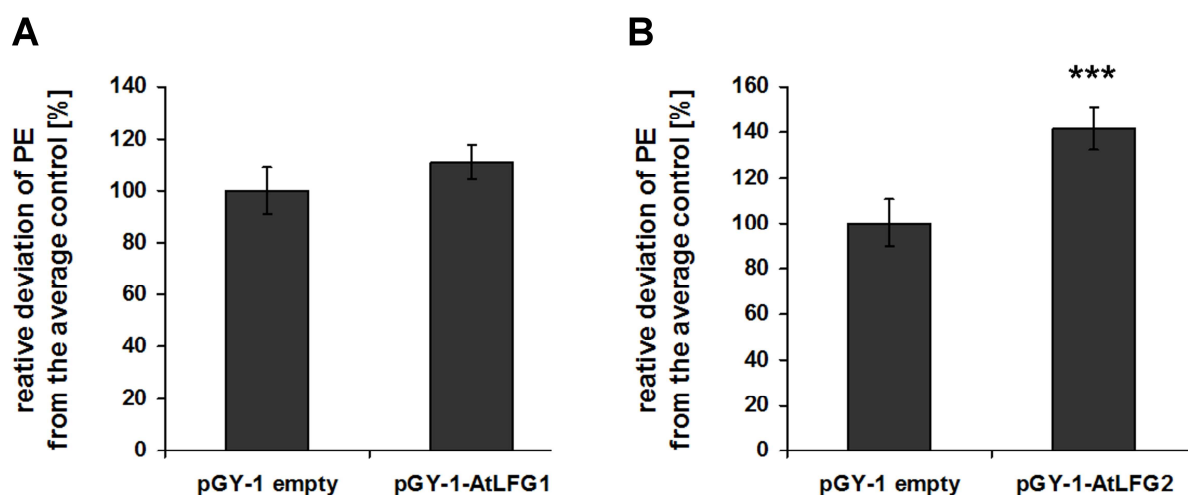
In contrast, the heterologous overexpression of *AtLFG2* significantly enhanced susceptibility of barley epidermal cells to *Bgh*. Here, the PE of *Bgh* changed from 42.2 ± 4.4% SE in empty vector control cells to 59.8 ± 4.0% SE in *AtLFG2* overexpressing cells, resulting in a relative deviation of PE from the average control of 41.7 ± 9.4% SE (fig. 3.3B). Like HvLFG1 (chapter 3.1.1), AtLFG2 enhanced susceptibility to *Bgh* when overexpressed in barley epidermal cells, which indicated a conserved function of LFG proteins in plant - powdery mildew interactions.

3.1.3.2 *E. cruciferarum* development is affected on *Arabidopsis LFG* mutants

Since *Arabidopsis* LFG proteins seemed to be involved in the interaction of plants with powdery mildew fungi (chapter 3.1.3), their role in the pathosystem *Arabidopsis - E. cruciferarum* should be assessed. Therefore, I ordered appropriate *AtLFG1* and *AtLFG2* T-DNA insertion lines (table 2.1). PCR analysis confirmed positions of T-DNA insertions, described in TAIR (supplementary figure 2). Both *AtLFG1* SALK-lines, SALK_147263C and SALK_111590, carry their T-DNA insertion in the promoter region. The T-DNA position in the *AtLFG2* SALK-line SALK_052507C is located in the 3'UTR. Furthermore, I assessed the expression level of *AtLFG1* and *AtLFG2* in the wild type Col-0 and in respective *AtLFG* T-DNA insertion lines by amplifying full-length sequences using semi-quantitative RT-PCR. Public expression data analyzed in Genevestigator (http://genevestigator.com/, ZIMMERMANN et al. 2004) indicate a generally low expression of *AtLFG1* and a considerably high expression of *AtLFG2* in *Arabidopsis* leaves (supplementary figure 3). Regarding *AtLFG1*, I also observed a very low expression level in wild type Col-0, as expected. *AtLFG1* T-DNA insertion line SALK_147263C turned out to be a knock-out mutant, since no *AtLFG1* could be amplified by PCR. *AtLFG1* T-DNA insertion line SALK_111590, showed a strongly reduced *AtLFG1* expression, indicating this mutant as a knock-down mutant (fig 3.4B). As predicted, expression of the *AtLFG2* coding sequence turned out to be quite high in Col-0, while no expression could be detected at all in the *AtLFG2* T-DNA insertion line SALK_ 052507C, indicating this mutant as a real knock-out mutant (fig 3.4B). From here on, *AtLFG1* T-DNA insertion lines SALK_147263C and SALK_111590 are named *Atlfg1-1* and *Atlfg1-2*, respectively, and *AtLFG2* T-DNA insertion line SALK_ 052507C is named *Atlfg2*.

I inoculated *Atlfg1-1*, *Atlfg1-2,* and *Atlfg2* mutants with *E. cruciferarum* and analyzed them macroscopically as well as microscopically. In three independent experiments,

there were no obvious differences in powdery mildew symptom development on the *Atlfg1* and *Atlfg2* mutants compared to Col-0 at 9 dai (supplementary figure 4). However, on all analyzed *Atlfg* mutants, the fungal development was reduced at 5 dai, as measured by the number of conidiophores per colony (c/c). *E. cruciferarum* developed 30 ± 3 SE c/c on Col-0 and significantly reduced numbers of c/c on both knock-out mutants, *Atlfg1-1* (14 ± 1 SE c/c) and *Atlfg2* (15 ± 4 SE c/c). On the *Atlfg1-2* knock-down mutant I observed 18 ± 5 SE c/c (fig. 3.4A).
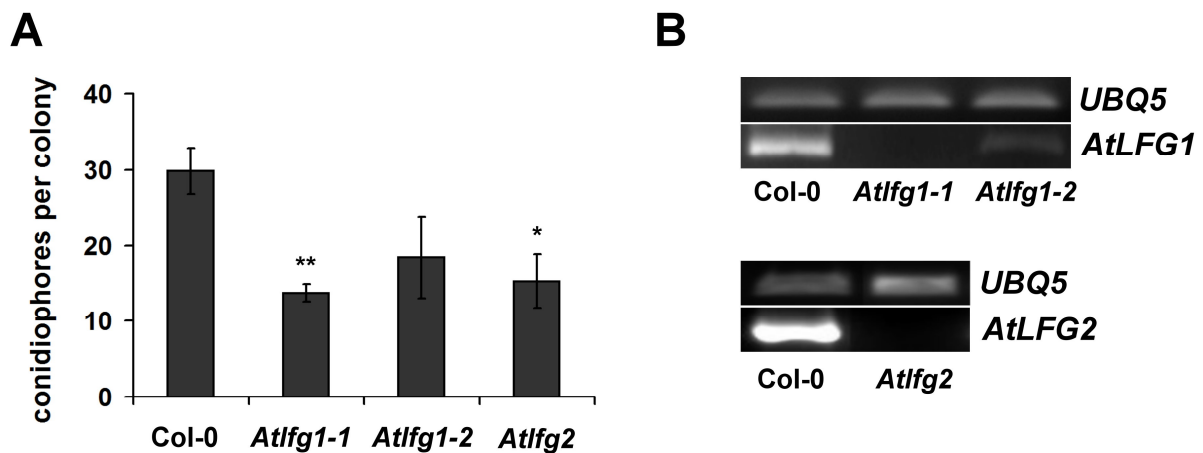
Fig. 3.4: Development of *E. cruciferarum* is reduced on *Atlfg* mutants. A 5-weeks-old Col-0 and *Atlfg* mutant plants were inoculated with 3-5 *E. cruciferarum* spores per mm^2. Leaves were harvested 5 dai, discolored and stained with acetic ink for subsequent microscopic analysis. Conidiophores per colony (c/c) were counted on five individual plants per mutant. 50 colonies per line were evaluated. Columns represent mean values, bars represent standard errors, * and ** indicate significance at $P <$ 0.05 and 0.01, respectively, according to two-sided unpaired Student's *t* test, calculated over the mean values of c/c on the single plants. The experiment was repeated twice with similar results. **B** Expression of *AtLFG1* and *AtLFG2* in respective SALK-lines and in wild type Col-0. Gel photographs after ethidium bromide staining of semi-quantitative RT-PCR products are shown. Upper panel illustrates *AtLFG1* expression in wild type Col-0, *Atlfg1-1* (SALK_147263C), and *Atlfg1-2* (SALK_111590). Lower panel shows *AtLFG2* expression in Col-0 and in *Atlfg2* (SALK_ 052507C). Amplification of *UBIQUITIN 5* (*UBQ5*) served as control for constitutive gene expression.

Furthermore, I created stable *AtLFG1* and *AtLFG2* overexpressing (OE) *Arabidopsis* mutants by *A. tumefaciens*-mediated transformation. Expression of *AtLFG1* and *AtLFG2* was controlled by the strong constitutive CaMV 35S promoter. Elevated expression of the respective full-length *AtLFG* coding sequences was confirmed by semi-quantitative RT-PCR (fig 3.5B). I inoculated OE and empty vector-carrying mutants with *E. cruciferarum*. Subsequently, the fungal development was evaluated by means of counting c/c 5 dai. On *AtLFG1* as well as on *AtLFG2* OE mutants, *E. cruciferarum* showed a significantly accelerated development compared to Col-0.

The amount of c/c raised from 19 ± 1 SE on empty vector control plants to 37 ± 2 SE on *AtLFG1* OE, and to 51 ± 7 SE on *AtLFG2* OE (fig.3.5A).

A

B
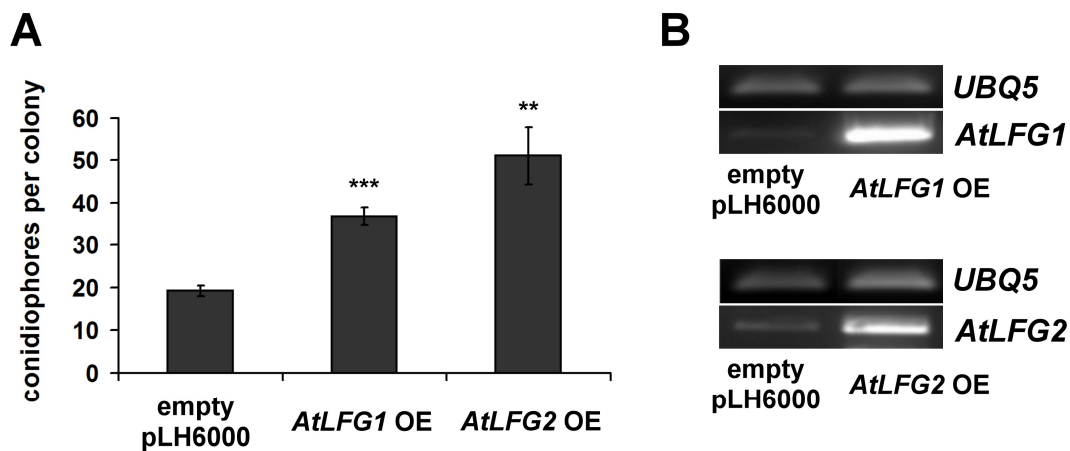
Fig. 3.5: Accelerated *E. cruciferarum* development on *AtLFG* overexpressing mutants. A *AtLFG1* and *AtLFG2* overexpressing (OE) mutants were created via *A. tumefaciens*-mediated transformation. 5-weeks-old *AtLFG* OE mutant plants and control plants, carrying the empty vector pLH6000, were inoculated with 3-5 *E. cruciferarum* spores per mm^2. Leaves were harvested 5 dai, discolored and stained with acetic ink for subsequent microscopic analysis. Conidiophores per colony (c/c) were counted on five individual plants per mutant. 50 colonies per line were evaluated. Columns represent mean values, bars represent standard errors; ** and *** indicate significance at *P* < 0.01 and 0.001, respectively, according to two-sided unpaired Student's *t* test, calculated over the mean values of c/c of the single plants. The experiment was repeated twice with similar results. **B** Expression of *AtLFG1* and *AtLFG2* in respective mutants and in wild type Col-0. Gel photographs after ethidium bromide staining of semi-quantitative RT-PCR products are shown. Upper panel illustrates *AtLFG1* expression in wild type Col-0 and in the *AtLFG1* OE mutant. Lower panel shows *AtLFG2* expression in Col-0 and in the *AtLFG2* OE mutant. Amplification of *UBIQUITIN 5* (*UBQ5*) served as control for constitutive gene expression.

To summarize, *E. cruciferarum* development was affected on *AtLFG* mutants. *E. cruciferarum* developed significantly less conidiophores per colony on *Atlfg1* and *Atlfg2* knock-out mutants than on Col-0. Vice versa, a significantly enhanced conidiophore production was observed on *AtLFG1* and *AtLFG2* OE mutants. These results support a function of AtLFG1 and AtLFG2 as susceptibility factors in the *Arabidopsis - E. cruciferarum* interaction.

3.1.4 Subcellular localization of a GFP-AtLFG1 and a GFP-AtLFG2 fusion protein

WoLF PSORT predicts AtLFG1 and AtLFG2 to be localized in the PM, in the tonoplast, in the ER, and/or in the Golgi apparatus. The actual protein localization was investigated by ballistic delivery of GFP-AtLFG1 and GFP-AtLFG2 fusion constructs into *Arabidopsis* Col-0 epidermal cells. GFP-AtLFG1 localized in the PM, in cytoplasmic strands, and in punctate structures reminiscent of Golgi organelles. However, co-transformation studies with the Golgi marker GmMAN1-RFP (YANG et al. 2005) indicated no clear co-localization of GFP-AtLFG1 with Golgi organelles (fig. 3.6).
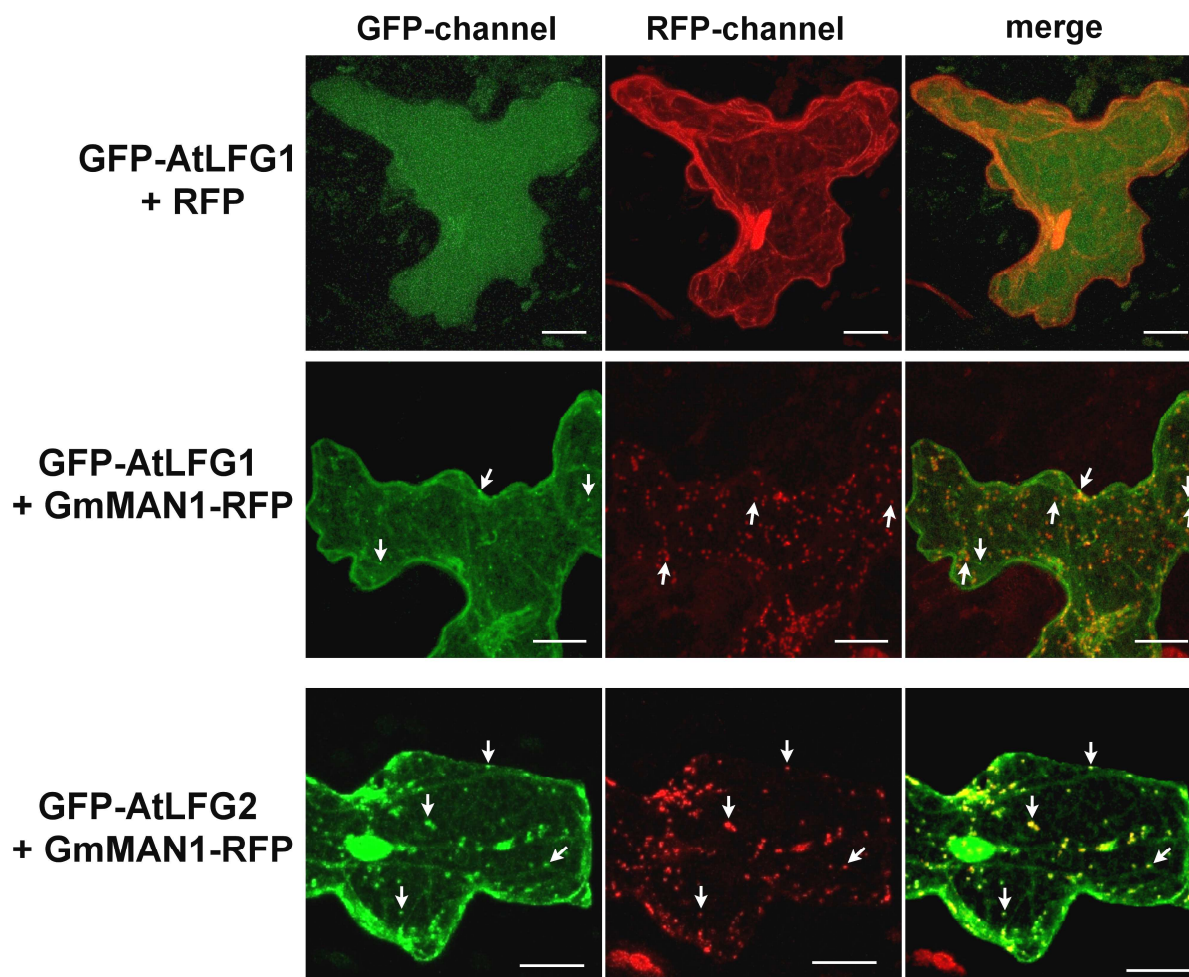
Fig 3.6: Localization of GFP-AtLFG1 and GFP-AtLFG2 fusion proteins. GFP-AtLFG1 and GFP-AtLFG2 constructs were ballistically delivered into *Arabidopsis* epidermal cells together with RFP or Golgi marker GmMAN1-RFP. Whole cell projections are displayed, imaged by CLSM 2 dab. Scale bars = 20 µm. Arrows mark punctate accumulation of GFP-AtLFG1, GFP-AtLFG2, and/or Golgi organelles. Yellow pixels in the merge image indicate co-localization.

Several other cells showed a diffuse, homogenously distributed GFP-AtLFG1 accumulation throughout the whole cell (fig. 3.6), presumably inside the vacuole. GFP-AtLFG2 was also detected in the PM, in cytoplasmic strands or in the ER, in punctate structures, and additionally in the nucleus. In contrast to GFP-AtLFG1, GFP-AtLFG2 co-localized with GmMAN1-RFP-labeld Golgi organelles (fig. 3.6).

3.1.5 *Atlfg* mutants are more sensitive to cell death inducing AAL toxin

AtBI-1 suppresses cell death reactions induced by various stimuli (KAWAI-YAMADA et al. 2004, WATANABE and LAM 2008). For instance, WATANABE and LAM (2006) showed accelerated cell death reactions in two *atbi-1* knock-out mutants upon treatment with the fungal toxin fumonisin B1 (FB1). To investigate the potential of AtLFG proteins in cell death inhibition, I treated *Atlfg1* and *Atlfg2* mutants with *Alternaria alternata* f.sp. lycopersici (AAL) toxin to induce cell death (LYNCH 1999, SPASSIEVA et al. 2002). All tested *Atlfg* mutants showed a tendency to enhanced accelerated cell death upon AAL toxin drop application. 9 days after treatment, 48 ± 17% SE of Col-0 leaves displayed AAL toxin-induced cell death symptoms (fig. 3.7). *Atlfg1-1* and *Atlfg1-2* mutants revealed symptoms on 75 ± 13% SE and 68 ± 16% SE of AAL toxin-treated leaves and *Atlfg2* mutant showed 60 ± 21% SE affected leaves (fig. 3.7). Distilled water treated control leaves showed no symptoms at all (data not shown). Infiltration of the AAL toxin gave basically the same results and confirmed accelerated cell death reactions in *Atlfg* mutants (data not shown).
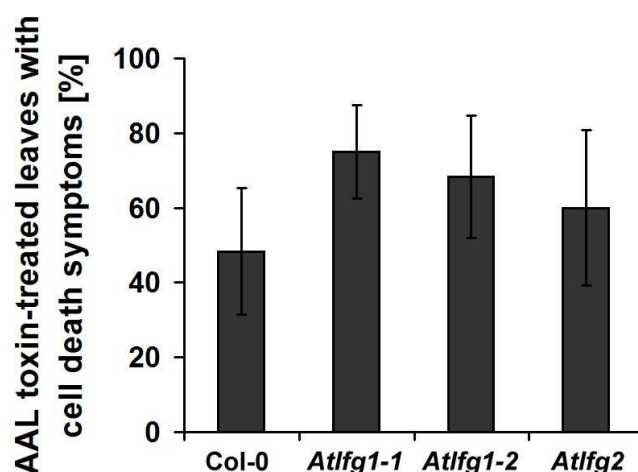
Fig. 3.7: *Atlfg* mutants are more sensitive to cell death inducing AAL toxin. Leaves of 5-weeks-old *Arabidopsis* WT Col-0 and *Atlfg* mutants were treated with 10 µl of a 100 µM AAL toxin solution. Evaluation of symptoms took place 9 days after drop application. Mean values of three independent experiments are displayed. Bars represent standard errors. No significant differences were observed using two-sided unpaired Student's *t* test.

Together, AtLFG1 and AtLFG2 seem to be involved in the inhibition of cell death reactions, as was shown for BI-1 proteins.

3.2 Investigation of putative components of BI-1-dependent signaling in susceptibility towards *Bgh*

To contribute to the understanding of BI-1-dependent signaling towards *Bgh* susceptibility, putative components of the signaling pathway were investigated. On the one hand, I assessed, whether BI-1 is part of MLO signaling, since *mlo5*-mediated resistance can be overcome by the overexpression of *HvBI-1* (HÜCKELHOVEN et al. 2003). On the other hand, I asked, whether CaM, a putative BI-1-interacting protein (IHARA-OHORI et al. 2007) is required for BI-1-mediated susceptibility towards *Bgh*.

3.2.1 Knock-down of *BI-1* expression by TIGS does not suppress supersusceptibility induced by *MLO* overexpression

Overexpression of *HvBI-1* compromises *mlo5*-mediated resistance to *Bgh* (HÜCKELHOVEN et al. 2003). To analyze whether supersusceptibility mediated by *MLO*-overexpression (SHIRASU et al. 1999) can be reduced by the knock-down of *BI-1*, a transient transformation assay was performed. For this, *MLO* was overexpressed during simultaneous knock-down of *BI-1* in epidermal cells of the resistant barley backcross line BCPallas-*mlo5*.

Control cells, transformed with the empty vector pGY-1 together with the TIGS construct pIPKTA30N-BI-1, showed a very low PE (2 ± 2% SE). As expected, overexpression of *MLO* significantly increased *Bgh* PE to 65 ± 4% SE. Simultaneous knock-down of *BI-1* expression did not affect *MLO*-overexpression-mediated supersusceptibility to *Bgh*. Here, the fungal PE reached 69 ± 5% SE (fig. 3.8A).

To examine the capacity of the *BI-1* RNAi construct to knock-down *GFP-BI-1* expression, I delivered pGY-1-GFP-BI-1 and either empty vector pIPKTA30N or pIPKTA30N-BI-1 into barley cv. Ingrid epidermal cells by transient transformation. *DsRED* served as transformation marker. DsRED fluorescing cells were analyzed concerning an additive GFP-BI-1 accumulation, 2 dab. While 78 ± 4% SE of DsRED expressing control cells displayed GFP-BI-1 expression as well, the delivery of the TIGS construct pIPKTA30N-BI-1 significantly reduced the amount of DsRED and GFP-BI-1 co-expressing cells to 31 ± 10% SE (fig. 3.8B).

A

B
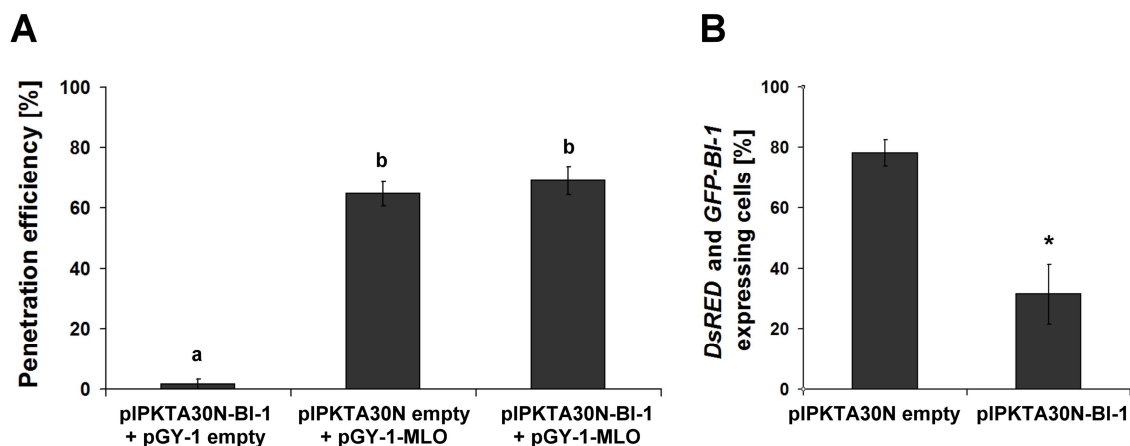
Fig. 3.8: Knock-down of *BI-1* expression does not affect supersusceptibility to *Bgh* mediated by *MLO*-overexpression. A Leaf segments of the *Bgh*-resistant barley backcross line Pallas-*mlo5* were ballistically co-transformed with the expression construct pGY-1-MLO together with either *BI-1* RNAi construct pIPKTA30N-BI-1 or empty vector pIPKTA30N. Control cells were co-bombarded with pIPTKTA30N-BI-1 and empty vector pGY-1. 2 days after transformation, leaves were inoculated with *Bgh* conidia and penetration efficiency was determined via microscopy 2 days later. Columns represent mean values of three independent experiments. Bars represent standard errors. Averages highlighted with the same letter are not statistically different at *P* < 0.05 according to two-sided paired Student's *t* test. **B** Barley cv. Ingrid leaf segments were co-bombarded with pGY-1-DsRED, pGY-1-GFP-BI-1, and TIGS vector pIPKTA30N-BI-1 or empty pIPKTA30N. 2 days after transformation, *DsRED*-expressing cells were analyzed for an additional GFP-BI-1 expression. Bars represent standard errors; * indicate significance at *P* < 0.05 according to two-sided unpaired Student's *t* test.

3.2.2 CaM is likely not required for HvBI-1-mediated susceptibility to *Bgh*

In barley, MLO was shown to interact with the cytoplasmic calcium sensor CaM, which contributes to full susceptibility towards *Bgh* (KIM et al. 2002a,b). In 2007, IHARA-OHORI and co-workers could demonstrate the interaction of CaM with AtBI-1. This interaction turned out to be crucial for the AtBI-1-mediated cell death suppression (KAWAI-YAMADA et al. 2009). To investigate whether CaM is required for HvBI-1-mediated susceptibility towards *Bgh*, a transient transformation assay was conducted, where *CaM* expression was knocked-down during simultaneous overexpression of *HvBI-1*.

While the PE increased from 37.7 ± 1.7% SE in control cells, co-transformed with the empty vector pIPKTA30N and empty vector pGY-1, to 53.7 ± 6.4% SE in *BI-1* overexpressing cells, the penetration success of *Bgh* was not reduced in cells where *CaM* expression was additionally silenced. Here, the PE reached 58.3 ± 7.9% SE (fig. 3.9).
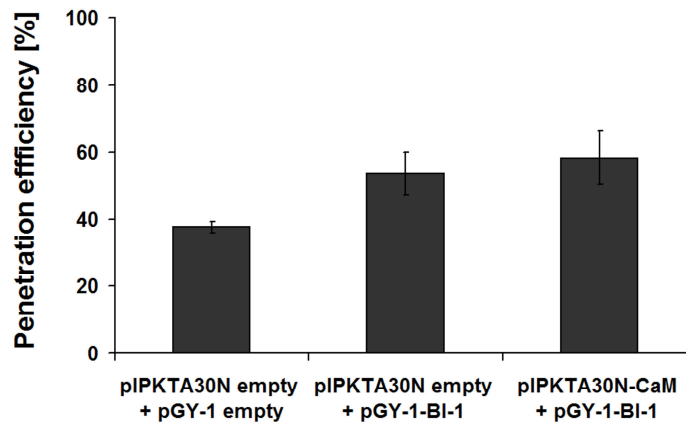
Fig. 3.9: CaM is likely not required for HvBI-1-mediated susceptibility to *Bgh*. Via particle bombardment, a *HvBI-1* overexpression construct was either co-delivered with the TIGS construct pIPKTA30N-CaM or empty vector pIPKTA30N. Control cells were co-transformed with both empty vectors. Leaf segments were inoculated with *Bgh* 24 hab and PE was assessed by microscopy 2 dai. GFP served as transformation marker. Mean PE of three independent experiments is displayed. Bars represent standard errors. No significant differences were observed using two-sided paired Student's *t* test.

I tested the efficiency of the *CaM* RNAi construct pIPKTA30N-CaM by the examination of its ability to knock-down the expression of *YFP-CaM* in cells expressing RFP, which served as reporter gene. Control cells, co-transformed with the empty RNAi vector pIPKTA30N and pGY-1-YFP-CaM showed 95% co-expression of RFP and YFP-CaM 2 dab. Replacing the empty vector with the *CaM* RNAi construct pIPKTA30N reduced the co-expressionrate to 10% (supplementary figure 5). The experiment was conducted only once.

Together, analysis of putative components of BI-1-mediated signaling in susceptibility to *Bgh* revealed that BI-1 most likely does not act as downstream factor of MLO, since simultaneous knock-down of *BI-1* expression did not affect *MLO* overexpression-mediated supersusceptibility to *Bgh*. Moreover, CaM is probably no essential components for BI-1-mediated signaling towards susceptibility to *Bgh*, since TIGS of *CaM* did not alter supersuceptibility to *Bgh* mediated by *BI-1*-overexpression.

3.3 Identification of putative AtBI-1-interacting proteins using a Co-immunoprecipitation assay

In order to further asses the operating mode of BI-1 as susceptibility factor towards powdery mildew fungi and as cell death suppressor, I established co-immunoprecipitation (co-IP) to identify new interaction partners of BI-1. Since heterologous transient overexpression of *AtBI-1* in barley epidermal cells resulted in enhanced susceptibility towards *Bgh*, a conserved function of BI-1 proteins in plant - powdery mildew interactions can be assumed (own unpublished results, Diploma thesis). Due to available molecular-biological tools, e.g. *AtBI-1-GFP* overexpressing *Arabidopsis* mutants (KAWAI-YAMADA et al. 2001) and corresponding GFP-tagged sepharose beads (GFP-TRAP A®, ROTHBAUER et al. 2008), the co-IP was carried out as follows: *AtBI-1-GFP* overexpressing *Arabidopsis* mutants as well as control plants, transformed with the empty overexpression vector pBin19 (KAWAI-YAMADA et al. 2001) served as starting material. Both *Arabidopsis* mutants were either non-inoculated or inoculated with adapted *E. cruciferarum* and non-adapted *Bgh*. I extracted total protein from a mixed sample of each variety. AtBI-1-GFP and putative interaction partners were co-immunoprecipitated using GFP-TRAP A®. Western blot analysis and silver staining visualized a successful AtBI-1-GFP immunoprecipitation (Fig. 3.10).
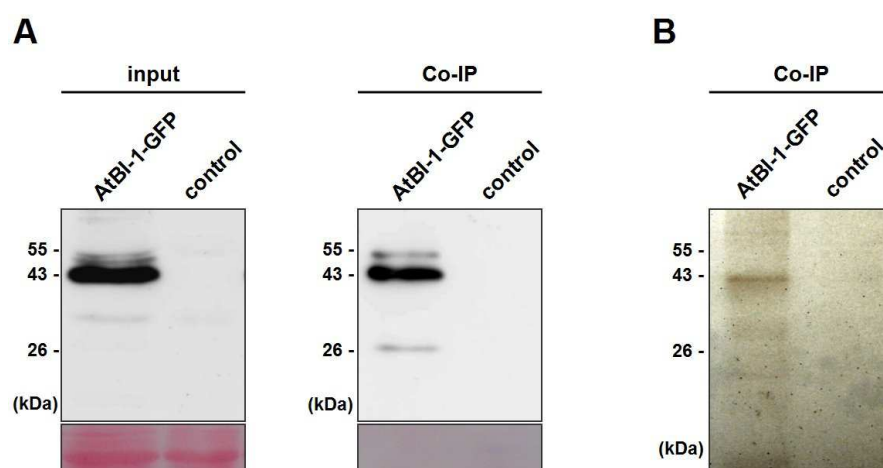
Fig. 3.10: Co-IP of AtBI-1-GFP and putative interacting proteins. I performed a co-IP by using GFP-TRAP A® (ROTHBAUER et al. 2008) and protein extracts of 4-weeks-old *Arabidopsis* leaves expressing AtBI-1-GFP or of control plant, transformed with the empty vector pBin19. **A** Total protein extracts (input, 50 µg) and co-immunoprecipitates (Co-IP, 15 µl) of both *Arabidopsis* mutants were separated by a 12% SDS-PAGE and analyzed by Western blotting using antibodies against GFP. Ponceau staining is displayed as loading control below each panel. **B** Total protein content was visualized by silver staining of a 12% SDS-PAGE, loaded with 5 µl of each co-immunoprecipitate.

The predicted molecular weight of AtBI-1-GFP is approximately 55 kDa (http://bioinformatics.org/sms/prot_mw.html). In the total protein extract of AtBI-1-GFP overexpressing *Arabidopsis* leaves as well as in the AtBI-1-GFP co-immunoprecipitate a predominant anti-GFP immunodetected band is visible at about 43 kDa in the Western blots. Preliminary characterization studies of human BI-1 showed that the protein was also running as a lower band on SDS gels than expected (COWLING and BIRNBOIM 1998). A less pronounced band is detectable at the predicted weight of about 55 kDa. Additionally, a weak band at about 27 kDa likely displayed a partial GFP-tag separation from the AtBI-1 protein in the co-immunoprecipitate. Control samples showed no anti-GFP-specific detection at all (fig 3.10A). Silver staining of the AtBI-1-GFP co-immunoprecipitate revealed a strong accumulation of a 43 kDa protein as well. The AtBI-1-GFP co-immunoprecipitate additionally showed a background smear indicating a generally higher protein amount, while no clear protein bands or protein smear were visible in the control (fig. 3.10B), indicating a successful co-IP.

LC-MS/MS was performed in cooperation with the chair of Proteomics and Bioanalytics (Prof. B. Küster, H. Hahne/F. Pachl, TUM) in order to identify precipitated proteins. The Mascot search result files were analyzed using Scaffold version 2.6.2 (Proteome Software Inc., Portland, OR, see chapter 2.3.3). Threshold parameters were set as follows: protein probability, 80 %; minimum number of peptides, 1; peptide probability, 80 %, yielding a false-discovery rate of 8.8% on the protein level and 7.0% on the peptide-spectrum match level.

In total, 168 proteins could be identified by searching against the whole NCBI database and against the NCBI database of viridiplantae. A search against the NCBI database of viridiplantae only, identified 127 proteins, of which 95 proteins were not identified in the control sample. These 95 AtBI-1-GFP co-immunoprecipitated proteins are listed in supplementary table 1, providing information on the representative NCBI hit, corresponding accession number, and the number of identified peptides. Moreover, supplementary table 1 provides information about the classification of the precipitated proteins (see below). One BI-1 peptide ((K)AHLGDMDYVK(H), AS 201-212) was identified, and search against the NCBI database exhibited an enrichment of GFP peptides in the AtBI-1-GFP co-immunoprecipitate, validating a successful AtBI-1-GFP precipitation.

I classified the 95 co-immunoprecipitated proteins in unknown (37%), chloroplast-associated (25%), energy/metabolism involved (21%), and nuclear trafficking proteins (3%). Proteins of diverse other functions were summarized as 'others' (14%), including AtBI-1 itself (see supplementary table 1).

Since during the plant - powdery mildew interplay the physical interaction is restricted to epidermal cells, I excluded all chloroplast-associated proteins from further examinations. AtBI-1-interacting candidates were selected predominantly according to their presumed BI-1-associated function and predicted subcellular localization. The following eight mostly membrane-associated AtBI-1-interacting candidate proteins were selected: HAPLESS 6 (HAP6), TRANSPORTIN 1 (TRN1), VACUOLAR H$^+$-ATPASES SYNTHASE SUBUNIT A (VHA-A), MYOSIN HEAVY CHAIN-RELATED (MYHC), CYTOCHROME P450 83A1 (CYP83A1, syn. REDUCED EPIDERMAL FLUORESCENCE 2 (REF2)), GLYCOSYLPHOSPHATIDYL INOSITOL TRANSAMIDASE SUBUNIT PIG-U (GPI), PLASMA MEMBRANE PROTON ATPASE 1 (AHA1), and PROHIBITIN 2 (PHB2).

HAP6 is predicted to have dolichyl-diphosphooligosaccharide-protein glycotransferase activity in N-glycosylation of proteins (TAIR) in the ER e.g. during the inhibition of ER stress (KANG et al. 2008, LIU and HOWELL 2010). WATANABE and LAM (2008) showed a role of AtBI-1 in the suppression of ER stress. This might functionally link BI-1 with HAP6.

WALTER et al. realized already in 1994 that the C-terminal sequence of the rat BI-1 protein is reminiscent of a nuclear targeting motif. In plant cells, BI-1 proteins localize in the ER and in the nuclear envelope (XU and REED 1998, KAWAI-YAMADA et al. 2001, EICHMANN et al. 2004). Interestingly, I co-immunoprecipitated three importin *β*-like nuclear transport receptors, namely, TRN1, CELLULAR APOPTOSIS SUSCEPTIBILITY PROTEIN/IMPORTIN-ALPHA RE-EXPORTER (CAS, putative), and EXPORTIN 1 (XPO1, MERKLE 2003). However, since no SALK-lines were available for CAS, and since the identified peptide of XPO1 fits to both, XPO1A and XPO1B, I went on with TRN1, as a start.

V-ATPases function in processes in the *trans*-Golgi network, involved in the synthesis and trafficking of cell wall components (DETTMER et al. 2005, 2006). Moreover, V-ATPases have essential roles in stress responses (DIETZ et al. 2001). Therefore, I picked the AtBI-1-GFP co-immunoprecipitated VHA-A as a candidate protein.

KEINATH et al. (2010) recently showed that flg22-triggered PAMP-signaling was affected in the *AHA1* mutant *ost2*-1D. In barley, PM H$^+$-ATPases are suggested to be involved in HR-mediated resistance to *Bgh* (ZHOU et al. 2000, FINNI et al. 2002). This gives cause to further investigate AHA1. However, the identified peptide (table 3.1) is also part of AHA2.

Actin cytoskeleton reorganization during plant - powdery mildew interactions is a well known process (OPALSKI et al. 2005). Since myosins are suggested to be involved in Ca^{2+}-/CaM-dependent transports of organelles along actin filaments (SHIMMEN and YOKOTA 2004), MYHC seemed to be another interesting candidate.

In human cells, BI-1 was shown to inhibit ROS production and resulting cell death by regulating cytochrome P450 2E1 (P450 2E1, KIM et al. 2009). BLAST search of human P450 2E1 against the *Arabidopsis thaliana* database of NCBI (state August 31, 2011) identifies CYP83A1 as first hit, which is the same protein I identified via AtBI-1-GFP co-IP. The protein was therefore also included in further investigations.

Furthermore, GPI was chosen as candidate protein for further investigations, even though the protein was identified in only one co-IP experiment. GPI anchors anchor proteins, such as arabinogalactan proteins (AGPs), to the cell wall (SCHULTZ et al. 1998). Amongst others, AGPs are suggested to be part of a signal transduction pathway involved in PCD (GAO and SHOWALTER 1999). Moreover, since array data (unpublished) showed an upregulation of AGPs upon *Bgh* infection in *GFP-BI-1* overexpressing barley plants when compared to the wild type cv. Golden Promise, there might be a link of GPI anchored AGPs and BI-1-mediated susceptibility to *Bgh*.

Another interesting candidate was PHB2. PHBs are involved in the prevention of stress responses and seem to play a major role in cell death-related mitochondrial function (DI et al. 2010, VAN AKEN et al. 2007, 2010).

Candidates were selected after quality check of respective mass spectra by manual inspection, although not all identified peptides showed significant mascot ion scores. Selected putative AtBI-1-interacting proteins are listed in table 3.1, including information about the AGI code, the number and amino acid sequence of identified peptides, and the mascot ion score (threshold: 46, for *P* < 0.05). Additionally, the NCBI annotation is given, when it differed from TAIR annotation.

Assumed subcellular localization of candidate proteins according to TAIR, is listed in supplementary table 2, also providing information of predicted protein domains and motifs, according to InterProScan (http://ebi.ac.uk/interpro/, HUNTER et al. 2009).

Out of the eight selected candidates, six, namely HAP6, TRN1, VHA-A, MYHC, AHA1, and PHB2 were AtBI-1-GFP co-immunoprecipitated in two further independent experiments. CYP83A1 was identified in one further independent repetition, when lower identification criteria were set, whereas GPI was not detected again.

Table 3.1: AtBI-1-interacting candidate proteins selected for further investigations.

protein name	AGI code	# peptides₁	mascot ion score	identified peptide
HAPLESS 6 (HAP6)ₐ	At4g21150	4	38.96, 48.82*, 38.24, 47.89*	(K)TLEILGIDKK(S), (K)VLQSSSTLK(D), (K)SVDSSVINNQELK(F), (K)FDADSATYFLDSFPK(N)
TRANSPORTIN 1 (TRN1)	At2g16950	3	38.15, 41.73, 42.77	(R)QSAFALMGDLAR(V), (R)LLDFLEIASQQLSANLNR(E), (R)GAYPSMTQENQK(Y)
VACUOLAR ATP SYNTHASE SUBUNIT A (VHA-A)	At1g78900	3	44.6, 35.59, 68.24*	(K)LAADTPLLTGQR(V), (R)LVSQKFEDPAEGEDTLVEK(F), (R)TTLVANTSNMPVAAR(E)
MYOSIN HEAVY CHAIN-RELATED (MYHC)ᵦ	At4g31340	2	44.87, 37.53	(R)ALESQIDEK(T), (R)EVQGKDEVVAEKEK(L)
CYTOCHROME P450 83A1 (CYP83A1), REDUCED EPIDERMAL FLUORESCENCE 2 (REF2)	At4g13770	1	41.4	(K)LPPGPSPLPVIGNLLQLQK(L)
GLYCOSYLPHOSPHATIDYL INOSITOL TRANSAMIDASE SUBUNIT PIG-U (GPI)_d	At1g63110	1	42.31	(R)SVENEESSTSTVSK(Q)
PLASMA MEMBRANE PROTON ATPASE 1 (AHA1), PLASMA MEMBRANE PROTON ATPASE 2 (AHA2)	At2g18960, At4g30190	1	35.8	(R)EGLTTQEGEDR(I)
PROHIBITIN 2 (PHB2)	At1g03860	1	52.81*	(R)EIAQTIAQSANK(V)

Selected candidate proteins are sorted by # peptides₁ and alphabetically. AGI code and gene descriptions are based on TAIR annotations (30th august 2011). ₁ number of identified individual peptides of each protein, ₐ NCBI annotation: dolichyl-diphosphooligosaccharide-protein glycotransferase (gi|22328844), ᵦ NCBI annotation: unknown protein (gi|18417787), c NCBI annotation: importin-alpha export receptor/ protein transporter (gi|15226001), d NCBI annotation: unknown protein; 55290–58984 (gi|12323255), ₐ-d state February 16, 2007, * *P* < 0.05.

3.4   Analysis of putative AtBI-1-interacting proteins

BI-1 is a conserved cell death inhibitor and a susceptibility factor in the barley - powdery mildew interaction (HÜCKELHOVEN et al. 2003, EICHMANN et al. 2004, 2006b, 2010). Therefore, I functionally analyzed several selected putative AtBI-1-interacting proteins in response to the adapted powdery mildew fungus *E. cruciferarum* and upon cell death stimuli. Furthermore, I studied the subcellular localization of promising candidates.

3.4.1   Investigations on the function of putative AtBI-1-interacting proteins in response to *E. cruciferarum*

To analyze the function of AtBI-1-interacting candidate proteins in the pathosystem *Arabidopsis - E. cruciferarum*, I conducted an inoculation assay using available homozygous T-DNA insertion lines of the selected candidates (table 2.3). Additionally, *ref2-1*, containing a point mutation in *CYP83A1*, was used (HEMM et al. 2003). *CYP83A1*, *PHB2*, *HAP6*, *AHA1*, and *VHA-A* T-DNA insertion lines as well as *ref2-1* were inoculated with *E. cruciferarum* and macroscopically analyzed 8-13 dai.
T-DNA insertion lines of *PHB2* (SALK_004663C and SALK_061282C) as well as of *HAP6* (SALK_019955C and SALK_017994C) were slightly more infected with *E. cruciferarum* than the wild type (supplementary figure 6). An accelerated fungal development was observed on both *PHB2* and *HAP6* T-DNA insertion lines 5 dai, respectively, measured as number of conidiophores per colony (c/c). On Col-0, the fungus developed an average number of about 20 ± 3 c/c, while the conidiophore production was enhanced to 23 ± 2 c/c and to 25 ± 2 c/c on the *PHB2* mutants, SALK_004663C and SALK_061282C (fig. 3.11A). On the *HAP6* mutants SALK_019955C and SALK_017994C, *E. cruciferarum* developed 17.2 ± 2.0 c/c and 18.5 ± 1.4 c/c, respectively. Here, on the wild type control, the fungus developed only 12.2 ± 1.2 c/c (fig. 3.11B).
Furthermore, I checked the expression level of *PHB2* and *HAP6* in the respective SALK-lines compared to Col-0 by amplifying the full-length coding sequence, respectively. I observed no *PHB2* accumulation in both *PHB2* SALK-lines used, assigning both lines as knock-out mutants (fig. 3.11C). Henceforward, SALK_004663C and SALK_061282C are named *phb2-1* and *phb2-2*. In contrast, the expression level of *HAP6* in both used mutants was only reduced compared to Col-0

in both lines used, defining SALK_019955C and SALK_017994C as *HAP6* knock-down mutants (fig. 3.11D), which were renamed to *hap6-1* and *hap6-2*. The T-DNA position in *phb2-2*, *hap6-1*, and *hap6-2* could be located (supplementary figure 7). In *phb2-1*, a T-DNA insertion was confirmed (data not shown). An adequate PCR to confirm the exact T-DNA position in *phb2-1* failed.
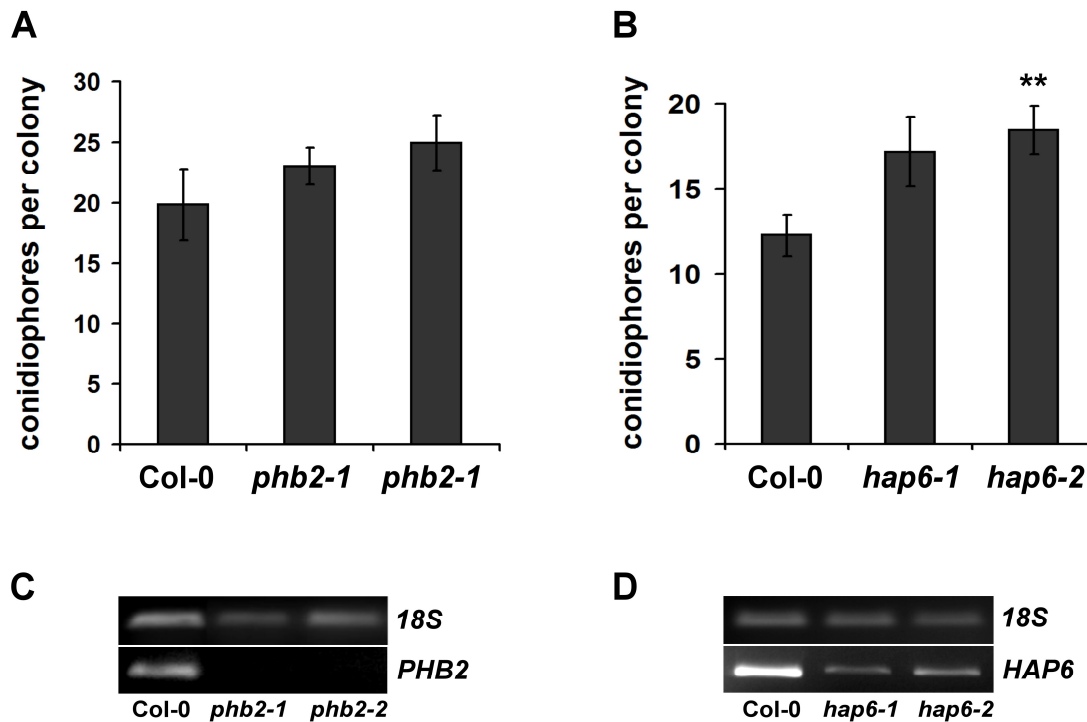
Fig. 3.11: *E. cruciferarum* development on *PHB2* and *HAP6* T-DNA insertion lines. Plants of 5-weeks-old wild type Col-0 and **A** *PHB2* (SALK_004663C and SALK_061282C) or **B** *HAP6* (SALK_019955C and SALK_017994C) T-DNA insertion lines were inoculated with 3-5 *E. cruciferarum* spores per mm^2. Leaves were harvested 5 dai, discolored and stained with acetic ink for subsequent microscopic analysis. Conidiophores per colony (c/c) were counted on five individual plants per line. 50 colonies per line were evaluated. Columns represent mean values. The experiment was repeated twice with similar results. Bars represent standard errors, ** indicate significance at $P < 0.01$ according to two-sided unpaired Student's t test, calculated over the mean values of c/c on the single leaves. **C** *PHB2* expression in wild type Col-0, *phb2-1* (SALK_004663C), and *phb2-2* (SALK_061282C) is displayed. **D** Pictures show *HAP6* expression in Col-0, *hab6-1* (SALK_019955C), and *hab6-2* (SALK_017994C). **C**, **D** Ethidium bromide-stained semi-quantitative RT-PCR products are displayed. Amplification of 18S served as control for constitutive gene expression.

VHA-A T-DNA insertion lines (SALK_081473C, SALK_089595C) and an *AHA1* T-DNA insertion line (SALK_065288C) seemed to be equally infected with *E. cruciferarum* as Col-0 (data not shown), and were not further analyzed in this pathosystem.

In contrast, the *CYP83A1* T-DNA insertion line SALK_123405C and the *cyp83a1* point mutant *ref2-1* stood out, due to a pronounced macroscopic *E. cruciferarum* resistance phenotype, when compared to Col-0 (fig. 3.12A). First, I checked the

expression level of *CYP83A1* in SALK_123405C and *ref2-1* compared to Col-0 by amplifying the coding sequence. SALK_123405C turned out to be a *cyp83a1* knock-out mutant, while *ref2-1* showed a strongly reduced *CYP83A1* expression, as previously described (HEMM et al. 2003, fig. 3.12C). Henceforth, SALK_123405C was named *cyp83a1.* The confirmation of the T-DNA position, as described in TAIR, is displayed in supplementary figure 8.

As a first parameter to quantify *E. cruciferarum* development, I counted c/c 5 dai. As expected, the amount of c/c was significantly decreased on both *cyp83a1* mutants analyzed, compared to the wild type. *E. cruciferarum* developed an average of 36 ± 6 SE c/c on Col-0 and only 1 ± 0.2 SE c/c and 2 ± 0.4 SE c/c on *cyp83a1* and *ref2-1,* respectively (fig. 3.12B).
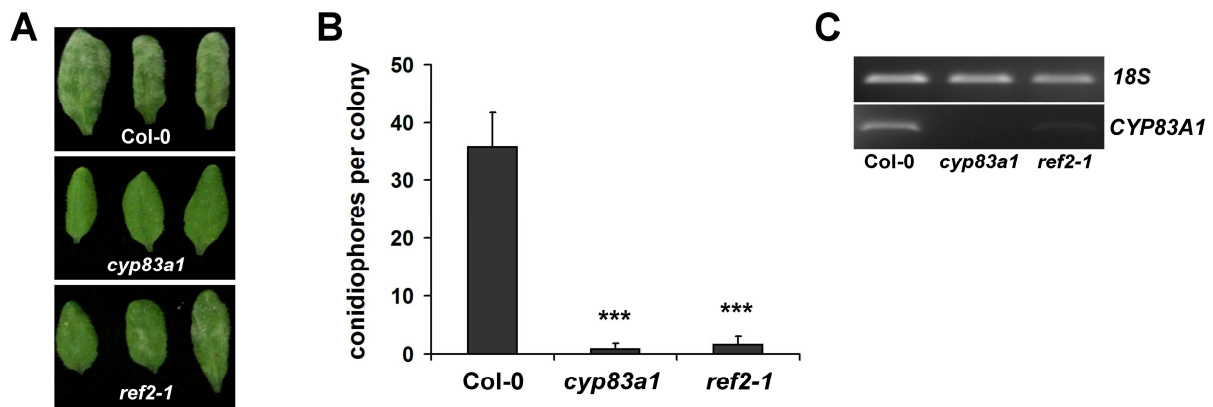
Fig. 3.12: *E. cruciferarum* **resistance phenotype of** *cyp83a1* **mutants.** 5-weeks-old Col-0, *cyp83a1* (SALK_123405C), and *ref2-1* (HEMM et al. 2003) plants were inoculated with 3-5 *E. cruciferarum* conidia per mm^2. **A** Photographs were taken 8 dai with *E. cruciferarum*. **B** For analyzing the amount of conidiophores per colony (c/c), leaves were harvested 5 dai, discolored and stained with acetic ink for subsequent microscopic analysis. 50 colonies per line were evaluated on five individual plants. Columns represent mean values. The experiment was repeated twice with similar results. Bars represent standard errors, *** represent $p < 0.001$ according to two-sided unpaired Student's *t* test, calculated over the mean values of c/c on the single leaves. **C** *CYP83A1* expression in Col-0, *cyp83a1* (SALK_123405C), and *ref2-1* is displayed. 18S was amplified to confirm an equal cDNA loading. Ethidium bromide-stained semi-quantitative RT-PCR products are shown.

In order to specify the resistance phenotype of the *cyp83a1* mutants, a detailed analysis was carried out 2 dai with *E. cruciferarum*. As a first result, this approach revealed no genotype-specific differences in the germination of the fungal spores (data not shown). Secondly, significant differences were observed, regarding the developmental stage of the germinated spores 2 dai on *cyp83a1* and *ref2-1,* respectively, compared to Col-0 (fig. 3.13A). On the wild type, about 13.9 ± 2.3% SE of the spores were in a stage, where the appressorium (APP) had been formed. However, the majority of fungi, 71.0 ± 3.6% SE, had established a haustorium and

elongated hyphae (EH) by this time. 14.6 ± 2.4% SE of the fungi already established a secondary haustoria in their host. In contrast, the number of spores with an APP only, was significantly enhanced on *cyp83a1* and *ref2-1* to 44.6 ± 4.9% SE and 40.1 ± 5.6% SE, respectively. Consistent with this, the number of fungi with haustoria and EH was significantly reduced to 53.2 ± 4.8% SE on *cyp83a1* and to 59.0 ± 5.7% SE on *ref2-1*. The percentage of secondary haustoria was significantly reduced on both *cyp83a1* mutants as well. On *cyp83a1* only 0.9 ± 0.4% SE, and on *ref2-1* 1 ± 0.4% SE of the germinated *E. cruciferarum* spores had established secondary haustoria.

Finally, the interaction sites were observed regarding local and whole cell callose deposition, using methyl blue staining. No significant differences in callose deposition were detected in both *cyp83a1* mutants compared to the wild type. In Col-0, *cyp83a1*, and *ref2-1*, a callose deposition was visible in about 90% of the attacked or penetrated epidermal cells (fig. 3.13B). Whole cell callose accumulation, indicative of cell death, appeared nearly exclusively in penetrated epidermal cells. Thereby, the percentage of interaction sites with cell death was enhanced on *cyp83a1* and *ref2-1*, compared to the wild type (fig. 3.13B). In Col-0, 3.7 ± 1.4% SE of the interaction sites showed cell death reactions, in *cyp83a1* 6.0 ± 1.4% SE, and in *ref2-1* 9.7 ± 1.6% SE.
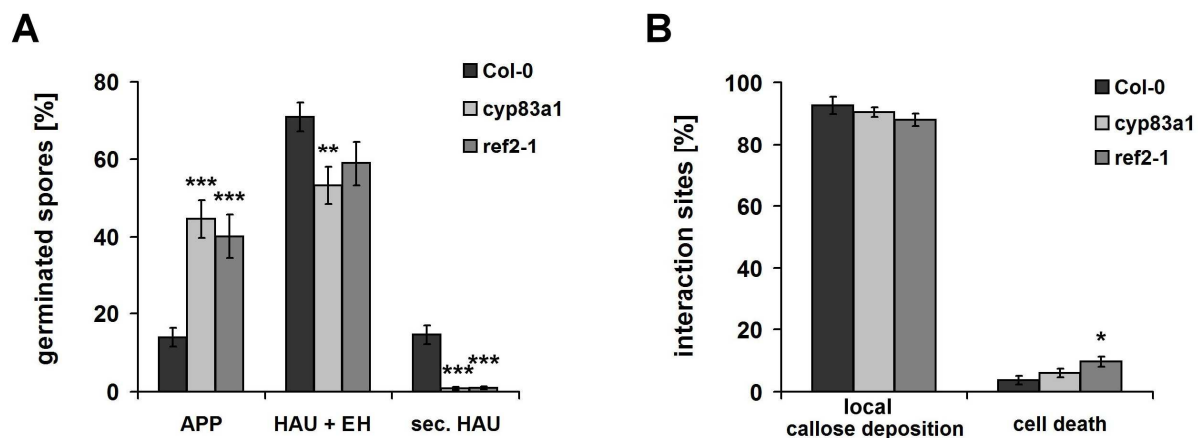
Fig. 3.13: *E. cruciferarum* development on *cyp83a1* mutants and analysis of the interaction sites 2 dai. 5-weeks-old Col-0, *cyp83a1*, and *ref2-1* plants (five per line) were inoculated with about 3-5 *E. cruciferarum* spores per mm^2. Two leaves per plant were harvested 2 dai, discolored, and stained with WGA-TMR and methyl blue for subsequent microscopic analysis. A minimum of 400 germinated spores were evaluated per line. **A** The developmental stage of the germinated spores was analyzed 2 dai, regarding appressorium formation only (APP), establishment of a haustorium (HAU) and formation of elongated hyphae (EH), or the formation of secondary haustoria (sec. HAU). **B** The interaction sites were analyzed regarding local callose deposition and whole cell callose accumulation (cell death). **A, B** Columns represent the mean values, bars represent standard errors, *, **, and *** represent p < 0.05, 0.01, and .001, respectively, according to two-sided unpaired Student's *t* test, calculated over the mean values of single leaves. The experiment was repeated twice with similar results.

Together, several AtBI-1-interacting candidate proteins seemed to be involved in the *Arabidopsis - E. cruciferaum* interaction. While on *phb2* and *hap6* mutants the fungus showed an accelerated development, macroscopic and microscopic analysis revealed an *E. cruciferarum* resistance phenotype of *Arabidopsis cyp83a1* mutants.

3.4.2 Co-localization of a AtBI-1-GFP fusion protein and RFP- or mCherry-labeled candidate proteins

CYP83A1, HAP6, and PHB2 turned out as promising AtBI-1-interacting candidates, since these proteins seemed to be involved in the interaction of *Arabidopsis* with *E. cruciferarum* (chapter 3.4.1). For a further characterization, I performed co-localization studies of AtBI-1 with CYP83A1, HAP6, or PHB2, respectively, by transiently expressing fluorescing protein fusions.

A PHB2-RFP fusion construct was transiently transformed into tobacco leaf segments via *A. tumefaciens*-infiltration, together with an AtBI-1-GFP fusion construct. As already shown by KAWAI-YAMADA et al. (2001), AtBI-1-GFP localized in the ER and in the nuclear envelope. RFP served as transformation marker and was localized in the cytoplasm and in the nucleus.
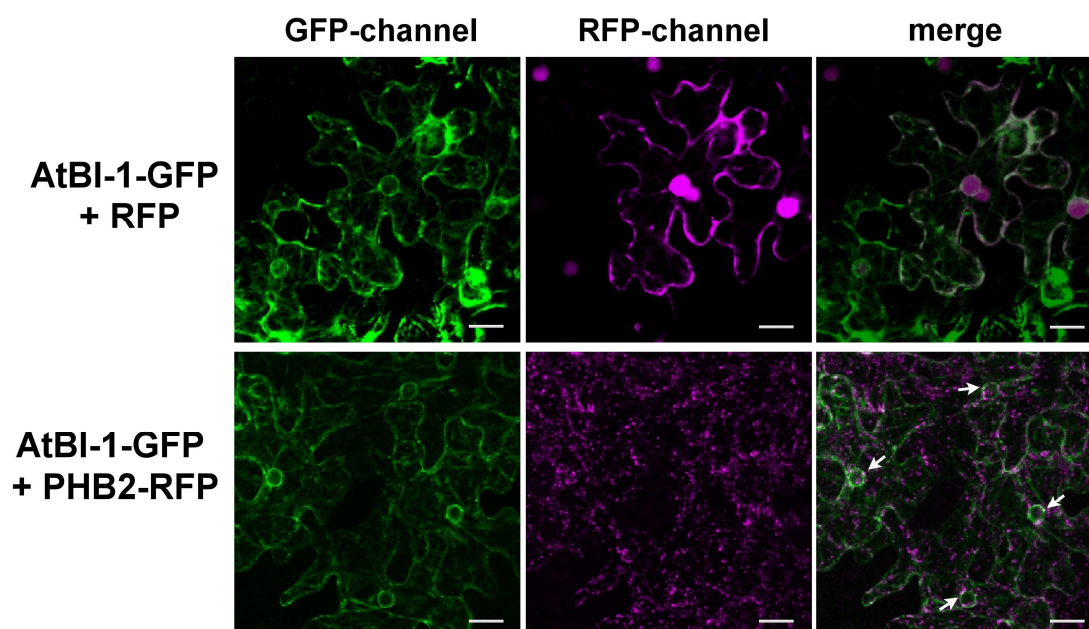
Fig. 3.14: Co-localization of AtBI-1-GFP and PHB2-RFP in tobacco cells. Tobacco leaf-segments were transiently co-transformed with pBI101+-AtBI-1-GFP together with pBI101+-RFP or pBI101+-PHB2-RFP via *A. tumefaciens*-infiltration. RFP served as marker for cytoplasmic and nuclear localization. Fluorescence was visualized by CLSM 5 days after transformation. Whole cell projections are displayed. Scale bars = 20 µm. Arrows mark nuclei. White pixels in the merge image indicate overlapping fluorescence signals.

Like mammalian prohibitins, AtPHB2 is thought to be associated with mitochondria (NIJTMANS et al. 2000, MILLAR et al. 2001). As shown in fig. 3.14, PHB2-RFP accumulated in small dots all over the cell, most likely representing mitrochondria (TAKAHASHI et al. 2003). The same localization pattern were observed by transiently transforming *Arabidopsis* epidermal cells via particle bombardment, but flourescence intensities were very low (data not shown). Co-localization of AtBI-1-GFP and PHB2-RFP was visible in small contact points, for instance at the nuclear envelope (fig. 3.14, arrows).
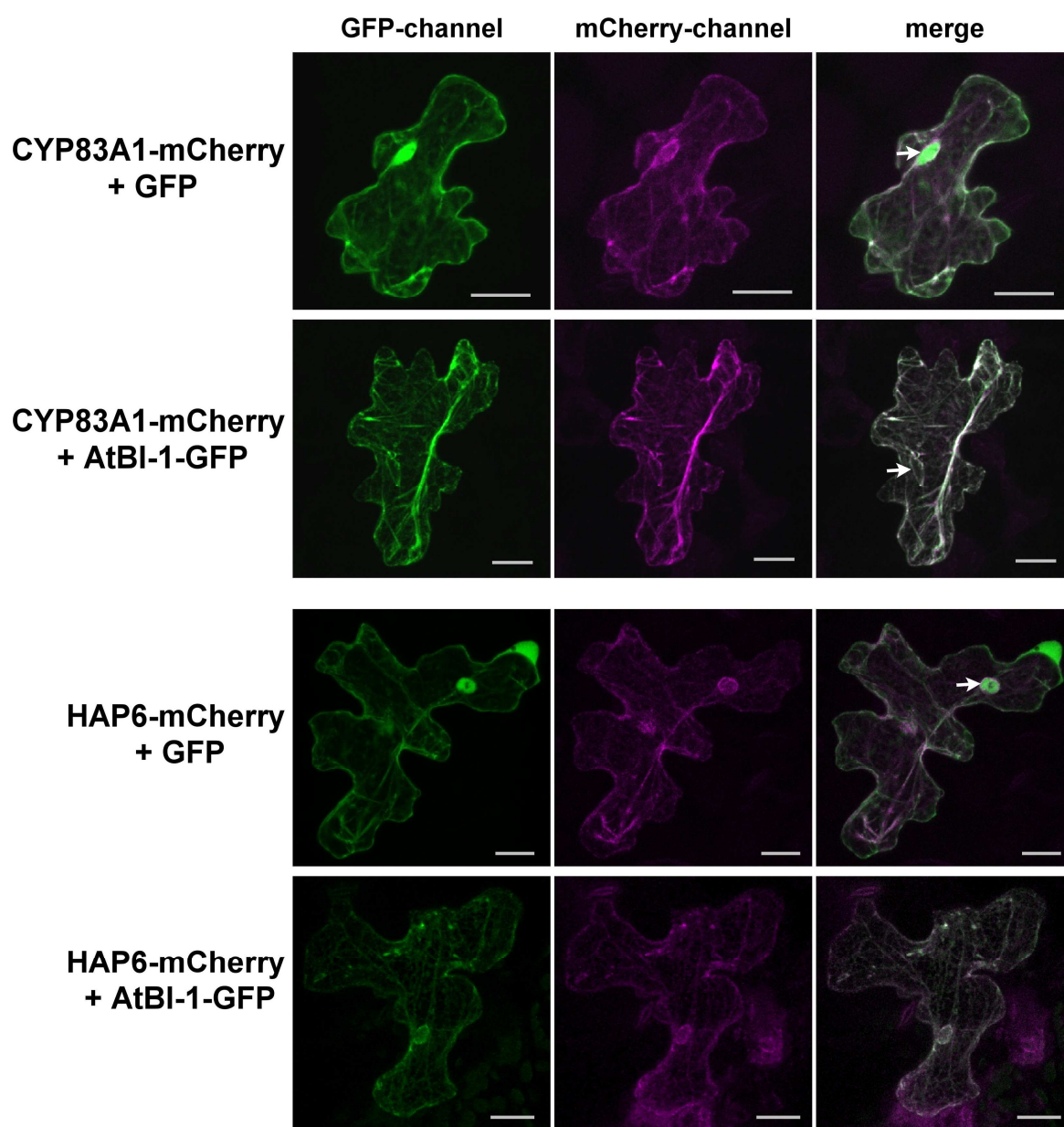
Fig. 3.15: Co-localization of AtBI-1-GFP and CYP83A1-mCherry or HAP6-mCherry in *Arabidopsis* epidermal cells. *Arabidopsis* leaves were transiently co-transformed by ballistically delivering pGY1-AtBI-1-GFP or pGY-1-GFP together with pGY-1-CYP83A1-mCherry or pGY-1-HAP6-mCherry, respectively. Fluorescence was visualized by CLSM 1 dab. Whole cell projections are displayed. Scale bars = 20 µm. Arrows mark nuclei. White pixels in the merge image indicate overlapping fluorescence signals.

Cytochrome P450 proteins are typically localized in the ER (SCHULER and WERCK-REICHHART 2003). Since CYP79F1 and CYP79F2 synthesize aliphatic aldoximes, the substrate of CYP83A1, at the ER, CYP83A1 is suggested to be localized to this compartment as well (REINTANZ et al. 2001, NAFISI et al. 2006). HAP6, also annotated as DOLICHYL-DIPHOSPHOOLIGOSACCHARIDE-PROTEIN GLYCO-TRANSFERASE, is also predicted to be (amongst others) ER-resident, where N-glycosylation takes place (NCBI, TAIR).

As expected, CYP83A1-mCherry and HAP6-mCherry fusion proteins accumulated in the ER and around the nucleus in transiently transformed *Arabidopsis* epidermal cells (fig. 3.15). GFP served as marker for cytosolic and nuclear localization. *HAP6-mCherry* was only weakly expressed. Co-expression of *AtBI-1-GFP* and *CYP83A1-mCherry* or *HAP6-mCherry* resulted in overlapping fluorescence signals, confirming the accumulation of both putative AtBI-1-interacting proteins in the ER and around the nucleus.

3.4.3 Functional analysis of putative AtBI-1-interacting proteins in cell death reactions

To assess whether selected AtBI-1-interacting candidates might be involved in AtBI-1-mediated cell death suppression, Col-0, *atbi1-2*, *cyp83a1*, *ref2-1*, *phb2-1*, *phb2-1*, and *hap6-1* mutants, as well as the *VHA-A* T-DNA insertion line SALK_089595C were treated with AAL toxin to induce cell death.

Cell death symptoms were evaluated 9-10 days after AAL toxin application. When compared to Col-0, accelerated cell death reactions appeared on *atbi-1* mutants (fig. 3.16A). The relative deviation of AAL toxin-affected leaf area of *atbi-1* from the average affected leaf area on the wild type control was 126.6 ± 109.8% SE. Control leaves, treated with distilled water, showed no cell death reactions at all.

cyp83a1 mutants, *cyp83a1* and *ref2-1*, revealed strongly enhanced cell death symptoms compared to Col-0 and *atbi1-2*. The relative deviation of affected leaf area from the respective average wild type control reached 778.6 ± 326.5% SE on *cyp83a1*, and 675.0 ± 331.5% SE on *ref2-1* (fig 3.16A).

Since at the same time a putative cuticle defect was observed on both *cyp83a1* mutants (chapter 3.5.1), I conducted another AAL toxin experiment, where the toxin was directly infiltrated into the leaves. As displayed in fig 3.16B, the affected leaf area

was also increased on *cyp83a1* and *ref2-1*, compared to the wild type control. Here, the relative deviation of affected leaf area from the average wild type control was significantly enhanced to 109.3 ± 28.9% SE and to 87.0 ± 21.5% SE on *cyp83a1* and *ref2-1*, respectively.
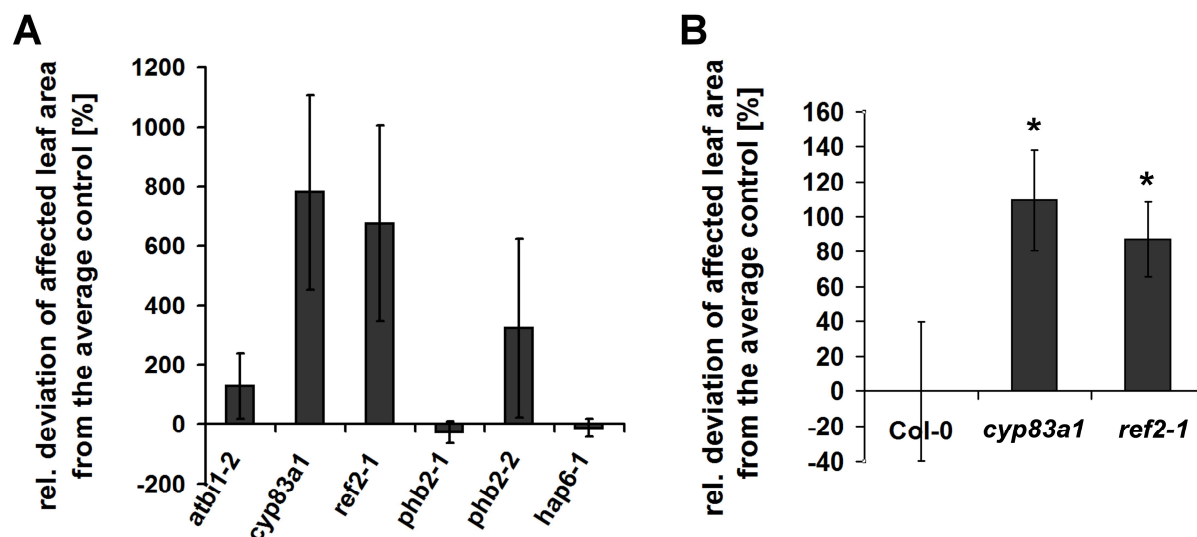
Fig. 3.16: Functional analysis of AtBI-1-interacting candidate proteins in cell death reactions. A 10 µl of a 100 µM AAL toxin solution were dropped on leaves of about 5-weeks-old Col-0, *atbi1-2*, *cyp83a1*, *ref2-1*, *phb2-1*, *phb2-1*, and *hap6-1* plants. Leaves were evaluated 9-10 days after treatment. Per experiment, 10 leaves per line were used. Mean values of a minimum of three independent experiments are displayed. Bars represent standard errors. **B** Leaves of about 5-weeks-old Col-0, *cyp83a1*, and *ref2-1* plants were infiltrated with 50 µl of a 100 µM AAL toxin solution and evaluated 3-4 days later. Per experiment, 8 leaves per line were treated. Columns represent mean values of three independent experiments, bars represent standard errors, and * indicates significance at $P < 0.05$ according to two-sided unpaired Student's *t* test.

There was no significant effect of the AAL toxin application on *phb2-1* and *hap6-1* compared to Col-0. However, on *phb2-2*, the relative deviation of affected leaf area from the average control was strongly enhanced to 322.0 ± 302.3% SE (fig. 3.16A). Typical symptoms of AAL toxin treated Col-0, *atbi1-2*, *cyp83a1*, *ref2-1*, *phb2-1*, *phb2-1*, and *hap6-1* leaves are displayed in supplementary figure 9.

VHA-A T-DNA insertion line SALK_089595C also displayed an accelerated cell death progression upon AAL toxin application compared to Col-0. The relative deviation of affected leaf area from the average wild type control was enhanced to 45.7 ± 61.0% SE.

WATANABE and LAM (2006) observed accelerated cell death reactions upon heat shock treatment in two *atbi-1* knock-out mutants compared to Col-0. Therefore, I also used heat shock, as a second cell death-inducing treatment. Consistent with the AAL toxin experiments, *atbi1-2*, *cyp83a1*, *phb2-2*, and the *VHA-A* T-DNA insertion line SALK_089595C showed stronger cell death phenotypes after heat shock compared

to Col-0. In contrast to the AAL toxin treatment, the heat shock application resulted in stronger cell death symptoms of *phb2-1* plants, compared to Col-0, as well. *hap6-1* was less affected after exposure to heat shock, compared to Col-0, or *atbi1-2* (supplementary table 3).

To summarize, the selected putative AtBI-1-interacting candidates, CYP83A1, PHB2, and HAP6, which already showed a function in *Arabidopsis - E. cruciferarum* interactions, seemed to be involved in cell death regulation as well. While CYP83A1 and PHB2 seemed to be involved in the suppression of cell death reactions, HAP6 rather supported these.

3.5   Phenotypic characterization of *cyp83a1* mutants

3.5.1   Morphological phenotypes

In the course of my work, I observed diverse phenotypes of the *cyp83a1* mutants, *cyp83a1* and *ref2-1*. Quite obviously, *cyp83a1* and *ref2-1* mutants showed a retarded plant development, concerning leaf size (fig. 3.17B) and the time of flowering (fig. 3.17A), when compared to the wild type. Interestingly, the leaf size phenotype was more pronounced, when the plants grew under short-day conditions, compared to long-day conditions.
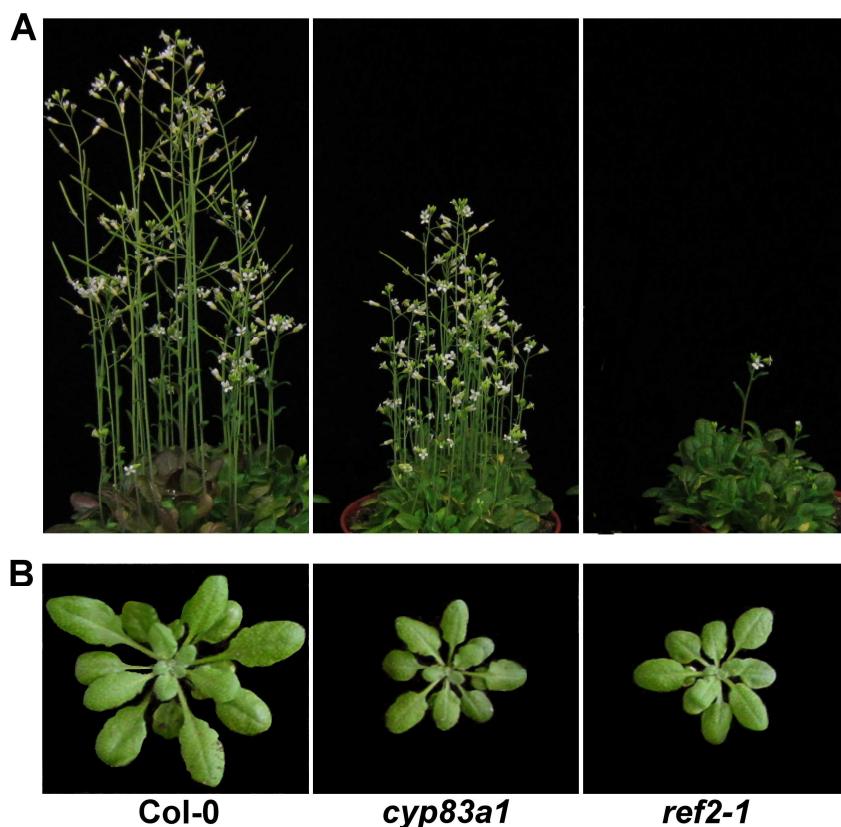
Fig. 3.17: Leaf size and flowering phenotype of *cyp83a1* mutants. A Photographs of 5-weeks-old Col-0, cyp83a1, and *ref2-1* plants, grown under long day conditions. **B** Photographs show an example of 4-weeks-old Col-0, *cyp83a1*, and *ref2-1* plants, respectively, grown under short day conditions.

| Col-0 | *cyp83a1* | *ref2-1* |

Furthermore, I observed a cuticle permeability phenotype, since acetic ink staining of fungal structures also visualized haustoria (fig. 3.18A) and chloroplasts (not shown) in both *cyp83a1* mutants. To confirm an increased cuticle permeability, calcofluor white-staining of *cyp83a1* and *ref2-1* leaves was conducted as previously described by BESSIRE et al. (2007). I observed a strong laminar fluorescence of *cyp83a1* and *ref2-1* leaves compared to Col-0, where only partial fluorescence was observable (fig. 3.18B). Since fluorescence of calcofluor white occurs by binding to cellulose, a cuticle phenotype of the *cyp83a1* mutants was supported.
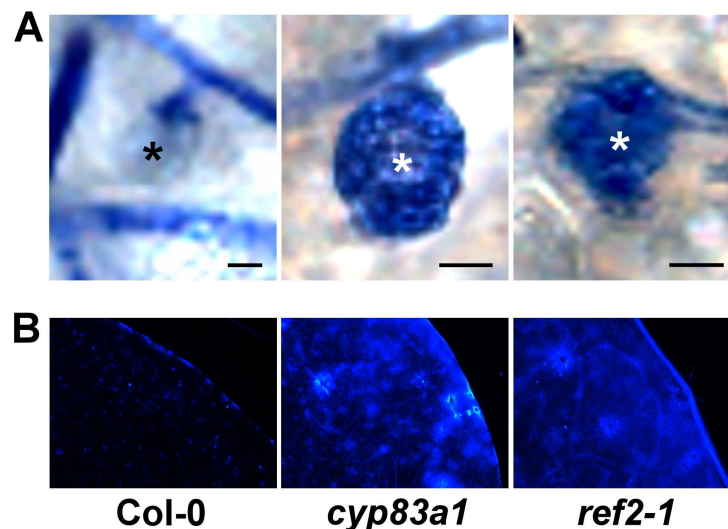
Fig. 3.18: Cuticle phenotype of *cyp83a1* mutants. A 5-weeks-old *Col-0*, *cyp83a1*, and *ref2-1* plants were inoculated with *E. cruciferarum*. Leaves were harvested 5 dai, discolored, and stained with acetic ink. Strongly magnified haustoria (asterisk) are displayed. Bars = 4 µm. **B** Leaves of about 4-weeks-old Col-0, *cyp83a1*, and *ref2-1* plants were discolored and stained with calcofluor white for 30 sec. Leaves were imaged under a fluorescence microscope with 5x magnification, using identical settings. The experiment was repeated twice with similar results.

For the purpose of propagation, approximately 3-weeks-old *cyp83a1* and *ref2-1* plants were transferred to long-day conditions to induce florescence. During the next 1-2 weeks, chlorotic, transparent spots appeared all over the leaves, on the upper as well as on the lower side of the leaves, especially on older ones (fig. 3.19A). After more than 2 month of cultivation, the same symptoms started to occur under short-day conditions (not shown). Exemplary, macroscopic and microscopic pictures of this long-day-induced spot phenotype are displayed for *cyp83a1* in fig. 3.19. Bright field microscopy revealed anthocyanin accumulation around affected areas on the lower leaf side, and nicely demonstrated the transparency of these spots (fig. 3.19B). Cells of affected areas seemed to be enlarged, reminiscent of hypertrophy (fig. 3.19B,C).

Moreover, DAB staining indicative of H_2O_2 accumulation in the chlorotic dots, likely indicate cell death reactions (fig. 3.19C).

Moreover, microscopic analysis of leaves of *cyp83a1* and *ref2-1* mutants with spot phenotypes revealed generally enlarged mesophyll cell sizes compared to Col-0 control leaves (fig. 3.19D).
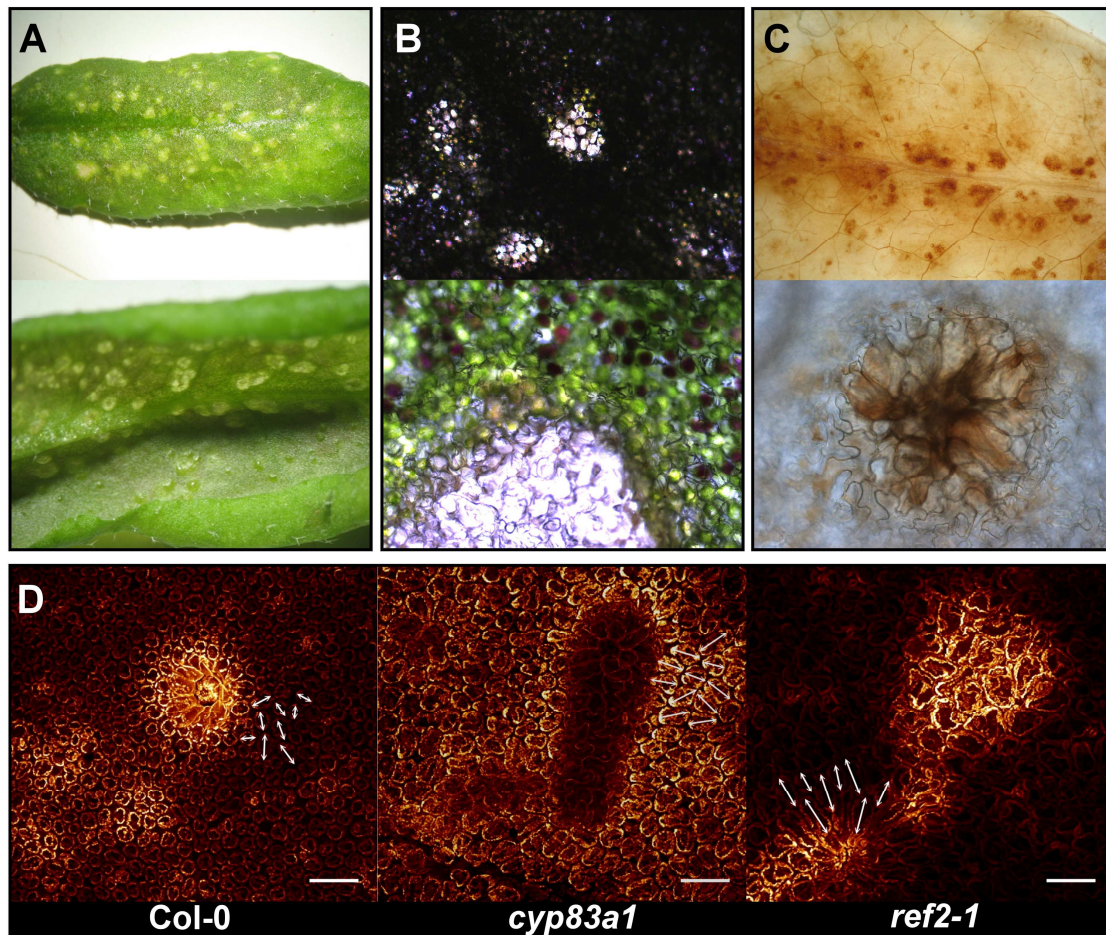
Fig. 3.19: Leaf spot phenotype of *cyp83a1*. Pictures display exemplary leaves of *cyp83a1*, 2 weeks after transfer to long-day conditions. **A** Photographs of the upper and lower leaf side are shown. **B** Upper (upper panel, 5x magnification) and lower (lower panel, 20x magnification) leaf side of *cyp83a1* viewed under a bright field microscope. **C** DAB-stained leaf was photographed (upper panel). A single spot was observed under 40x magnification using the bright field microscope (lower panel). **D** Col-0, *cyp83a1*, and *ref2-1* leaves were stained with mPS-PI (TRUERNIT et al. 2008). Bars represent 100 μm. Arrows mark diameter of single mesophyll cells. The experiment was repeated once with similar results.

3.5.2   *cyp83a1* mutants promote development of *B. cinerea*

The *Arabidopsis* mutant *botrytis-resistant 1* (*bre1*) exhibits a permeable cuticle and is resistant to *Botrytis cinerea* (BESSIRE et al. 2007). Since I observed a cuticle phenotype of the *cyp83a1* mutants (see above), I asked whether these mutants might also be resistant to the necrotrophic fungus *B. cinerea*.

Unexpectedly, *cyp83a1* and *ref2-1* showed increased disease symptoms 4 dai with *B. cinerea*, compared to Col-0. On the wild type control, about 15.2 ± 8.9% SE of the leaf area was necrotic or chlorotic. The affected leaf area was increased on *cyp83a1* to 45.8 ± 22.0% SE and significantly increased on *ref2-1* to 38.7 ± 10.1% SE (fig. 3.20).
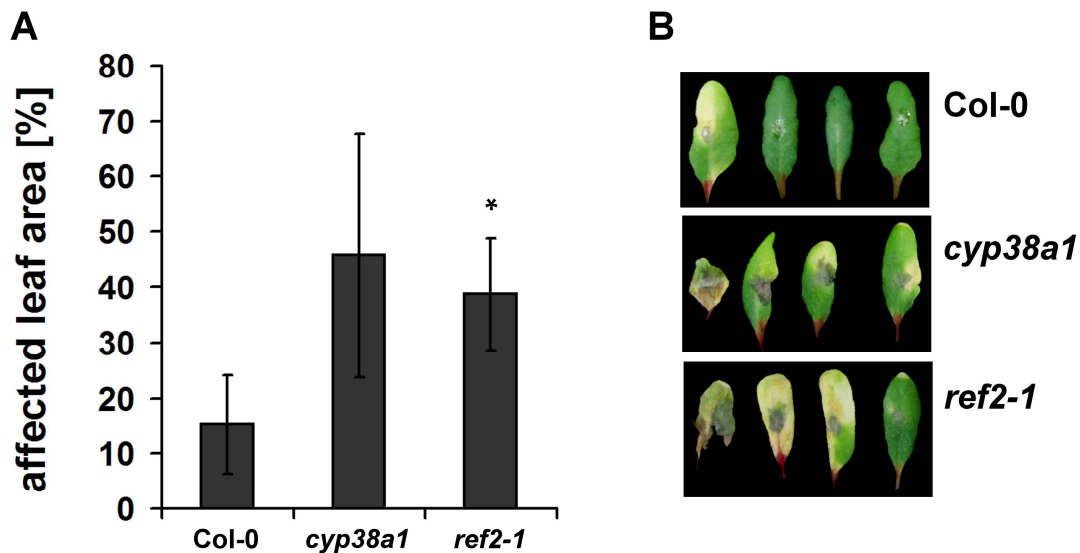
Fig. 3.20: *cyp83a1* mutants promote *B. cinerea* development. Leaves of about 5-weeks-old Col-0, *cyp83a1*, and *ref2-1* plants were drop inoculated with 20 µl of a *B. cinerea* spore solution (800,000 spores per ml) and evaluated 4 dai. **A** Columns represent mean values calculated over three independent experiments. Bars represent standard errors, and * indicates statistical significance at $p < 0.05$ according to two-sided paired Students *t*-test. **B** Typical *B. cinerea* symptoms on Col-0, *cyp83a1*, and *ref2-1*, photographed 4 dai.

3.6 Functional analysis of barley homologs of AtBI-1-interacting candidate proteins

Finally, I investigated the impact of the barley homologs of the selected putative AtBI-1-interacting candidate proteins in the barley - *Bgh* interaction.

To identify homologs, amino acid (AA) sequences of putative AtBI-1-interacting proteins were compared to the NCBI database, selected for *Hordeum vulgare*. The fist BLAST hit was accepted, except for CYP83A1. Here, the AA sequence identity with the first three NCBI hits ranged between 24-31%, only. Therefore, a CYP83A1 barley homolog was not selected.

Table 3.2 provides information about identified accession numbers of barley homologs. Moreover, AA identity of *Arabidopsis* and barley homologs is given, respectively.

Table 3.2: Barley homologs of AtBI-1-intreracting candidate proteins

candidates	accession number	AA identity [%]
PROHIBITIN 2	BAK00720	74
MYOSIN HEAVY CHAIN-RELATED	BAJ97759	46
VACUOLAR ATP SYNTHASE SUBUNIT A	BAB18682	90
TRANSPORTIN 1	BAJ93230	70
PLASMA MEMBRANE PROTON ATPASE 1	BAK05828	78
GPI TRANSAMIDASE SUBUNIT PIG-U	BAK07917	43
HAPLESS 6	BAJ85530	56

Accession number according to NCBI, AA identity of *Arabidopsis* and barley homologs according to ClustalW2 (http://ebi.ac.uk/Tools/msa/clustalw2/). State July 8, 2011.

To functionally analyze barley homologs of putative AtBI-1-interacting proteins (table 3.2) in the interaction of barley with *Bgh*, a transient transformation assay was performed. Via particle bombardment, I delivered overexpression constructs of *HvGPI*, *HvVHA-A*, *HvMYHC*, and *HvPHB2*, into barley cv. Ingrid epidermal cells. Control cells were transformed with empty vector pGY-1. The numbers of the individual experiments depend on the effects of the first two repetitions. I could not further investigate HvTRN1 and HvAHA1 in the barley - *Bgh* interaction, since the isolation of the coding sequences failed.

Overexpression of *HvGPI* and of *HvVHA-A* had no effects towards an altered PE of *Bgh*, respectively. In *HvGPI* overexpressing cells, a PE of 36 ± 12% SE was determined, control cells displayed 37 ± 3 SE % PE. The relative deviation of PE from the average control was 0.5 ± 41.5% SE, as a mean of two experiments (fig. 3.21A). A PE of *Bgh* of 38.7 ± 4.5% SE was archived by overexpressing *HvVHA-A*. In respective control cells, a PE of 37.3 ± 4.4% SE was calculated. Over three independent experiments, the relative deviation of PE from the average control was 5.3 ± 7% SE (fig. 22A).

Overexpression of *HvMYHC* significantly enhanced PE of *Bgh* from 39.8 ± 2.1% SE in control cells to 50 ± 4.7% SE. The relative deviation of PE from the average control was 26.2 ± 10.9% SE, calculated over six independent experiments (fig 3.21A).

A significantly enhanced susceptibility to *Bgh* was also achieved by transiently overexpressing *HvPHB2*. Here, the PE of the fungus reached 52.2 ± 3.1% SE, while control cells showed a PE of 42.8 ± 1.9% SE, resulting in a relative deviation of PE from the average control of 21.8 ± 6.1% SE. Five independent experiments were conducted (fig 3.21A).
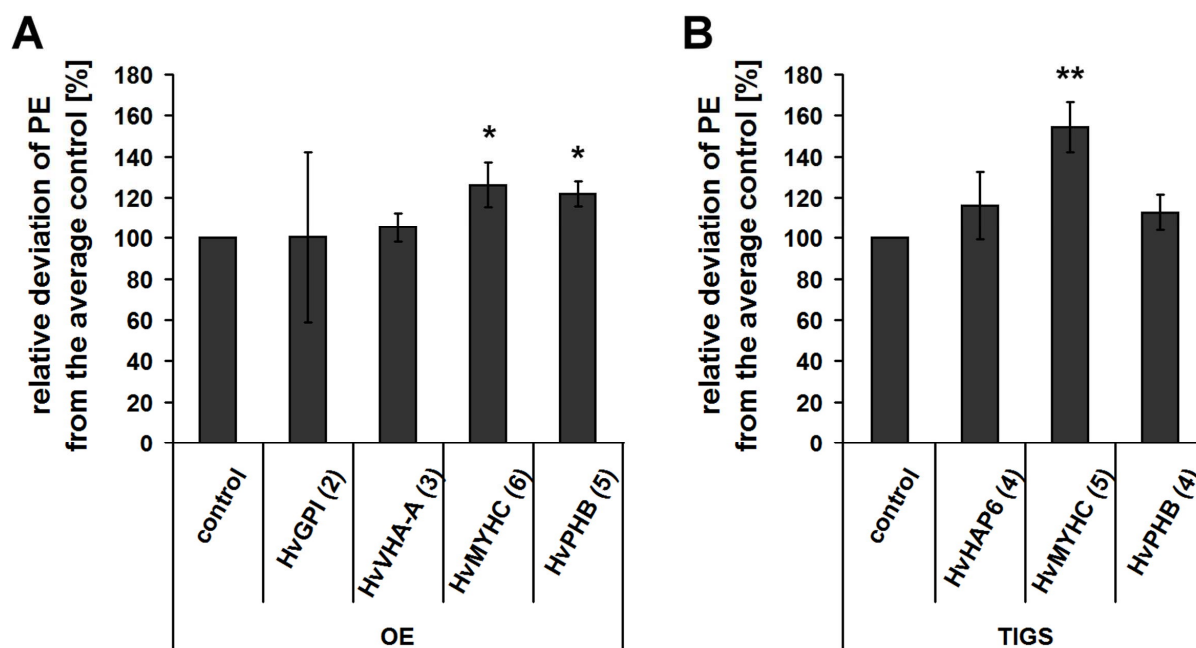
Fig. 3.21: Functional analysis of barley homologs of AtBI-1-interacting candidates. A Via particle bombardment, *HvGPI*, *HvVHA-A*, *HvMYHC*, and *HvPHB2* were transiently overexpressed (OE) in single barley epidermal cells. Empty vector pGY-1 was delivered into control cells. **B** Expression of *HvHAP6*, *HvMYHC*, and *HvPHB2* was transiently knocked-down via TIGS. Empty TIGS vector pIPKTA30N served as control. **A, B** GFP was co-delivered as transformation marker. Leaf segments were inoculated with *Bgh* 1 dab and microscopically analyzed 2 dai. Numbers in brackets indicate numbers of individual experiments. The relative deviation of penetration efficiency (PE) from the average control is displayed, in which the respective control was set to 100%, respectively. Bars represent standard errors, * and ** indicate significance at $P < 0.05$ and 0.01, respectively, according to two-sided paired Student's *t* test.

Since the overexpression of *HvMYHC* and *HvPHB2* showed significant effects towards enhanced susceptibility of barley cells against *Bgh*, I further analyzed these two candidates via TIGS. Unexpectedly, the knock-down of *HvMYHC* expression also led to a significantly enhanced PE. Here, PE of *Bgh* reached 55.2 ± 8.6% SE, while control cells showed 36.8 ± 6.4% SE PE of *Bgh*. Hence, the relative deviation of PE from the average control was 54.4 ± 12.1% SE. Five independent experiments were performed (fig 3.21B).

In contrast, no effect was observed after knocking-down *HvPHB2* expression. Here, the PE of *Bgh* reached to 49.2 ± 8.2% SE, and control cells showed 47.8 ± 6.8% SE PE. Out of four independent experiments, a relative deviation of only 2.8 ± 8.7% SE was calculated (fig 3.21B).

Since the full-length *HvHAP6* coding sequence (BAJ85530) was not available for overexpression experiments at that time, *HvHAP6* expression was transiently knocked-down via TIGS, which led to a slightly enhanced PE of *Bgh* of 54.5 ± 7.6%

SE compared to 47.8 ± 5% SE in control cells. Here, the relative deviation of PE from the average control was 16 ± 16.6% SE. The *HvHAP6* TIGS experiment was performed four times (fig 3.21B).

Together, at least two analyzed barley homologs of the AtBI-1-interacting candidate proteins, namely HvMYHC and HvPHB2, might have an influence on the barley - *Bgh* interaction, since the overexpression of both proteins resulted in a significantly enhanced PE of *Bgh*. TIGS of *HvMYHC* led to an increased susceptibility to *Bgh* as well, which might indicate a general role for HvMYHC in the barley - *Bgh* interaction.

To summarize, the applied approach to identify new AtBI-1-interacting proteins, led to the identification of several interesting candidate proteins. The analysis of selected candidates demonstrated a function of several of these proteins in BI-1-associated processes. CYP83A1, PHB2, and HAP6 turned out as the functionally most interesting AtBI-1-interacting candidates, due to their observed impact on the *Arabidopsis - E. cruciferarum* interaction and their potential involvement in cell death reactions.

In barley, the functional analysis of several homologs of putative AtBI-1-interacting proteins revealed that HvMYHC and HvPHB2 seemed functionally related to BI-1 proteins, since they might be involved in the barley - *Bgh* interaction.

4 Discussion

The interplay between plants and biotrophic pathogens is based on highly specific molecular interactions during all stages of pathogenesis. Therefore, the lack of an essential host factor can result in enhanced resistance against pathogens, if it is an effector target, or required for appropriate physiological or structural conditions leading to compatibility. This type of resistance, which can be independent of constitutive defense reactions, is assumed to be effective against pathogen species/classes rather than being isolate-specific (O'CONNELL and PANSTRUGA 2006, HÜCKELHOVEN 2005). In barley, only recently BI-1 was designated as a susceptibility factor to *Bgh* (HÜCKELHOVEN et al. 2003, EICHMANN et al. 2004, 2006b, 2010). Since LFG proteins are similar to BI-1 proteins in structure and cell death inhibiting function, one may assume that these proteins could also share functional properties in the pathosystem barley - *Bgh*. My results supported this hypothesis, and showed a conserved role of plant LFG proteins as susceptibility factors in powdery mildew interactions of monocots and dicots.

Since the mode of action of BI-1 in modulating basal defense reactions against *Bgh* is largely unknown, the second part of this thesis dealt with investigations of potential signaling components, namely MLO and CaM. My results indicate that BI-1 acts independently to rather than downstream of MLO. Moreover, I demonstrated that CaM is probably not essential for HvBI-1-mediated susceptibility towards *Bgh*, unlike it was shown for the MLO-mediated susceptibility to *Bgh* (KIM et al. 2002a,b).

Finally, in order to identify BI-1-interacting proteins, involved in the BI-1-mediated susceptibility to *Bgh* and/or cell death suppression, I conducted a co-immunoprecipitation assay. By this, 95 putative AtBI-1-interacting proteins were identified. I further analyzed selected candidate proteins, by which CYP83A1, PHB2 and HAP6 turned out as the most promising putative AtBI-1-interaction partners, since their involvement in plant - powdery mildew interactions as well as in cell death reactions could be demonstrated. Moreover, several barley homologs of the candidate proteins were analyzed in the interaction with *Bgh*, whereby barley HvPHB2 and HvMYHC showed an impact during the infection.

Together, the investigations revealed new insights into the involvement of BI-1, BI-1-like, and putative BI-1-interacting proteins in biotic and abiotic stress reactions.

4.1 Characterization of LFG proteins

4.1.1 LFG proteins: conserved susceptibility factors in plant - powdery mildew interactions

Overexpression of susceptibility factors to powdery mildew fungi, including MLO and HvBI-1, promote the penetration success of the fungus, while their knock-out or knock-down induce enhanced resistance (HÜCKELHOVEN 2005, EICHMANN et al. 2010). Since RNAi-based TIGS of *HvLFG1* in single barley epidermal cells significantly reduced the penetration success of *Bgh*, while vice versa the transient overexpression of *HvLFG1* led to a significantly enhanced susceptibility to the fungus (fig. 3.1), a function of *HvLFG1* as susceptibility factor to *Bgh* can be assumed.

The heterologous overexpression of *AtLFG1* and *AtLFG2*, respectively, in barley epidermal cells resulted in enhanced susceptibility to *Bgh* as well (fig 3.3). Moreover, on *Arabidopsis Atlfg1* as well as on *Atlfg2* mutants *E. cruciferarum* showed a reduced development, while stable *AtLFG1* and *AtLFG2* overexpression promoted the fungal development (fig 3.4, fig 3.5).

BI-1 and LFG proteins contain the *Bax1-I* motif (PF01027, formerly UPF0005) and are predicted to possess most likely seven transmembrane domains. Moreover, like BI-1, several LFG proteins are involved in the prevention of apoptosis (HU et al. 2009, SHUKLA et al. 2010). Due to this structural and functional analogy of LFG to BI-1 proteins, one can speculate that HvBI-1 and HvLFG1 are involved in similar processes leading to susceptibility to *Bgh*. The mode of action of HvBI-1 in mediating susceptibility to *Bgh* is largely unknown. Until now, it is not clear whether HvBI-1 is a direct *Bgh* effector target, as assumed for MLO (PANSTRUGA 2005). Yet, HvBI-1 is discussed to be involved in delay of HR-associated cell death and in the suppression of local oxidative burst, which is associated with penetration resistance (HÜCKELHOVEN et al. 1999, EICHMANN et al. 2006b). In plants and mammals, the conserved function of BI-1 as cell death inhibitor is associated with the modulation of intracellular Ca^{2+} homeostasis, possibly by regulating ion channels or forming one itself (CHAE et al. 2004, IHARA-OHORI et al. 2007, KIM et al. 2008, BULTYNCK et al. 2011). Besides this, cytosolic Ca^{2+} concentrations $[(Ca^{2+})_{cyt}]$ play an important role in defense signaling, e.g. for H_2O_2 production or callose deposition at the site of attempted fungal penetration, associated with penetration resistance (HAMMOND-KOSACK and JONES 1996, LEVINE et al. 1996, THORDAL-CHRISTENSEN et al. 1997, BLUME et al. 2000, GRANT et al. 2000, SAGI and FLUHR 2001). Therefore, EICHMANN et

al. (2010) postulated a pivotal role of HvBI-1 in the regulation of $[(Ca^{2+})_{cyt}]$ by limiting Ca^{2+} flux out of the ER during pathogenesis of *Bgh*. In turn, this could lead to the suppression of diverse processes involved in penetration resistance, finally conferring susceptibility to the fungus. Whether both processes, BI-1-mediated cell death suppression and BI-1-mediated susceptibility to *Bgh*, are functionally inked, remains to be investigated.

In mammals, LFG proteins are causally associated with the regulation of Ca^{2+}-homeostasis as well. For instance, the 71 kDa *N*-methyl-D-aspartate receptor protein NMDARP-71/LFG1 was shown to mediate Ca^{2+} influx in hippocampal neurons (MATTSON et al. 1993, CHEN et al. 1999). Furthermore, the function of h-GAAP/LFG4 as cell death inhibitor is linked with the regulation of intracellular Ca^{2+} fluxes. h-GAAP/LFG4 affect both, Ca^{2+} influx across the plasma membrane and Ca^{2+} release from intracellular stores, the latter by regulating inositol-1,4,5-triphosphate receptors (IP3Rs, DE MATTIA et al. 2009). Recently, ROJAS-RIVERA et al. (2012) demonstrated that TMBIM3/LFG1 controls ER-stress by regulating IP3Rs. Moreover, TMBIM3/LFG1 and BI-1 showed synergistic anti-apoptotic activities, probably through a physical interaction (ROJAS-RIVERA et al. 2012). Hence, HvLFG1, AtLFG1, and AtLFG2 might also be involved in the modulation of $[(Ca^{2+})_{cyt}]$, which might result in the suppression of cell death reactions and/or immune responses. Especially HvLFG1 seems to affect processes associated with penetration resistance, as shown for HvBI-1 and MLO. In contrast to HvBI-1, overexpression of HvLFG1 was not able to restore susceptibility to *Bgh* in the resistant barley backcross line BCPallas*mlo5*, when transiently overexpressed (data not shown, HÜCKELHOVEN et al. 2003).

AAL toxin treatment leads to the inhibition of sphingolipid biosynthesis, resulting in cell death (SPASSIEVA et al. 2002). *Atlfg* mutants showed a tendency to enhanced sensitivity to AAL toxin treatments (fig. 3.7), suggesting plant LFG proteins to be cell death inhibitors. Biotrophic fungi are assumed to actively suppress host cell death (JOHAL et al. 1995). Therefore, LFG proteins might mediate susceptibility to powdery mildew fungi by preventing cell death reactions, possibly through regulating $[(Ca^{2+})_{cyt}]$. By reducing Ca^{2+} influx, LFG proteins might also suppress other processes leading to penetration resistance to powdery mildew fungi, as assumed for BI-1. Ca^{2+} regulation might therefore be the functional link between BI-1 and LFG.

AtLFG2, also named BIL4, is supposed to be a positive regulator in brassinosteroid (BR) signaling (YAMAGAMI et al. 2009). BRs play pivotal roles in plant growth,

development, and responses to biotic and abiotic stress (Krishna 2003). Exogenous application of brassinolide (BL), the biologically most active BR hormone, to tobacco and rice induced resistance to tobacco mosaic virus, *Pseudomonas syringae*, *Oidium* sp., and to *Magnaporthe grisea* (now *oryzae*) and *Xanthomonas oryzae*, respectively (Nakashita et al. 2003). Besides increased crop yield, field application of BL to barley plants resulted in enhanced resistance to mixed fungal pathogens as well (Pshenichnaya et al. 1997). In contrast to that, in *Arabidopsis* an antagonistic interplay between PTI and BR signaling has been proposed, since Chinchilla et al. (2007) identified BAK1, as an interaction partner of FLS2 and EFR. BAK1 is also a coreceptor of BR INSENSITIVE 1 (BRI1) in BR signaling (Nam and Li 2002). Albrecht et al. (2011) recently showed that exogenously induced BR signaling in *Arabidopsis* does not lead to the onset of typical defense responses but rather to a suppression of early events in PTI, downstream or independent of BAK1, when co-applied with flg22, elf18, or chitin. BR signaling further contributes to stress prevention and cell wall loosening (Zurek et al. 1994, Che et al. 2010), attributes suggested to promote haustoria-forming fungi (Hückelhoven 2007a). These findings would go along with my results. The *AtLFG2 OE* mutant is supposed to exhibit enhanced BR signaling, as previously shown for the activation tagging mutant *bil4-1D* and the overexpression mutant *BIL4-OX* (Yamagami et al. 2009), and showed enhanced susceptibility to *E. cruciferarum*. Vice versa, lack of the putative positive BR synthesis regulator in *Atlfg2* mutants led to enhanced resistance. Since I observed analogous effects on *AtLFG1* mutants, one may speculate a potential function of AtLFG1 and AtLFG2 in BR signaling leading to enhanced susceptibility to powdery mildew fungi. However, I have no further evidence for a role of AtLFG1 or AtLFG2 in BR signaling. In contrast to *bil4-1D* and *BIL4-OX*, all *AtLFG* mutants used here showed wild type-like growth phenotypes. To what extent the discussed role of BRs might be relevant for the HvLFG1-mediated susceptibility to *Bgh* remains to be addressed as well.

Preliminary results indicate a *Bgh*-dependently elevated *HvLFG1* expression in barley cv. Ingrid leaves, mainly in the epidermal tissue, where the physical plant - fungus interaction takes place (supplementary figure 10). The expression of *HvLFG1* in the epidermis is a prerequisite for reliable results of transient overexpression and TIGS experiments. The expression seems to be enhanced 12 and 48 hai, coinciding with appressorium formation and a later stage, where haustoria are established, and

elongated secondary hyphae develop. Public microarray data analyzed in PLEXdb (Plant Expression Database, http://plexdb.org, DASH et al. 2012) show inconsistent expression profiles for *HvLFG1* as well as for *HvLFG2-5* during the barley - *Bgh* interaction. At least *HvLFG1* might have an unfavorable secondary structure, since it turned out as difficult to amplify. In recent experiments, *HvLFG4* and *HvLFG5* showed no *Bgh*-responsive expression (S. Rankl, TUM, personal communication).

Moreover, first results indicate an enhanced *AtLFG2* expression in wild type plants 24 h upon *E. cruciferarum* inoculation (supplementary figure 11). Gene-expression analysis of *AtLFG1* failed, maybe due to a constitutively low expression and/or an unfavorable secondary structure. Public expression data, analyzed in Genevestigator, show an enhanced *AtLFG2* expression upon inoculation with the adapted powdery mildew fungus *G. cichoracearum* and with the non-adapted barley powdery mildew fungus *Bgh* in Col-0. According to this data, *AtLFG1* and *AtLFG3-5* are hardly powdery mildew-regulated. However, since AtLFG1 was demonstrated to be involved in mediating susceptibility to *E. cruciferarum*, a role of AtLFG3-5 in similar processes cannot be excluded.

No differences in macroscopic *E. cruciferarum* phenotypes were visible on *AtLFG* mutants when compared to the wild type. Therefore, AtLFG1, AtLFG2, and maybe other AtLFG proteins might act redundantly. Double mutants would be a good tool to further study the role of AtLFG proteins in response to biotic and abiotic stress. And transgenic barley plants over- or underexpressing *HvLFG1*, will serve as tools in further investigations concerning the role of HvLFG1 during cell death reactions and challenges with pathogens. Whether HvLFG2-5 are involved in the barley - *Bgh* interaction as well, remains to be examined. Latest transient overexpression experiments suggest at least HvLFG5 to be involved in mediating susceptibility to *Bgh* as well (S. Rankl, TUM, personal communication).

Together, LFG proteins seem to have a conserved function in mediating susceptibility to powdery mildew fungi. Whether the underlying mechanisms in dicot *Arabidopsis* and monocot barley plants are based on LFG-regulated Ca^{2+} dynamics, leading to the suppression of cell death and immune responses, remains to be investigated in detail. Especially in *Arabidopsis*, a role of LFG proteins in BR signaling might be involved in promoting compatible plant - powdery mildew interactions.

4.1.2 Subcellular localization of GFP-LFG fusion proteins in barley and *Arabidopsis*

In mammals, LFG proteins localize to endomembrane structures, mainly to the Golgi apparatus (GUBSER et al. 2007, SHUKLA et al. 2010, NIELSEN et al. 2011). In order to get an idea about the subcellular localization of HvLFG1, AtLFG1, and AtLFG2, I examined transiently transformed single barley and *Arabidopsis* cells, expressing GFP fusion constructs.

Localization studies of GFP-AtLFG1 and GFP-AtLFG2 in transiently transformed *Arabidopsis* cells, respectively, were difficult. Both proteins are predicted to be localized in the PM, in the tonoplast, in the ER, and/or in the Golgi apparatus (WoLF PSORT). GFP-AtLFG1 accumulated in the PM, in cytoplasmic strands and in punctate structures that did not co-localize with the Golgi marker GmMAN1-RFP (YANG et al. 2005). Moreover, in other cells, GFP-AtLFG1 seemed to localize within the vacuole (fig. 3.6). As GFP-AtLFG1, GFP-AtLFG2 localized in the PM, in cytoplasmic strands, and in punctate structures. In contrast to GFP-AtLFG1, GFP-AtLFG2 co-accumulated with GmMAN1-labeld Golgi organelles and might be also located to the ER. Additionally, I detected GFP-AtLFG2 in the nucleus (fig. 3.6). Whether AtLFG proteins also accumulate in the tonoplast, as predicted, remains to be elucidated in further studies.

According to WoLF PSORT, HvLFG1 should reside in the tonoplast, in the PM, and/or in Golgi organelles. During my localization studies, a functional GFP-HvLFG1 fusion protein localized in the PM, confirmed by plasmolysis, and in punctate structures (fig. 3.2A,B), which were identified in further studies most likely as early endosomes (R. Eichmann, TUM, personal communication). A co-localization with Golgi organelles was not observed.

Next, transiently transformed barley leaf segments were inoculated with *Bgh*. In incompatible interactions, GFP-HvLFG1 localization was predominant in the PM and frequently in endosomes. I observed an additional weak accumulation at the site of non-successful attempted penetration (fig. 3.2E). In addition to the PM and endosomes, a localization of GFP-HvLFG1 around the haustoria was detectable in successfully *Bgh*-penetrated cells, associated with the PM and/or the tonoplast. Moreover, big moving GFP-HvLFG1-labeled bubble-like and tubular structures appeared two days after inoculation (fig. 3.2D), reminiscent of vacuolar compartments (REISEN et al. 2005, HIGAKI et al. 2006). Experiments with the tonoplast

marker rice two-pore K^+ channel isoform b (OsTPKb)-RFP (ISAYENKOV et al. 2011) revealed a localization or translocation of GFP-HvLFG1 in the tonoplast (R. Eichmann, TUM, personal communication). Besides the ER, the apoplast and the vacuole serve as Ca^{2+} stores (DODD et al. 2010). Therefore, the accumulation of GFP-HvLFG1 to both compartments goes with the assumption that HvLFG1 might support *Bgh* entry by suppressing cell death through regulating $[(Ca^{2+})_{cyt}]$. HvLFG1 might form or regulate a Ca^{2+} pore in the tonoplast and/or in the PM, as shown for BI-1 in the ER (CHAE et al. 2004, WESTPHALEN et al. 2005, XU et al. 2008, BULTYNCK et al. 2011). Generally, from two days upon *Bgh* inoculation onwards, a vacuolar reorganization seems to take place. Vacuolar reorganization, associated with enhanced endocytosis, might promote nutrient uptake through fungal haustoria. However, the underlying mechanisms need to be investigated in more detail.

Further studies are required to shed light on the subcellular localization and mechanisms of LFG proteins, in particular during plant - powdery mildew interactions.

4.2 BI-1 seems to act independently of MLO and does not require CaM to fulfill the function as susceptibility factor to *Bgh*

The MLO protein is the major susceptibility factor in barley - powdery mildew interactions. Barley *mlo* mutants display complete, race-non-specific resistance to all isolates of *Bgh* so far tested (JØRGENSEN 1992, PANSTRUGA 2005). Like BI-1, the plasma membrane-localized MLO protein possesses seven transmembrane domains and is a negative regulator of (developmental) cell death (BÜSCHGES et al. 1997, PIFFANELLI et al. 2002). Moreover, *BI-1* and *MLO* are both expressed in response to biotic stress (SANCHEZ et al. 2000, HÜCKELHOVEN et al. 2001, PIFFANELLI et al. 2002), and transient overexpression of *BI-1* and *MLO*, respectively, suppresses penetration resistance in already susceptible barley genotypes and in the nonhost interaction with *Bgt* (ELLIOT et al. 2002, HÜCKELHOVEN et al. 2003, EICHMANN et al. 2004, 2006b). Due to these similarities, it has been assumed that both proteins function in the same pathway. Since transient overexpression of *HvBI-1* can break *mlo*-mediated resistance to *Bgh*, a role of BI-1 as upstream factor in the MLO pathway has been excluded (HÜCKELHOVEN et al. 2003). Simultaneous co-overexpression of BI-1 and MLO resulted in only slightly enhanced susceptibility to *Bgt* compared to single overexpression experiments, which has been considered as a non-additive effect

(EICHMANN et al. 2004). Therefore, it has been hypothesized that BI-1 functions downstream or independently of MLO rather than synergistically (HÜCKELHOVEN et al. 2003, EICHMANN et al. 2004). However, merging pathways cannot be ruled out, since the effect of MLO in the co-expression experiments with BI-1 might already have reached the possible limit of susceptibility to *Bgt*. Here, I pursued the question whether BI-1 is a downstream component in MLO-mediated signaling. I could demonstrate that TIGS of *BI-1* did not affect MLO-mediated supersusceptibility to *Bgh*, although TIGS of BI-1 alone strongly limits susceptibility by using the same construct. This indicates that BI-1 does not act downstream of MLO (fig. 3.8, EICHMANN et al. 2010). Whether BI-1 and MLO function in parallel or in converging pathways remains to be elucidated.

KIM and co-workers (2002a,b) demonstrated an interaction of MLO with the cytoplasmic calcium sensor CaM, which is required for full susceptibility to *Bgh*. It has been suggested that Ca^{2+} and CaM are crucial components during successful penetration processes of barley powdery mildew fungi (PANSTRUGA 2003). In 2007, IHARA-OHORI et al. demonstrated the interaction of CaM with the C-terminus of AtBI-1. This interaction turned out to be crucial for AtBI-1-mediated cell death suppression (KAWAI-YAMADA et al. 2009). Therefore, the question arose whether CaM is required in BI-1-mediated susceptibility to *Bgh*. My results showed that TIGS of *CaM* did not suppress BI-1-mediated supersusceptibility to *Bgh* (fig 3.9). Therefore, CaM is most likely no essential signal component in BI-1-mediated signaling towards susceptibility to the barley powdery mildew fungus.

Together, analysis of putative elements of BI-1-dependent signaling in susceptibility to *Bgh* revealed that BI-1 probably acts synergistically or independently of MLO. Moreover, my findings do not support an essential role of CaM in BI-1-mediated susceptibility to *Bgh*.

However, a role of BI-1 in Ca^{2+} signaling was already demonstrated in mammals and has been suggested for plants (CHAE et al. 2004, WESTPHALEN et al. 2005, IHARA-OHORI et al. 2007, XU et al. 2008). In mammals, overexpression of BI-1 reduces the Ca^{2+} concentration in the ER lumen $[(Ca^{2+})_{ER}]$ upon ER stress stimulation. This is accompanied by reduced Ca^{2+} fluxes into the cytosol and goes along with enhanced rates of Ca^{2+} leakage from the ER. The lack of BI-1 results in the opposite effects (CHAE et al. 2004, WESTPHALEN et al. 2005, XU et al. 2008). In mammalian cells, BI-1 functions downstream of Bcl-2 family members and independently or in parallel to

Bax by regulating ER-releasable Ca^{2+} (Xu et al. 2008). Only recently, BULTYNCK et al. (2011) proposed a function of BI-1's C-terminus as an independent Ca^{2+}-permeable channel pore. At least three BI-1 proteins are assumed to be required for a functional pore (BULTYNCK et al. 2011). This goes along with findings from KIM and co-workers (2008), who reported a pH-dependent oligomerization of BI-1. IHARA-OHORI and co-workers (2007) suggested AtBI-1 to be involved in Ca^{2+} homeostasis since AtBI-1, besides interacting with Ca^{2+}-sensing CaM, failed to rescue Bax-induced cell death of yeast mutants lacking a Ca^{2+} ATPase. Moreover, I observed an oligomerization of AtBI-1-GFP even under reducing conditions (supplementary figure 12). This supports a role of plant BI-1 proteins in Ca^{2+} regulation, maybe by forming a pore in the ER through oligomerization as well. Further investigations contributing to the elucidation of the role of Ca^{2+} homeostasis during barley - *Bgh* interactions are eligible.

4.3 Co-immunoprecipitation-based identification of putative AtBI-1-interacting proteins

I conducted a co-IP to identify putative AtBI-1-interacting proteins that might be involved in susceptibility to powdery mildew fungi and/or in suppression of cell death reactions. Western blot analysis, silver staining, and LC-MS/MS-derived data confirmed a successful co-IP (fig.3.10).

In the total protein extract as well as in the AtBI-1-GFP co-immunoprecipitate, I detected an AtBI-1-GFP band at about 55 kDa as expected, but also a more pronounced band of a lower molecular weight than predicted from the primary AA sequence. COWLING and BIRNBOIM (1998) showed that human BI-1 was also running as a lower band on SDS gels than expected. Moreover, they demonstrated that human BI-1 was resistant to V8 and trypsin proteolysis. This might also explain the detection of only one AtBI-1 peptide compared to eleven GFP peptides in the AtBI-1-GFP co-immunoprecipitate.

HEMRAJANI et al. (2010) identified mammalian BI-1 as a target of NleH effectors of *Escherichia coli*, which leads to the inhibition of apoptosis. No putative fungal effector candidates were identified with the used approach. However, available protein sequences of *E. cruciferarum* and *Bgh* were limited at the time point of analysis.

The high number of AtBI-1-GFP co-immunoprecipitated proteins, associated with chloroplasts (25%) might hint at a chloroplast-associated function of AtBI-1. Upon

Bgh inoculation, the expression of BI-1 is enhanced in the epidermal tissue but also in the mesophyll of barley (HÜCKELHOVEN et al. 2003, EICHMANN et al. 2010). Moreover, barley *BI-1-GFP* overexpressing mutants contain higher chlorophyll contents as wild type plants (BABAEIZAD 2009). Furthermore, *AtBI-1* overexpression elevated the chlorophyll content upon treatment with cyclopiazonic acid, a specific inhibitor of sarcoplasmic/endoplasmic reticulum Ca^{2+} ATPase (SERCA), compared to the wild type and *AtBI-1* knock-out mutants (IHARA-OHORI et al. 2007). 21% of the AtBI-1-GFP co-immunoprecipitated proteins seem to be involved in general metabolic processes. Previous experiments revealed the differential expression of several chloroplast- and general metabolism-associated genes during compatible plant - powdery mildew interactions, likely supporting fungal nutrition (EICHMANN et al. 2006a, FABRO et al. 2008, CHANDRAN et al. 2010).

However, in this work the selection of putative AtBI-1-interacting candidate proteins relied on their presumed BI-1-associated function in cell death suppression and susceptibility to powdery mildew fungi as well as on the predicted subcellular localization (supplementary table 2). Therefore, chloroplast-associated proteins were excluded, since the actual physical plant - powdery mildew interaction is limited to chloroplast-free epidermal cells. AtBI-1-interacting candidates were selected predominantly according to their presumed BI-1-associated function in plant - powdery mildew interactions, in cell death reactions, and/or in biotic stress regulation. A further selection criterion was the predicted subcellular localization. The following eight mostly membrane-associated AtBI-1-interacting candidate proteins were selected: HAP6, TRN1, VHA-A, AHA1, MYHC, CYP83A1, GPI, and PHB2 (chapter 3.3).

Besides the chosen putative AtBI-1-interacting candidate proteins, several other AtBI-1-GFP co-immunoprecipitated proteins might be interesting candidates for further investigations (supplementary table 1).

4.4 Analysis of selected BI-1-interacting candidate proteins

The putative AtBI-1-interacting proteins HAP6, PHB2, CYP83A1, VHA-1, and AHA1 were analyzed concerning their role during biotic and abiotic stress responses. HAP6, PHB2, and CYP83A1 had an influence on the *Arabidopsis - E. cruciferarum* pathosystem and in cell death responses. Therefore, these three candidates are the most promising AtBI-1-interacting candidate proteins (see below), whereas no macroscopic *E. cruciferarum* phenotype was observed on *VHA-A* and *AHA1* T-DNA insertion lines, compared to the wild type. In former experiments, no apparently visible *E. cruciferarum* phenotype was visible on *atbi-1* mutants as well. However, a slightly reduced conidiophore production was observable (R. Eichmann, TUM, personal communication). Since at least three *Arabidopsis* BI-1 homologs were identified (AtBI-1, AtBI-2, and AtBI-3), redundant functions can be assumed (LAM et al. 2001). The same might be true for AHA1, one of 11 members of the PM H^+-ATPase gene family in *Arabidopsis* (ELMORE and COAKER 2011). LIU et al. (2009) already discussed redundant functions of AHA1 and AHA2. Since several working groups demonstrated a function of PM H^+-ATPases in plant - pathogen interactions, and especially given that in barley PM H^+-ATPases are suggested to be involved in HR-mediated resistance to *Bgh,* AHA1 and AHA2 are still interesting candidates (ZHOU et al. 2000, FINNI et al. 2002, LIU et al. 2009, KEINATH et al. 2010). Moreover, some phytotoxins, such as fumonisin B1 and fusicoccin, are known to affect PM H^+-ATPase activity (BAUNSGAARD et al. 1998, GUTIÉRREZ-NÁJERA et al. 2005, ELMORE and COAKER 2011). Interestingly, WATANABE and LAM (2006) demonstrated that two *atbi-1* mutants are more sensitive to fumonisin B1. Since Ca^{2+} and ROS regulate PM H^+-ATPases (KIM et al. 2010), one might assume that BI-1 inhibits PM H^+-ATPases activity by regulating Ca^{2+} and ROS.

V-ATPases consist of the two subclomplexes V_1 and V_0, which are again subdivided into subunits. VHA-A is one out of eight subunits (A-H) of the peripheral V_1 complex that is responsible for ATP hydrolysis. The V_0 complex is responsible for the proton translocation into the lumen of endomembrane compartments (DETTMER et al. 2005). I could not observe a role of *HvVHA-A* during the compatible barley - *Bgh* interaction by transiently overexpressing the gene (fig. 3.21A). However, since HvVHA-A is part of a complex, TIGS of *HvVHA-A* might result in an altered penetration success of the fungus. Public expression data analyzed in PLEXdb (experiment AT59) show that neither *AHA1* nor *VHA-A* are *G. orontii*-dependently regulated. Interestingly, the

VHA-A T-DNA insertion line SALK_089595C was more sensitive to cell death inducing treatments, compared to Col-0. Since in animals V-ATPase activity was shown to be involved in the regulation of BI-1-mediated ER stress responses (LEE et al. 2011), this might be a good starting point for future investigations.

The amplification of *HvTRN1* and *HvAHA1* coding sequence failed. Therefore, these interesting candidate proteins were not further investigated in the barley - *Bgh* pathosystem. HvGPI and HvMYHC were analyzed in the barley - *Bgh* interaction, exclusively. Although HvGPI was a promising candidate (see chapter 4.3), transient overexpression of *HvGPI* in single barley epidermal cells did not affect the penetration success of the fungus (fig. 3.21A). Interestingly, the transient overexpression as well as TIGS of *HvMYHC* in barley epidermal cells resulted in a significantly enhanced penetration success of *Bgh*, compared to control cells, respectively (fig.3.21). This might indicated that HvMYHC is involved in the regulation of general processes rather than in specific plant - pathogen interactions. One scenario might be that the transport of putative pathogenesis-associated cargo proteins could be impaired upon overexpressing or knocking-down *HvMYHC*, leading to susceptibility to *Bgh*. UEDA et al. (2010) demonstrated altered ER dynamics and actin filament bundle orientations in *Arabidopsis* MYOSIN XI-K-deficient mutants. Therefore, the disturbance of HvMYHC expression via transiently transforming barley epidermal cells might affect the ER movement pattern and the actin cytoskeleton organisation. RNAi off-target prediction by using SI-FI software tool (http://labtools.ipk-gatersleben.de/) identified a second off-target, namely BAJ93613, a protein with uncharacterized function, which could be also responsible for the enhanced susceptibility to *Bgh* in the TIGS experiment. The annotation of the AtBI-1-GFP-co-immunoprecipitated *Arabidopsis* MYHC remains cryptic, since no obvious MYOSIN HEAVY CHAIN-typical domain could be found in the AA sequence using InterProScan or NCBI. Interestingly, according to NCBI, the barley homolog HvMYHC possesses a V-SNARE domain (pfam05008), and InterProScan identified a twin-arginine translocation pathway signal sequence (IPR006311). However, it would be interesting to further elucidate the underlying mechanisms of HvMYHC in the barley - *Bgh* interaction.

4.4.1 PROHIBITIN 2 (PHB2)

Arabidopsis PHB proteins belong to a larger SPFH (STOMATIN, PROHIBITIN, FLOTILLIN, and HIGH FREQUENCY LYSOGENIZATION K AND C) superfamily. The *Arabidopsis* PHB family itself consists of seven genes (VAN AKEN et al. 2010). Plant PHBs are predicted to be localized in the mitochondrial fraction, probably to the inner mitochondrial membrane (IMM), as shown for yeast and mammalian PHBs (IKONEN et al. 1995, SNEDDEN and FROMM 1997, MILLAR et al. 2001, HEAZLEWOOD et al. 2004, TATSUTA et al. 2005). Here, localization studies revealed an accumulation of *Arabidopsis* PHB2-RFP to mitochondria in transiently transformed *Arabidopsis* (not shown) and tobacco cells. Co-localization studies with PHB2-RFP and the ER- and nuclear envelope-resident AtBI-1-GFP demonstrated small putative contact points, predominantly around the nucleus (fig. 3.14). Preliminary localization studies of an HvPHB2-GFP fusion protein demonstrated a potential accumulation in the mitochondria as well (not shown). The ER contains several attachment-domains to diverse organelles, such as the mitochondria (STAEHELIN 1997, FRIEDMAN and VOELTZ 2011). In yeast and mammalians, tethering proteins have already been identified, which regulate the contact of both dynamic organelles and therefore the functional connection, for instance in regulation of Ca^{2+} signaling-mediated apoptosis (HOPPINS et al. 2007, DE BRITO and SCORRANO 2008, KORNMANN et al. 2009, IWASAWA et al. 2011).

The function of *Arabidopsis* *PHB2* has not been analyzed specifically, so far. However, diverse biological functions are attributed to a couple of plant PHBs. Besides developmental functions, PHBs are predicted to be involved in the regulation of senescence, ethylene signaling, oxidative stress prevention, and mitochondrial biogenesis (CHEN et al. 2005, AHN et al. 2006, CHRISTIANS and LARSEN 2007). In animals, apoptosis is mostly initiated through the mitochondrial pathway, characterized by the occurrence of mitochondrial outer membrane permeability, leading to the release of caspase-activating molecules and other death effectors (GREEN and KROEMER 2004). Several studies indicated that plant PCD is regulated through similar processes (LAM et al. 2001).

In the present work, cell death-inducing AAL toxin and heat shock treatments provoked intensified symptoms on the *Arabidopsis PHB2* mutants, *phb2-1* and *phb2-2*, compared to the wild type (fig. 3.16A, supplementary table 3). Hence, a role of *Arabidopsis* PHB2 in stress-induced cell death suppression can be assumed, maybe

by interacting with AtBI-1 in the regulation of Ca^{2+} signaling or downstream of mitochondrial dysfunction. However, since PHBs are thought to be essential for mitochondrial homeostasis, the phenotype of the *phb2* mutants might be a common phenotype for mitochondrial damage under stress conditions as well.

Quite unexpectedly, both *Arabidopsis PHB2* knock-out mutants showed a tendency towards more susceptibility in the interaction with the adapted powdery mildew fungus *E. cruciferarum*, uncoupling toxin-induced cell death and resistance to biotrophs (fig. 3.11A). In contrast, transient overexpression of *HvPHB2* in Ingrid epidermal cells led to enhanced susceptibility to *Bgh*, while the knock-down did not alter the penetration success of the fungus (fig. 3.21). This indicates that the *PHB2*-dependent mechanisms during plant - powdery mildew interactions might be different in monocots and dicots. Although public microarray data (PLEXdb, experiment AT59) showed an upregulation of *Arabidopsis PHB2* 5 dai with *E. orontii*, the expression of *PHB2* during the compatible *Arabidopsis - E. cruciferarum* interaction was not obviously affected. Furthermore, no *AtBI-1*-dependent *PHB2* expression was observed (supplementary figure 13), whereas *HvPHB2* was apparently upregulated during pathogenesis of *Bgh* in a first experiment. The *Bgh*-dependent expression of barley *HvPHB2* was more pronounced in epidermal tissue (supplementary figure 10). Detailed analyses remain to be conducted to confirm an interaction between PHB2 and BI-1 proteins and its role in plant - powdery mildew interactions and cell death reactions.

4.4.2   HAPLESS 6 (HAP6)

HAP6 is a further promising putative AtBI-1-interacting protein, since it seems to be involved in the *Arabidopsis - E. cruciferarum* interaction and in cell death regulation. A slightly enhanced susceptibility to *E. cruciferarum* was observed on two independent *hap6* knock-down mutants, compared to the wild type (fig. 3.11B). Only heterozygous *hap6* mutants are cultivable, since a *hap6* mutation was found to hamper the growth of the pollen tube into the style (JOHNSON et al. 2004). Col-0 is a susceptible genotype. Therefore, a phenotype towards more susceptibility on compared mutants is hard to gain. A more pronounced effect towards enhanced resistance to *E. cruciferarum* might be detectable on mutants constitutively expressing *HAP6* under the control of a strong promoter. Public expression data analyzed in PLEXdb show an enhanced *HAP6* expression during a compatible

Arabidopsis - powdery mildew interaction (experiment AT59). Consistently, gene expression analysis indicated an *E. cruciferarum*-responsive *HAP6* expression as well. Moreover, the *E. cruciferarum*-induced *HAP6* expression seemed to be *AtBI-1*-dependent, indicating a possible transcriptional regulation of *HAP6* via *AtBI-1* (supplementary figure 13).

TIGS of *HvHAP6* in single barley epidermal cells led to a slightly enhanced penetration success of *Bgh* (fig. 3.21B). Since the full-length coding sequence of *HvHAP6* is available now, a transient overexpression experiment could be the next step to analyze the role of HvHAP6 in the barley - *Bgh* interaction. In a preliminary experiment, a *Bgh*-dependent *HvHAP6* expression was detectable in epidermal and mesophyll tissue, respectively (supplementary figure 10).

Until now, the knowledge about the function of HAP6 in plants, and especially during plant - pathogen interactions is limited. According to my results, one might assume a conserved function of HAP6 in the regulation of plant - powdery mildew interactions.

In *Arabidopsis*, the RLK FERONIA (FER) and AtMLO7, syn. NORTIA (NTA), function in pollen tube reception. In *fer* and *nta* mutants, pollen tubes show an overgrowth in the female gametophytes instead of bursting to release the sperm (ESCOBAR-RESTREPO et al. 2007, KESSLER et al. 2010). Interestingly, FER and several AtMLO proteins are involved in mediating susceptibility to powdery mildew fungi, linking pollen tube growth and fungal invasion (CONSONNI et al. 2006, KESSLER et al. 2010). In this context, vesicle transport-associated relocalization processes are discussed to be involved in both processes (KESSLER et al. 2010). Moreover, there are several evidences that lead ZOU et al. (2011) to the speculation that FER family members could act upstream of RAC/ROP signaling involved in NADPH oxidase-dependent ROS-mediated pollen tube growth.

The linkage of pollen tube growth and fungal invasion fits also to my results but in the opposite way. Here, *Arabidopsis hap6* mutants, impaired in pollen tube growth, showed an enhanced susceptibility to *E. cruciferarum*. Interestingly, unchallenged barley and *Arabidopsis mlo* mutants as well as *Arabidopsis fer* mutants develop spontaneous mesophyll cell death accompanied with H_2O_2 production (KESSLER et al. 2010). In contrast, the *hap6-1* mutant seemed to be more resistant to cell death-inducing treatments than wild type plants (fig. 3.16A, supplementary table 3).

HAP6 contains an almost entire protein-spanning RIBOPHORIN II domain (IPR008814, supplementary table 2), and was already mentioned as ortholog of

RIBOPHORIN II, an essential subunit of the yeast oligosaccharyltransferase (OST) complex, by LEROUXEL et al. (2005). The human RIBOPHORIN II protein localizes to the ER (CRIMAUDO et al. 1987). As expected, an *Arabidopsis* HAP6-mCherry fusion protein also accumulated in the ER and co-localized with AtBI-1-GFP in transiently transformed *Arabidopsis* cells (fig. 3.15). OSTs catalyze asparagin (N)-linked-glycosylation, a protein modification reaction accompanied with proper protein folding, which is highly conserved amongst eukaryotes (KNAUER and LEHLE 1999, KELLEHER and GILMORE 2006). In *Arabidopsis*, three OST subunits, DEFENDER AGAINST APOPTOTIC DEATH 1 (DAD1), DEFECTIVE GLYCOSYLATION1-1 (DGL1-1), and STAUROSPORINE- AND TEMPERATURE-SENSITIVE YEAST PROTEIN 3 (STT3), have already been characterized in some aspects. The analyses revealed a role of N-linked glycosylation in plant reproduction, growth, and development (GALLOIS et al. 1997, KOIWA et al. 2003, LEROUXEL et al. 2005). Moreover, regulatory functions during abiotic stress were discovered (KOIWA et al. 2003). For instance, DAD1 suppresses cell death upon UV-C irradiation (DANON et al. 2004).

However, HAP6 and its potential role in the plant OST complex are not well characterized. Given that disturbances in N-glycosylation lead to ER stress accompanied with cell death reactions, one could assume stronger cell death symptoms upon AAL toxin treatment or heat stress on *hap6* mutants compared to the wild type (CROSTI et al. 2001, HOEBERICHTS et al. 2007). Since leaves of *hap6-1* remained green and intact after cell death inducing treatments compared to Col-0, HAP6 might be a positive regulator of cell death. WATANABE and LAM (2008) demonstrated a role of AtBI-1 in the suppression of ER stress induced cell death. Therefore, HAP6 might likely act antagonistically by negatively regulating AtBI-1, leading to an enhanced cell death suppressing activity of AtBI-1 in the *hap6* mutant. Future studies are needed to uncover the mode of action of this interesting putative AtBI-1-interacting protein and to confirm a physical interaction between HAP6 and BI-1.

4.4.3 CYTOCHROME P450 83A1 (CYP83A1)

244 *CYTOCHROME P450* genes (and 28 pseudogenes) exist in the *Arabidopsis* genome. Strictly speaking, the CYP83 family phylogenetically belongs to the CYP71 family since it groups between the CYP71A and CYP71B subfamilies (HANSEN et al. 2001, BAK et al. 2011). The two members, CYP83A1 and CYP83B1, function non-redundantly in glycosinolate biosynthesis by catalyzing the initial conversion of aldoximes to thiohydroximates. Thereby, CYP83A1 has higher substrate specificity to methionine-derived aldoximes, while CYP83B1 preferentially catalyzes tryptophan-derived aldoximes, which are also the precursors of auxin (BAK and FEYEREISEN 2001, NAUR et al. 2003). HEMM et al. (2003) demonstrated a reduced level of aliphatic glycosinolates and a slightly increased level of indol-derived glucosinolates in *ref2* mutants. In cooperation with the Chair of Genetics (Dr. E. Glawischnig, TUM, Freising) the content of several glucosinolates was measured in *cyp83a1* and Col-0 leaves 5 dai with *E. cruciferarum* and in control leaves. The data confirmed the observations of HEMM et al. (2003). A pathogen-dependent influence on the glucosinolate contents was hardly detectable. Maybe a slight induction of 4-methoxy-indol-*3*-ylmethyl-glucosinolate can be assumed 5 dai with *E. cruciferarum* in both genotypes (supplementary figure 14). The same tendencies were observed in another biological experiment using *ref2-1* and Col-0 (data not shown). In contrast to HEMM et al. (2003), the *CYP83A1* mutants showed strong morphologic phenotypes, e.g. delayed development, under the conditions used (fig. 3.17). An impact of aliphatic glucosinolates on plant and inflorescence development has already been discussed. However, the underlying mechanisms are still unclear (CLOSSAIS-BESNARD and LARHER 1991, CHEN et al. 2003). In contrast, the role of glucosinolates, mostly indole-glycosinolates, in plant - herbivore interactions is described quite well (HOPKINS et al. 2009). However, the impact of CYP83 proteins in plant - pathogen interactions, specifically during the plant - powdery mildew interplay, is completely uncharacterized.

In most cases, P450 proteins are present in the ER (BAK et al. 2011). As expected, an *Arabidopsis* CYP83A1-mCherry fusion protein co-localized with AtBI-1-GFP in the ER and around the nucleus in transiently transformed *Arabidopsis c*ells (fig. 3.15).

A pronounced *E. cruciferarum* resistance phenotype was observed on *cyp83a1* and *ref2-1*, compared to Col-0 (fig. 3.12, fig. 3.13A). A generally enhanced *PR1* gene expression was not observed in *cyp83a1* mutants, when compared to Col-0 (data not

shown). Since indole-3-acetaldoxime is the branching point between auxin and glucosinolate biosynthesis (BAK et al. 2001), the lack of CYP83A1 might result in an enhanced biosynthesis of camalexin, a well known auxin-derived phytoalexin (GLAWISCHNIG 2007). Therefore, the content of this compound was determined as well (Dr. E. Glawischnig, TUM, Freising). However, since the content was even reduced in *cyp83a1* compared to Col-0 5 dai with *E. cruciferarum* (data not shown), camalexin can be excluded as responsible factor for the resistance phenotype.

A detailed analysis of fungal development 2 dai on Col-0 and *CYP83A1* mutants revealed no genotype-dependent differences in germination (data not shown). Interestringly, significantly more germinated spores were arrested at the pre-penetration stage on the *cyp83a1* mutants, compared to those on Col-0 (fig.3.13A).

Due to a reduced sinapate ester and lignin syringyl monomer contents in *ref2* mutants, a potential role of CYP83A1 in the phenylpropanoid pathway has been discussed (RUEGGER and CHAPPLE 2001, HEMM et al. 2003). Several CYP83 family members have been identified in plant species that do not belong to the order Capparales and do therefore not accumulate glucosinolates, giving a further argument for an involvement of these enzymes in other pathways (BILODEAU et al. 1999, SIMINSZKY et al. 1999). The observed cuticle phenotype of *cyp83a1* and *ref2-1* underpins this assumption (fig. 3.18). Several chytochrome P450 monooxygenases, such as members of the CYP86 family or CYP77A6, are involved in the biosynthesis of cutin monomers by the hydroxylation of C_{16} and C_{18} fatty acids. Mutations in respective genes resulted in cuticle defects (WELLESEN et al. 2001, XIAO et al. 2004, HÖFER et al. 2008, COMPAGNON et al. 2009, LI-BEISSON et al. 2009). CYP86A2-associated cutin biosynthesis seems to have an influence on bacterial type III gene expression (XIAO et al. 2004). Moreover, cutin monomers as well as cutin wax constituents are involved in germination and differentiation processes of fungal pathogens, as shown for very-long-chain aldehydes in barley, which promote prepenetration processes of *B. graminis* (FRANCIS et al. 1996, HANSJAKOB et al. 2010). ADAS et al. (1999) demonstrated a role of human P450 2E1 (see chapter 4.3) in the hydroxylation of free fatty acids, presumably as a process to maintain membrane integrity and therefore cell death, upon stress stimuli. Interestingly, the hydroxylation activity increased in the presence of the electron transfer protein cytochrome b_5 (ADAS et al. 1999). In *Arabidopsis*, NAGANO et al. (2009) showed the interaction of AtBI-1 with fatty acid 2-hydroxylases (AtFAHs) via cytochrome b_5

(AtCb5), which was suggested to be involved in cell death suppression. Therefore, it might be speculated that AtBI-1 interacts with CYP83A1, maybe via AtCb5, in the hydroxylation of fatty acids as well. In CYP83A1-deficient mutants, the content of free fatty acids might be enhanced, which could be responsible for the cuticle phenotype and maybe for the impaired fungal development.

Only a tendency to an increased amount of cell death reactions at the site of attempted penetrations was observed in both *CYP83A1* mutants 2 dai (fig. 3.13B). However, this observation might be more pronounced at a later point of time in pathogenesis of *E. cruciferarum*. Compared to the wild type, *cyp83a1* and *ref2-1* generally showed accelerated cell death reactions upon cell death-inducing AAL toxin and heat shock treatments (fig. 3.16, supplementary table 3). Moreover, unchallenged *CYP83A1* mutants showed spontaneous cell death reactions, which were promoted by long-day conditions (fig. 3.19). Therefore, one could assume a role of CYP83A1 in the prevention of cell death.

Several studies showed a relation between cuticle permeability and resistance to *B. cinerea*, associated with the release of antifungal compounds, such as ROS (BESSIRE et al. 2007, CHASSOT et al. 2007, L'HARIDON et al. 2011). However, *cyp83a1* and *ref2-1* are more susceptible to this necrotrophic fungus (fig. 3.20), reflecting a potential dual role of CYP83A1 in cuticle biosynthesis and cell death regulation. Consistently, *HvBI-1* over-expression in carrots results in partial resistance against *B. cinerea* (IMANI et al. 2006).

In mammals, BI-1 was shown to inhibit ROS production and resulting cell death by mediating the destabilization of the NADPH-dependent cytochrome P450 reductase (NPR)-cytochrome P450 2E1 complex. Thereby, BI-1 interacts with NPR, and to a lesser extent with P450 2E1, which leads to a reduced electron transfer from NPR to P450 2E1 and thus reduced ROS production (KIM et al. 2009). Furthermore, the protein level of P450 2E1 is suggested to be regulated through BI-1-mediated enhancement of lysosomal activity (LEE et al. 2012). Whether similar processes occur in *Arabidopsis* plants is questionable, since CYP83A1-deficient mutants demonstrated enhanced cell death symptoms upon stress stimuli compared to the wild type.

AtBI-1-genotype-dependent gene expression of *CYP83A1* during the *Arabidopsis - E. cruciferarum* interaction was not consistent in repeated experiments (data not shown). Online microarray data indicate a strong downregulation of *CYP83A1* during

a compatible *Arabidopsis* - powdery mildew interaction (PLEXdb, experiment AT59), as well as during the interaction with *B. cinerea* (PLEXdb, experiment AT51). This might probably indicate an AtBI-1-mediated downregulation of *CYP83A1* during pathogenesis on the transcriptional level.

In barley, ECKEY et al. (2004) observed an upregulation of a *CYTOCHROME P450* gene during compatible and incompatible interactions with powdery mildew fungi. This barley P450 protein contains all three IPR domains identified in the *Arabidopsis* CYP83A1 protein (supplementary table 2). However, TIGS showed no significant functional impact on the penetration success of *Bgh* (ECKEY et al. 2004).

Interestingly, the glucosinolate pathway has often been discussed to be evolutionarily related to the pathway of the structurally related cyanogenic glucosides (POULTON and MØLLER 1993, HALKIER and DU 1997). In both pathways, orthologous CYP79 enzymes convert amino acids to oximes. Oximes are further catalyzed by CYP71s (in the cyanogenic glucoside synthesis) or by the phylogenetically related CYP83s (in the glucosinolate pathway) to intermediates, which are further converted enzymatically into cyanogenic glucosides or glucosinolates (HALKIER et al. 1995, ANDERSEN et al. 2000, NIELSEN and MØLLER 2000, BAK et al. 2001, BAK and FEYEREISEN 2001, HANSEN et al. 2001, NAUR et al. 2003). The formations of enzyme complexes, so-called metabolons, lead to fast and efficient reactions of instable and/or toxic intermediates to stable and/or non-toxic compounds (JØRGENSEN et al. 2005). Dynamic dissociation processes of cyanogenic glucosides and glucosinolate metabolons might result in an enhanced production of free oximes, known to be toxic to fungi (DRUMM et al. 1995, MØLLER 2010). SAKURADA et al. (2009) reported the effect of oximes on mitochondria, leading to mitochondrial dysfunction, lipid peroxidation and the generation of ROS. Therefore, it cannot be excluded that in CYP83A1-deficient mutants, an accumulation of aldoximes could lead to a poisoning of the fungus during or short after penetration. Further investigations are needed to confirm the interaction of AtBI-1 with CYP83A1. In future studies, it will be a challenge to investigate the potential role of CYP83A1 proteins in AtBI-1-mediated susceptibility to powdery mildew fungi and cell death suppression, and the underlying molecular biologic mechanisms.

Together, the approach used was successful regarding the identified putative AtBI-1-interacting proteins. Several analyzed candidate proteins showed a function in AtBI-

1-associated processes, namely in the interaction with powdery mildew fungi and in the regulation of cell death. Moreover, the generated co-IP data constitute the basis of future research projects to further elucidate the mode of action of BI-1.

4.5 Conclusion

4.5.1 Postulated function of LFG proteins and of the BI-1-linked signaling components MLO and CaM in plant - powdery mildew interactions

The conserved cell death suppressor protein BI-1 functions as susceptibility factor to *Bgh* (HÜCKELHOVEN et al. 2003, EICHMANN et al. 2010). BI-1-mediated cell death suppression is associated with the regulation of cytosolic Ca^{2+} influx, which is also discussed to be important in the BI-1-mediated susceptibility to powdery mildew fungi (EICHMANN et al. 2010). Here, BI-1-related LFG proteins were identified as conserved susceptibility factors to powdery mildew fungi in *Arabidopsis* and barley. Therefore, and since mammalian LFG proteins are also associated with Ca^{2+}-regulation-mediated apoptosis-like cell death inhibition (DE MATTIA et al. 2009, ROJAS-RIVERA et al. 2012), a function of plant LFG proteins in the regulation of Ca^{2+}-flux might be postulated. Since GFP-LFG fusion proteins localized to the plasma membrane and most likely to the tonoplast, LFG is supposed to regulate the releasable $[Ca^{2+}]$ in the apoplast and/or the vacuole. This could lead to the suppression of cell death and defense reactions, such as callose deposition, H_2O_2 generation, and actin reorganization, supporting powdery mildew fungi.

Investigations on the role of the two potential BI-1-linked signaling components CaM and MLO in the barley - *Bgh* interaction led to following conclusions: Although CaM is required for full MLO-mediated susceptibility to *Bgh* in barley and for AtBI-1-mediated cell death suppression in *Arabidopsis* (KIM et al. 2000b, KAWAI-YAMADA et al. 2009), a role of CaM as potential component in HvBI-1-mediated signaling toward *Bgh* is unlikely, since TIGS of *CaM* did not suppress BI-1-mediated supersusceptibility to *Bgh*. Due to structural and functional similarities and since *mlo5*-mediated resistance can be overcome by the overexpression of *HvBI-1*, BI-1 and MLO have been discussed to function in the same pathway (HÜCKEHOVEN et al. 2003, EICHMANN et al. 2004). However, supersusceptibility mediated by *MLO* overexpression was not reduced by simultaneous knock-down of *BI-1* in a transient transformation assay

here, indicating that BI-1 acts independently or synergistically to rather than downstream of MLO.

4.5.2 General considerations on the function of putative BI-1-interacting proteins in compatible plant - powdery mildew interactions and in cell death regulation

Based on LC-MS/MS data of a successful AtBI-1-GFP co-immunoprecipitation assay, selected putative AtBI-1-interacting proteins were analyzed concerning their function during biotic and abiotic stress. Dependent on literature and on results of this study, a general consideration on the function of PHB2, HAP6, and CYP83A1 in BI-1-associated processes, namely in compatible plant - powdery mildew interactions and in cell death suppression, is given here.

Plant PHBs are involved in diverse processes associated with cell death regulation (CHEN et al. 2005, AHN et al. 2006, CHRISTIANS and LARSEN 2007). Consistent with this, two independent *Arabidopsis phb2* mutants were more sensitive to AAL toxin and heat shock treatment compared to Col-0, indicating a function of PHB2 in cell death suppression. Thereby PHB2, which is localized to mitochondria, could function together with the ER-resident BI-1 protein through ER-mitochondria attachment domains in regulating Ca^{2+} signaling leading to cell death inhibition. The role of PHB2 proteins in compatible plant - powdery mildew interactions is unclear, since on *Arabidopsis phb2* mutants, an accelerated fungal development was observed, and transient overexpression of *HvPHB2* in barley epidermal cells promoted the penetration efficiency of *Bgh*. Whether the *E. cruciferarum* phenotype of the *phb2* mutants is a common phenotype for mitochondrial damage under stress conditions or whether the role of PHB2 proteins in plant - powdery mildew interactions differs in monocots and dicots remains to be elucidated.

HAP6 is involved in pollen tube growth and suggested to be part of the OST complex (JOHNSON et al. 2004, LEROUXEL et al. 2005). Compared to wild type plants, on *Arabidopsis hap6* mutants an accelerated *E. cruciferarum* development could be observed, giving cause to the assumption that HAP6 is involved in resistance-associated processes towards powdery mildew fungi. Moreover, *HAP6* expression seemed to be AtBI-1- and *E. cruciferarum*-dependently regulated in *Arabidopsis*, and to be *Bgh*-regulated in barley. A linkage between pollen tube growth and fungal

invasion has been shown for FER and NTA, possibly involving vesicle transport-associated relocalization processes (ESCOBAR-RESTREPO et al. 2007, KESSLER et al. 2010). Therefore, HAP6 might be involved in such mechanisms as well. Furthermore, *Arabidopsis* HAP6 turned out as possible positive regulator of stress-induced cell death reactions. All these results led to the assumption that HAP6 functions antagonistically to BI-1, maybe by negatively regulating BI-1.

In glucosinolate biosynthesis, CYP83A1 catalyzes the initial conversion of methionine-derived aldoximes to thiohydroximates (BAK and FEYEREISEN 2001, NAUR et al. 2003). Here, CYP83A1 turned out to be ER-resistant and showed an impact in mediating susceptibility to *E. cruciferarum* and in cell death suppression, as shown for BI-1 proteins.
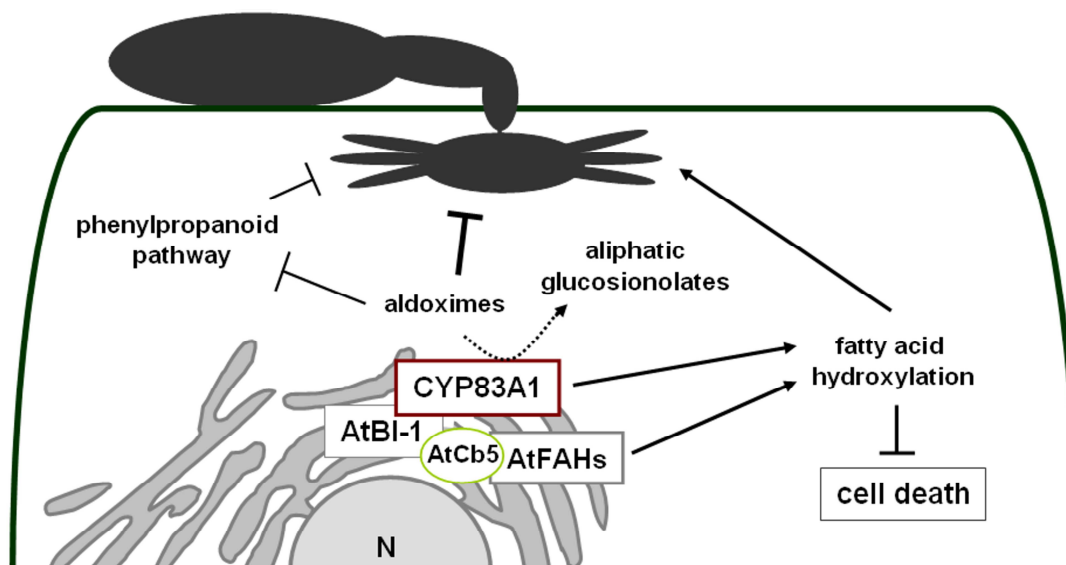
Fig. 4.2: Hypothetical model for the function of AtBI-1 and CYP83A1 in the compatible interaction of *Arabidopsis thaliana* (*At*) with powdery mildew fungi. CYTOCHROME P450 83A1 (CYP83A1) detoxifies aldoximes by catalyzing the initial conversion of methionine-derived aldoximes to thiohydroximates, which are further converted into aliphatic glucosinolates. Although aldoximes might inhibit the resistance-related phenylpropanoid pathway, their predominant effect in this plant - powdery mildew interaction might be the poisoning of the fungus. An interaction of *Arabidopsis* BAX INHIBITOR-1 (AtBI-1) with fatty acid 2-hydroxylases (AtFAHs) via cytochrome b_5 (AtCb5) leads to an enhancement of 2-hydroxylation of fatty acids, which is associated with cell death suppression. BI-1 might also interact with CYP83A1 in the hydroxylation of fatty acids, leading to the inhibition of cell death, supporting the development of the biotrophic powdery mildew fungus, and restricting necrotrophic fungi, such as *Botrytis cinerea*.

However, the *E. cruciferarum* resistance phenotype of the CYP83A1-deficient mutants might result from an enrichment in aldoximes, which are toxic to fungal pathogens (DRUMM et al. 1995), causing a poisoning of the fungus during the penetration progress. A potential role of CYP83A1 in the regulation of the phenylpropanoid pathway has been discussed as well (BILODEAU et al. 1999,

SIMINSZKY et al. 1999, HEMM et al. 2003). Due to a cuticle defect phenotype of *cyp83a1* mutants, a function of CYP83A1 in the hydroxylation of fatty acids is postulated here, as described for other chytochrome P450 monooxygenases (WELLESEN et al. 2001, XIAO et al. 2004, HÖFER et al. 2008, COMPAGNON et al. 2009, LI-BEISSON et al. 2009). The hydroxylation of free fatty acids could be involved in cell death prevention by maintaining the membrane integrity (ADAS et al. 1999). NAGANO et al. (2009) demonstrated the interaction of AtBI-1 with AtFAHs via AtCb5, which is supposed to be required for AtBI-1-mediated cell death suppression. Therefore, CYP83A1 might interact with AtBI-1, possibly also via AtCb5, in the hydroxylation of fatty acids, leading to cell death inhibition, promoting powdery mildew fungi and restricting the growth of necrotrophic pathogens, such as *B. cinerea*.

Together, the co-immunoprecipitation applied was successful in the identification of interesting putative AtBI-1-interacting proteins. The interaction of AtBI-1 with PHB2, HAP6, or CYP83A1 remains to be confirmed in future studies. Furthermore, it will be a challenge to elucidate mechanisms involving AtBI-1 and PHB2, HAP6, or CYP83A1 in resistance or susceptibility to powdery mildew fungi and in the regulation of cell death reactions.

5 Summary/Zusammenfassung

The conserved cell death suppressor protein BAX INHIBITOR-1 (BI-1) is involved in plant - pathogen interactions. In the pathosystem barley (*Hordeum vulgare*, *Hv*) - barley powdery mildew fungus (*Blumeria graminis* f.sp. *hordei*, *Bgh*) BI-1 was identified as susceptibility factor. LIFEGUARD (LFG) proteins are structurally related to BI-1 and suppress apoptotic-like cell death in animals. Barley and *Arabidopsis thaliana* (*At*) homologs have been identified. Transient and/or stable knock-out and overexpression experiments demonstrated that LFG proteins are also conserved regulators of susceptibility to powdery mildew fungi. Moreover, an impact of LFG proteins on cell death regulation can be assumed.

Investigations on the role of potential BI-1-linked signaling components should contribute to the elucidation of the mode of BI-1 during the barley - *Bgh* interaction. AtBI-1 interaction with CALMODULIN (CaM) is important for cell death suppression. However, CaM is likely not limiting for HvBI-1-mediated susceptibility towards *Bgh*.

BI-1 function in susceptibility to *Bgh* resembles that of MILDEW LOCUS O (MLO). Results presented here indicate that BI-1 likely acts independently to rather than downstream of MLO, since supersusceptibility mediated by MLO overexpression was not reduced by simultaneous knock-down of BI-1.

Heterologous overexpression of AtBI-1 enhanced penetration success of *Bgh* in barley epidermal cells, indicating functional conservation. A co-immunoprecipitation assay using AtBI-1-GFP overexpressing mutants identified 95 putative AtBI-1-interacting proteins. Selected candidates were investigated concerning their impact in BI-1-assosiated processes in *Arabidopsis* and/or barley. In *Arabidopsis*, PROHIBITIN 2 (PHB2), HAPLESS 6 (HAP6), and CYTOCHROME P450 83A1 (CYP83A1) had a function in the *Arabidopsis - Erysiphe cruciferarum* interaction and in regulation of stress-related cell death. Additionally, altered expression of barley homologs of PHB2 and a MYROSIN-HEAVY CHAIN-RELATED (MYHC) protein influenced the barley - *Bgh* interplay. Thus, the approach was successful in the identification of conserved elements of BI-1-related processes in monocot and dicot plants.

Together, investigations on BI-1, BI-1-like, and putative BI-1-interacting proteins demonstrated new insights into mechanisms involved in resistance or susceptibility to powdery mildew fungi and in the regulation of cell death reactions.

BAX INHIBITOR-1 ist ein konserviertes Zelltodsuppressor-Protein, das an verschiedenen Pflanze - Pathogen Interaktionen beteiligt ist. Im Pathosystem Gerste (*Hordeum vulgare*, *Hv*) - Echter Gerstenmehltaupilz (*Blumeria graminis* f.sp. *hordei*, *Bgh*) wurde BI-1 als Anfälligkeitsfaktor beschrieben. LIFEGUARD (LFG) Proteine ähneln BI-1 Proteinen in ihrere Struktur, und inhibieren im tierischen System Apoptose-assoziierten Zelltod. Sowohl in Gerste als auch in *Arabidopsis thaliana* (*At*) wurden Homologe identifiziert. In dieser Arbeit wurde durch transiente und/oder stabile Unter- und Überexpressionsexperimente gezeigt, dass LFG Proteine auch konservierte Anfälligkeitsregulatoren gegenüber Echten Mehltaupilzen sind. Darüber hinaus kann ein Einfluss von pflanzlichen LFG Proteinen in Zelltodregulationen angenommen werden.

Untersuchungen von potentiellen BI-1-vermittelten Signalweg-Komponenten sollten zur Aufklärung der Wirkungsweise von BI-1 in der Gersten - *Bgh* Interaktion beitragen. Die Interaktion von AtBI-1 mit CALMODULIN (CaM) ist wichtig für die Zelltodinhibition. Allerdings scheint CaM nicht essentiell für die HvBI-1-vermittelte Anfälligkeit gegenüber *Bgh* zu sein. Die Funktionen von BI-1 und MILDEW LOCUS O (MLO) in der Anfälligkeit gegenüber *Bgh* ähneln sich. Die hier gezeigten Ergebnisse demonstrieren, dass BI-1 eher unabhängig von MLO agiert als unterhalb im Signalweg, da in einem transienten Transformationsassay die durch MLO-Überexpression induzierte Super-Anfälligkeit nicht durch das gleichzeitige Herunterregulieren von BI-1 verringert werde konnte.

Die heterologe Überexpression von AtBI-1 erhöht den Penetrationserfolg von *Bgh* in Gerstenepidermiszellen und lässt eine konservierte Funktion von BI-1 Proteinen vermuten. Unter der Verwendung von *AtBI-1-GFP* überexpremierenden Mutanten wurde ein Co-Immunoprezipitationsassay durchgeführt und 95 putative AtBI-1-interagierende Proteine identifiziert. Ausgewählte Kandidaten wurden in *Arabidopsis*- und/oder Gerstenpflanzen hinsichtlich ihrer Funktion in BI-1-assoziierten Prozessen untersucht. *Arabidopsis* PROHIBITIN 2 (PHB2), HAPLESS 6 (HAP6), and CYTOCHROME P450 83A1 (CYP83A1) zeigten eine Funktion in der Interaktion von *Arabidopsis* mit *Erysiphe cruciferarum* und in der Regulation von Stress-induziertem Zelltod. In transienten Transformationsassays zeigte die veränderte Expression von PHB2 und eines MYROSIN-HEAVY CHAIN-RELATED (MYHC) Gerstenhomolgs einen Einfluss auf die Gerste - *Bgh* Interaktion. Demnach führte die angewandte Methode zur Identifizierung von konservierten Elementen von BI-1-assoziierten Prozessen in mono- und dicotylen Pflanzen.

Die Untersuchungen von BI-1, BI-1-ähnlichen und putativen BI-1 interagierenden Proteinen gewährten neue Einblicke in Resistenz- oder Anfälligkeitsmechanismen gegenüber Echten Mehltaupilzen und in Zelltodregulationsprozessen.

6 References

ADAS, F., SALAÜN, J.P., BERTHOU, F., PICART, D., SIMON, B. and AMET, Y. (1999) Requirement for omega and (omega;-1)-hydroxylations of fatty acids by human cytochromes P450 2E1 and 4A11. J Lipid Res. 40: 1990-97.

ADE, J., DEYOUNG, B.J., GOLSTEIN, C. and INNES, R.W. (2007) Indirect activation of a plant nucleotide binding site-leucine-rich repeat protein by a bacterial protease. Proc Natl Acad Sci U S A. 104: 2531-36.

AHN, C.S., LEE, J.H., REUM HWANG, A., KIM, W.T. and PAI, H.S. (2006) Prohibitin is involved in mitochondrial biogenesis in plants. Plant J. 46: 658-67.

ALBRECHT, C., BOUTROT, F., SEGONZAC, C., SCHWESSINGER, B., GIMENEZ-IBANEZ, S., CHINCHILLA, D., RATHJEN, J.P., DE VRIES, S.C. and ZIPFEL, C. (2011) Brassinosteroids inhibit pathogen-associated molecular pattern–triggered immune signaling independent of the receptor kinase BAK1. Proc Natl Acad Sci U S A. 109: 303-308.

AMES, G.F. (1974) Resolution of bacterial proteins by polyacrylamide gel electrophoresis on slabs. J Biol Chem. 249: 634-44.

ANDERSEN, M.D., BUSK, P.K., SVENDSEN, I. and MØLLER, B.L. (2000) Cytochromes P-450 from cassava (*Manihot esculenta* Crantz) catalyzing the first steps in the biosynthesis of the cyanogenic glucosides linamarin and lotaustralin. J Biol Chem. 275: 1966-75.

ASSAAD, F.F., QIU, J.L., YOUNGS, H., EHRHARDT, D., ZIMMERLI, L., KALDE, M., WANNER, G., PECK, S.C., EDWARDS, H., RAMONELL, K., SOMERVILLE, C.R. and THORDAL-CHRISTENSEN, H. (2004) The PEN1 syntaxin defines a novel cellular compartment upon fungal attack and is required for the timely assembly of papillae. Mol Biol Cell. 15: 5118-29.

AUSUBEL, F. M. (2005) Are innate immune signaling pathways in plants and animals conserved? Nature Immunol. 6: 973-79.

AZEVEDO, C., SADANANDOM, A., KITAGAWA, K., FREIALDENHOVEN, A., SHIRASU, K. and SCHULZE-LEFERT, P. (2002) The RAR1 interactor SGT1, an essential component of R gene-triggered disease resistance. Science. 295: 2073-76.

BABAEIZAD, V. (2009) Generation and molecular analyses of transgenic barley (*Hordeum vulgare* L.) in response to relevant pathogens. JLU, Giessen, Dissertation.

BABAEIZAD, V., IMANI, J., KOGEL, K.H., EICHMANN, R. and HÜCKELHOVEN, R. (2009) Over-expression of the cell death regulator BAX inhibitor-1 in barley confers reduced or enhanced susceptibility to distinct fungal pathogens. Theor Appl Genet. 118: 455-63.

BAI, Y., PAVAN, S., ZHENG, Z., ZAPPEL, N.F., REINSTÄDLER, A., LOTTI, C., DE GIOVANNI, C., RICCIARDI, L., LINDHOUT, P., VISSER, R., THERES, K. and PANSTRUGA, R. (2008) Naturally occurring broad-spectrum powdery mildew resistance in a Central American tomato accession is caused by loss of mlo function. Mol Plant Microbe Interact. 21: 30-39.

BAK, S. and FEYEREISEN, R. (2001) The involvement of two p450 enzymes, CYP83B1 and CYP83A1, in auxin homeostasis and glucosinolate biosynthesis. Plant Physiol. 127: 108-18.

BAK, S., BEISSON, F., BISHOP, G., HAMBERGER, B., HÖFER, R., PAQUETTE, S. and WERCK-REICHHART, D. (2011) Cytochromes p450. Arabidopsis Book. 9: e0144.

BAK, S., TAX, F.E., FELDMANN, K.A., GALBRAITH, D.W. and FEYEREISEN, R. (2001) CYP83B1, a cytochrome P450 at the metabolic branch point in auxin and indole glucosinolate biosynthesis in *Arabidopsis*. Plant Cell. 13: 101-11.

BAUNSGAARD, L., FUGLSANG, A.T., JAHN, T., KORTHOUT, H.A.A., DE BOER, A.H. and PALMGREN, M.G. (1998) The 14-3-3 proteins associate with the plant plasma membrane H^+-ATPase to generate a fusicoccin binding complex and a fusicoccin responsive system. Plant J. 13: 661-71.

BEDNAREK, P., PISLEWSKA-BEDNAREK, M., SVATOS, A., SCHNEIDER, B., DOUBSKY, J., MANSUROVA, M., HUMPHRY, M., CONSONNI, C., PANSTRUGA, R., SANCHEZ-VALLET, A., MOLINA, A. and SCHULZE-LEFERT, P. (2009) A glucosinolate metabolism pathway in living plant cells mediates broad-spectrum antifungal defense. Science. 323: 101-106.

BERNOUX, M., TIMMERS, T., JAUNEAU, A., BRIERE, C., DE WIT, P.J., MARCO, Y. and DESLANDES, L. (2008) RD19, an *Arabidopsis* cysteine protease required for RRS1-R-mediated resistance, is relocalized to the nucleus by the *Ralstonia solanacearum* PopP2 effector. Plant Cell. 20: 2252-64.

BESSIRE, M., CHASSOT, C., JACQUAT, A.C., HUMPHRY, M., BOREL, S., PETETOT, J.M., METRAUX, J.P. and NAWRATH, C. (2007) A permeable cuticle in *Arabidopsis* leads to a strong resistance to *Botrytis cinerea*. EMBO J. 26: 2158-68.

BILODEAU, P., UDVARDI, M.K., PEACOCK, W.J. and DENNIS, E.S. (1999). A prolonged cold treatment-induced cytochrome P450 gene from *Arabidopsis thaliana*. Plant Cell Environ. 22: 791-800.

BLOCK, A., LI, G., FU, Z.Q. and ALFANO, J.R. (2008) Phytopathogen type III effector weaponry and their plant targets. Curr Opin Plant Biol. 11: 396-403.

BLUM, H., BEIER, H. and GROSS, H.J. (1987) Improved silver staining of plant proteins, RNA and DNA in polyacrylamide gels. Electrophoresis. 8: 93-99.

BLUME, B., NÜRNBERGER, T., NASS, N. and SCHEEL, D. (2000) Receptor-mediated increase in cytoplasmic free calcium required for activation of pathogen defense in parsley. Plant Cell 12: 425-40.

BOCH, J., SCHOLZE, H., SCHORNACK, S., LANDGRAF, A., HAHN, S., KAY, S., LAHAYE, T., NICKSTADT, A. and BONAS, U. (2009) Breaking the code of DNA binding specificity of TAL-type III effectors. Science. 326: 1509-12.

BOGDANOVE, A.J., SCHORNACK, S. and LAHAYE, T. (2010) TAL effectors: Finding plant genes for disease and defense. Curr Opin Plant Biol. 13: 394-401.

BOLDUC, N., OUELLET, M., PITRE, F. and BRISSON, L.F. (2003) Molecular characterization of two plant BI-1 homologues which suppress Bax-induced apoptosis in human 293 cells. Planta. 216: 377-86.

BOLLER, T. and FELIX, G. (2009) A renaissance of elicitors: perception of microbe-associated molecular patterns and danger signals by pattern-recognition receptors. Annu Rev Plant Biol. 60: 379-406.

BOUDSOCQ, M., WILLMANN, M.R., MCCORMACK, M., LEE, H., SHAN, L., HE, P., BUSH, J., CHENG, S.H. and SHEEN, J. (2010) Differential innate immune signalling via Ca^{2+} sensor protein kinases. Nature. 464: 418-22.

BOYD, L.A., SMITH, P.H., FOSTER, E.M. and BROWN, J.K. (1995) The effect of allelic variation at the Mla resistance locus in barley on the early development of *Erysiphe graminis* f. sp. *hordei.* Plant J. 7: 959-96.

BRAUN, U., COOK, R.T.A., INMAN, A.J. and SHIN, H.-D. (2002) The taxonomy of powdery mildew fungi. The Powdery Mildews: A Comprehensive Treatise. (Bélanger, R.R., Bushnell, W.R., Dik, A.J. and Carver, T.L. Eds.), St. Paul, Minnesota, pp. 13-55.

BRECKENRIDGE, D.G. and XUE, D. (2004) Regulation of mitochondrial membrane permeabilization by BCL-2 family proteins and caspases. Curr Opin Cell Biol. 16: 647-52.

BUCAN, V., ADILI, M.Y., CHOI, C.Y., EDDY, M.T., VOGT, P.M. and REIMERS, K. (2010) Transactivation of lifeguard (LFG) by Akt-/LEF-1 pathway in MCF-7 and MDA-MB 231 human breast cancer cells. Apoptosis. 15: 814-21.

BÜSCHGES, R., HOLLRICHER, K., PANSTRUGA, R., SIMONS, G., WOLTER, M., FRIJTERS, A., VAN DAELEN, R., VAN DER LEE, T., DIERGAARDE, P., GROENENDIJK, J., TÖPSCH, S., VOS, P., SALAMINI, F. and SCHULZE-LEFERT, P. (1997) The barley *Mlo* gene: a novel control element of plant pathogen resistance. Cell. 88: 695-705.

BULTYNCK, G., KIVILUOTO, S., HENKE, N., IVANOVA, H., SCHNEIDER, L., RYBALCHENKO, V., LUYTEN, T., NUYTS, K., DEBORGGRAEVE, W., BEZPROZVANNY, I., PARYS, J.B., DE SMEDT, H., MISSIAEN, L. and METHNER A. (2011) The C-terminus of bax inhibitor-1 forms a Ca^{2+}-permeable channel pore. J Biol Chem. 287: 2544-57.

BUSHNELL, W.R. (1981) Incompatibility conditioned by the *Mla* gene in powdery mildew of barley: the halt in cytoplasmic streaming. Phytopathology. 71: 1062-66.

CARVER, T.L,, KUNOH, H., THOMAS, J. and NICHOLSON, R.L. (1999) Release and visualization of the extracellular matrix of conidia of *Blumeria graminis*. Mycol Res. 103: 547-60.

CATANZARITI, A.M., DODDS, P.N., LAWRENCE, G.J., AYLIFFE, M.A. and ELLIS, J.G. (2006) Haustorially expressed secreted proteins from flax rust are highly enriched for avirulence elicitors. Plant Cell. 18: 243-56.

CATANZARITI, A.M., DODDS, P.N., VE, T., KOBE, B., ELLIS, J.G. and STASKAWICZ, B.J. (2010) The AvrM effector from flax rust has a structured C-terminal domain and interacts directly with the M resistance protein. Mol Plant Microbe Interact. 23: 49-57.

CHAE, H.J., KIM, H.R., XU, C., BAILLY-MAITRE, B., KRAJEWSKA, M., KRAJEWSKI, S., BANARES, S., CUI, J., DIGICAYLIOGLU, M., KE, N., KITADA, S., MONOSOV, E., THOMAS, M., KRESS, C.L., BABENDURE, J.R., TSIEN, R.Y., LIPTON, S.A. and REED, J.C. (2004) BI-1 regulates an apoptosis pathway linked to endoplasmic reticulum stress. Mol Cell. 15: 355-66.

CHANDRAN, D., INADA, N., HATHER, G., KLEINDT, C.K. and WILDERMUTH, M.C. (2010) Laser microdissection of *Arabidopsis* cells at the powdery mildew infection site reveals site-specific processes and regulators. Proc Natl Acad Sci U S A. 107: 460-65.

CHASSOT, C., NAWRATH, C. and MÉTRAUX, J.P. (2007) Cuticular defects lead to full immunity to a major plant pathogen. Plant J. 49: 972-80.

CHE, P., BUSSELL, J.D., WENXU ZHOU, W., ESTAVILLO, G., POGSON, B.J. and SMITH, S.M. (2010) Signaling from the endoplasmic reticulum activates brassinosteroid

signaling and promotes acclimation to stress in *Arabidopsis*. Sci Signal. 3: ra69.

CHEN, J.C., JIANG, C.Z. and REID, M.S. (2005) Silencing a prohibitin alters plant development and senescence. Plant J. 44: 16-24.

CHEN, L.Q., HOU, B.H., LALONDE, S., TAKANAGA, H., HARTUNG, M.L., QU, X.Q., GUO, W.J., KIM, J.G., UNDERWOOD, W., CHAUDHURI, B., CHERMAK, D., ANTONY, G., WHITE, F.F., SOMERVILLE, S.C., MUDGETT, M.B. and FROMMER, W.B. (2010) Sugar transporters for intercellular exchange and nutrition of pathogens. Nature. 468: 527-32.

CHEN, S., GLAWISCHNIG, E., JØRGENSEN, K., NAUR, P., JØRGENSEN, B., OLSEN, C.E., HANSEN, C.H., RASMUSSEN, H., PICKETT, J.A. and HALKIER, B.A. (2003) CYP79F1 and CYP79F2 have distinct functions in the biosynthesis of aliphatic glucosinolates in *Arabidopsis*. Plant J. 33: 923-37.

CHEN, X., MOORE-NICHOLS, D., NGUYEN, H. and MICHAELIS, E.K. (1999) Calcium influx through NMDA receptors, chronic receptor inhibition by ethanol and 2-amino-5-phosponopentanoic acid, and receptor protein expression. J Neurochem. 72: 1969-80.

CHINCHILLA, D., BAUER, Z., REGENASS, M., BOLLER, T. and FELIX, G. (2006) The *Arabidopsis* receptor kinase FLS2 binds flg22 and determines the specificity of flagellin perception. Plant Cell. 18: 465-76.

CHINCHILLA, D., ZIPFEL, C., ROBATZEK, S., KEMMERLING, B., NÜRNBERGER, T., JONES, J.D., FELIX, G. and BOLLER, T. (2007) A flagellin-induced complex of the receptor FLS2 and BAK1 initiates plant defence. Nature. 448: 497-500.

CHISHOLM, S.T., COAKER, G., DAY, B. and STASKAWICZ, B.J. (2006) Host-microbe interactions: shaping the evolution of the plant immune response. Cell. 124: 803-14.

CHRISTIANS, M.J. and LARSEN, P.B. (2007) Mutational loss of the prohibitin AtPHB3 results in an extreme constitutive ethylene response phenotype coupled with partial loss of ethylene-inducible gene expression in *Arabidopsis* seedlings. J Exp Bot. 58: 2237-48.

CLOSSAIS-BESNARD, N. and LARHER, F. (1991) Physiological role of glucosinolates in *Brassica napus*. Concentration and distribution pattern of glucosinolates among plant organs during a complete life cycle. J Sci Food Agric. 56: 25-38.

CLOUGH, S.J. and BENT, A.F. (1998) Floral dip: a simplified method for *Agrobacterium*-mediated transformation of *Arabidopsis thaliana.* Plant J. 16: 735-43.

COLLIER, S.M. and MOFFETT, P. (2009) NB-LRRs work a "bait and switch" on pathogens. Trends Plant Sci. 14: 521-29.

COLLINS, N.C., THORDAL-CHRISTENSEN, H., LIPKA, V., BAU, S., KOMBRINK, E., QIU, J.-J., HÜCKELHOVEN, R., STEIN, M., FREIALDENHOVEN, A., SOMMERVILLE, S.C. and SCHULZE-LEFERT, P. (2003): SNARE-protein-mediated disease resistance at the plant cell wall. Nature. 425: 973-77.

COMPAGNON, V., DIEHL, P., BENVENISTE, I., MEYER, D., SCHALLER, H., SCHREIBER, L., FRANKE, R. and PINOT, F. (2009) CYP86B1 is required for very long chain omega-hydroxyacid and alpha, omega-dicarboxylic acid synthesis in root and seed suberin polyester. Plant Physiol. 150: 1831-43.

CONSONNI, C., HUMPHRY, M.E., HARTMANN, H.A., LIVAJA, M., DURNER, J., WESTPHAL, L., VOGEL, J., LIPKA, V., KEMMERLING, B., SCHULZE-LEFERT, P., SOMERVILLE, S.C. and PANSTRUGA, R. (2006) Conserved requirement for a plant host cell protein in powdery mildew pathogenesis. Nat Genet. 38: 716-20.

CORY, S. and ADAMS, J.M. (2002) The Bcl2 family: regulators of the cellular life-or-death switch. Nat Rev Cancer. 2: 647-56.

COWLING, R.T. and BIRNBOIM, H.C. (1998) Preliminary characterization of the protein encoded by human testis-enhanced gene transcript (TEGT). Mol Membr Biol. 15: 177-87.

CRIMAUDO, C., HORTSCH, M., GAUSEPOHL, H. and MEYER, D.I. (1987) Human ribophorins I and II: the primary structure and membrane topology of two highly conserved rough endoplasmic reticulum-specific glycoproteins. EMBO J. 6: 75-82.

CROSTI, P., MALERBA, M. and BIANCHETTI, R. (2001) Tunicamycin and Brefeldin A induce in plant cells a programmed cell death showing apoptotic features. Protoplasma. 216: 31-38.

DANON, A., ROTARI, V.I., GORDON, A., MAILHAC, N. and GALLOIS, P. (2004) Ultraviolet-C overexposure induces programmed cell death in *Arabidopsis*, which is mediated by caspase-like activities and which can be suppressed by caspase inhibitors, p35 and Defender against Apoptotic Death. J Biol Chem. 279: 779-87.

DASH, S., VAN HEMERT, J., HONG, L., WISE, R.P. and DICKERSON, J.A. (2012) PLEXdb: gene expression resources for plants and plant pathogens. Nucleic Acids Res. 40 (Database issue): D1194-201.

DE BRITO, O.M. and SCORRANO, L. (2008) Mitofusin 2 tethers endoplasmic reticulum to mitochondria. Nature. 456: 605-10.

DE JONGE, R., BOLTON, M.D. and THOMMA, B.P. (2011) How filamentous pathogens co-opt plants: the ins and outs of fungal effectors. Curr Opin Plant Biol. 14: 400-406.

DE JONGE, R., VAN ESSE, H.P., KOMBRINK, A., SHINYA, T., DESAKI, Y., BOURS, R., VAN DER KROL, S., SHIBUYA, N., JOOSTEN, M.H. and THOMMA, B.P. (2010) Conserved fungal LysM effector Ecp6 prevents chitin-triggered immunity in plants. Science. 329: 953-55.

DE MATTIA, F., GUBSER, C., VAN DOMMELEN, M.M., VISCH, H.J., DISTELMAIER, F., POSTIGO, A., LUYTEN, T., PARYS, J.B., DE SMEDT, H., SMITH, G.L., WILLEMS, P.H. and VAN KUPPEVELD, F.J. (2009) Human GAAP modulates intracellular calcium fluxes. Mol Biol Cell. 20: 3638-45.

DE MENDOZA, T.H., PEREZ-GARCIA, C.G., KROLL, T.T., HOONG, N.H., O'LEARY, D.D. and VERMA, I.M. (2011) Antiapoptotic protein Lifeguard is required for survival and maintenance of Purkinje and granular cells. Proc Natl Acad Sci U S A. 108: 17189-94.

DE WIT, P.J., MEHRABI, R., VAN DEN BURG, H.A. and STERGIOPOULOS, I. (2009) Fungal effector proteins: past, present and future. Mol Plant Pathol. 106: 735-47.

DEAN, R.A., TALBOT, N.J., EBBOLE, D.J., FARMAN, M.L., MITCHELL, T.K., ORBACH, M.J., THON, M., KULKARNI, R., XU, J.R., PAN, H., READ, N.D., LEE, Y.H., CARBONE, I., BROWN, D., OH, Y.Y., DONOFRIO, N., JEONG, J.S., SOANES, D.M., DJONOVIC, S., KOLOMIETS, E., REHMEYER, C., LI, W., HARDING, M., KIM, S., LEBRUN, M.H.,

BOHNERT, H., COUGHLAN, S., BUTLER, J., CALVO, S., MA, L.J., NICOL, R., PURCELL, S., NUSBAUM, C., GALAGAN, J.E. and BIRREN, B.W. (2005) The genome sequence of the rice blast fungus *Magnaporthe grisea*. Nature. 434: 980-86.

DESHMUKH, S., HÜCKELHOVEN, R., SCHÄFER, P., IMANI, J., SHARMA, M., WEISS, M., WALLER, F. and KOGEL, K.H. (2006) The root endophytic fungus *Piriformospora indica* requires host cell death for proliferation during mutualistic symbiosis with barley. Proc Natl Acad Sci U S A. 103: 18450-57.

DESLANDES, L., OLIVIER, J., PEETERS, N., FENG, D.X., KHOUNLOTHAM, M., BOUCHER, C., SOMSSICH, I., GENIN, S. and MARCO, Y. (2003) Physical interaction between RRS1-R, a protein conferring resistance to bacterial wilt, and PopP2, a type III effector targeted to the plant nucleus. Proc Natl Acad Sci U S A. 13: 8024-29.

DETTMER, J., HONG-HERMESDORF, A., STIERHOF, Y.D. and SCHUMACHER, K. (2006) Vacuolar H^+-ATPase activity is required for endocytic and secretory trafficking in *Arabidopsis*. Plant Cell. 18: 715-30.

DETTMER, J., SCHUBERT, D., CALVO-WEIMAR, O., STIERHOF, Y.D., SCHMIDT, R. and SCHUMACHER, K. (2005) Essential role of the V-ATPase in male gametophyte development. Plant J. 41: 117-24.

DEVOTO, A., PIFFANELLI, P., NILSSON, I., WALLIN, E., PANSTRUGA, R., VON HEIJNE, G. and SCHULZE-LEFERT, P. (1999) Topology, subcellular localization, and sequence diversity of the Mlo family in plants. J Biol Chem. 274: 34993-5004.

DI, C., XU, W., SU, Z. and YUAN, J.S (2010) Comparative genome analysis of PHB gene family reveals deep evolutionary origins and diverse gene function. BMC Bioinformatics. 11: S22.

DIETRICH, C. and MAISS, E. (2002) Red fluorescent protein DsRed from *Discosoma* sp. as a reporter protein in higher plants. Biotechniques. 32: 286-93.

DIETZ, K.J., TAVAKOLI, N., KLUGE, C., MIMURA, T., SHARMA, S.S., HARRIS, G.C., CHARDONNENS, A.N. and GOLLDACK, D. (2001) Significance of the V-type ATPase for the adaptation to stressful growth conditions and its regulation on the molecular and biochemical level. J Exp Bot. 52: 1969-80.

DJAMEI, A., SCHIPPER, K., RABE, F., GHOSH, A., VINCON, V., KAHNT, J., OSORIO, S., TOHGE, T., FERNIE, A.R., FEUSSNER, I., FEUSSNER, K., MEINICKE, P., STIERHOF, Y.D., SCHWARZ, H., MACEK, B., MANN, M. and KAHMANN, R. (2011) Metabolic priming by a secreted fungal effector. Nature. 478: 395-98.

DODD, A.N., KUDLA, J.R. and SANDERS, D. (2010) The language of calcium signalling. Annu Rev Plant Biol. 61: 593-620.

DODDS, P.N. and RATHJEN, J.P. (2010) Plant immunity: towards an integrated view of plant-pathogen interactions. Nat Rev Genet. 118: 539-48.

DODDS, P.N., LAWRENCE, G.J., CATANZARITI, A.M., AYLIFFE, M.A. and ELLIS, J.G. (2004) The *Melampsora lini* AvrL567 avirulence genes are expressed in haustoria and their products are recognized inside plant cells. Plant Cell. 16: 755-68.

DODDS, P.N., LAWRENCE, G.J., CATANZARITI, A.M., TEH, T., WANG, C.I., AYLIFFE, M.A., KOBE, B. and ELLIS, J.G. (2006) Direct protein interaction underlies gene-for-gene specificity and coevolution of the flax resistance genes and flax rust avirulence genes. Proc Natl Acad Sci U S A. 103: 8888-93.

DOUCHKOV, D., NOWARA, D., ZIEROLD, U. and SCHWEIZER, P. (2005) A high-throughput gene-silencing system for the functional assessment of defense-related genes in barley epidermal cells. Mol Plant Microbe Interact. 18: 755-61.

DRUMM, J.E., ADAMS, J.B. JR, BROWN, R.J., CAMPBELL, C.L., ERBES, D.L., HALL, W.T., HARTZELL, S.L., HOLLIDAY, M.J., KLEIER, D.A., MARTIN, M.J., PEMBER, S.O. and RAMSEY, G.R. (1995) Oxime fungicides. Highly active broad-spectrum protectants. ACS Symp Ser. 584: 396-405.

ECKARDT, N.A. (2002) Plant disease susceptibility genes? Plant Cell. 14: 1983-86.

ECKEY, C., KORELL, M., LEIB, K., BIEDENKOPF, D., JANSEN, C., LANGEN, G. and KOGEL, K.H. (2004) Identification of powdery mildew-induced barley genes by cDNA-AFLP: functional assessment of an early expressed MAP kinase. Plant Mol Biol. 55: 1-15.

EDWARDS, H.H. (2002) Development of primary germ tubes by conidia of *Blumeria graminis* f.sp. *hordei* on leaf epidermal cells of *Hordeum vulgare*. Can J Bot. 80: 1121-25.

EICHMANN, R. and HÜCKELHOVEN, R. (2008) Accommodation of powdery mildew fungi in intact plant cells. J Plant Physiol. 165: 5-18.

EICHMANN, R., BIEMELT, S., SCHÄFER, P., SCHOLZ, U., JANSEN, C., FELK, A., SCHÄFER, W., LANGEN, G., SONNEWALD, U., KOGEL, K.-H. and HÜCKELHOVEN, R. (2006a) Macroarray expression analysis of barley susceptibility and nonhost resistance to *Blumeria graminis*. J Plant Physiol. 163: 657-70.

EICHMANN, R., BISCHOF, M., WEIS, C., SHAW, J., LACOMME, C., SCHWEIZER, P., DUCHKOV, D., HENSEL, G., KUMLEHN, J. and HÜCKELHOVEN, R. (2010) BAX INHIBITOR-1 is required for full susceptibility of barley to powdery mildew. Mol Plant Microbe Interact. 23: 1217-27.

EICHMANN, R., DECHERT, C., KOGEL, K.-H. and HÜCKELHOVEN, R. (2006b) Transient over-expression of barley BAX Inhibitor-1 weakens oxidative defence and *MLA12*-mediated resistance to *Blumeria graminis* f.sp. *hordei*. Mol Plant Pathol. 7: 543-52.

EICHMANN, R., SCHULTHEISS, H., KOGEL, K.-H. and HÜCKELHOVEN, R. (2004) The barley apoptosis suppressor homologue Bax Inhibitor-1 compromises nonhost penetration resistance of barley to the inappropriate pathogen *Blumeria graminis* f. sp. *tritici*. Mol Plant Microbe Interact. 17: 484-90.

ELLIOTT, C., ZHOU, F., SPIELMEYER, W., PANSTRUGA, R. and SCHULZE-LEFERT, P. (2002) Functional conservation of wheat and rice *Mlo* orthologs in defense modulation to the powdery mildew fungus. Mol Plant Microbe Interact. 15: 1069-77.

ELMORE, J.M. and COAKER, G. (2011) The role of the plasma membrane H$^+$-ATPase in plant-microbe interactions. Mol Plant. 4: 416-27.

ESCOBAR-RESTREPO, J.M., HUCK, N., KESSLER, S., GAGLIARDINI, V., GHEYSELINCK, J., YANG, W.C. and GROSSNIKLAUS, U. (2007) The FERONIA receptor-like kinase mediates male-female interactions during pollen tube reception. Science. 317: 656-60.

FABRO, G., DI RIENZO, J.A., VOIGT, C.A., SAVCHENKO, T., DEHESH, K., SOMERVILLE, S. and ALVAREZ, M.E. (2008) Genome-wide expression profiling *Arabidopsis* at the stage of *Golovinomyces cichoracearum* haustorium formation. Plant Physiol. 146: 1421-39.

FENG, J., WANG, F., LIU, G., GREENSHIELDS, D., SHEN, W., KAMINSKYJ, S., HUGHES, G.R., PENG, Y., SELVARAJ, G., ZOU, J. and WEI, Y. (2009) Analysis of a *Blumeria graminis*-secreted lipase reveals the importance of host epicuticular wax components for fungal adhesion and development. Mol Plant Microbe Interact. 22: 1601-10.

FERNÁNDEZ, M., SEGURA, M.F., SOLÉ, C., COLINO, A., COMELLA, J.X. and CEÑA, V. (2007) Lifeguard/neuronal membrane protein 35 regulates Fas ligand-mediated apoptosis in neurons via microdomain recruitment. J Neurochem. 103: 190-203.

FINER, J.J., VAIN, P., JONES, M.W. and MCMULLEN, M.D. (1992) Development of the particle inflow gun for DNA delivery to plant cells. Plant Cell Report. 11: 323-28.

FINNI, C., ANDERSEN, C.H., BORCH, J., GJETTING, S., CHRISTENSEN, A.B., DE BOER, A.H., THORDAL-CHRISTENSEN, H. and COLLINGE, D.B. (2002) Do 14-3-3 proteins and plasma membrane H+-AtPases interact in the barley epidermis in response to the barley powdery mildew fungus? Plant Mol Biol. 49: 137-47.

FRANCIS, S.A., DEWEY, F.M. and GURR, S.J. (1996) The role of cutinase in germling development and infection by *Erysiphe graminis* f. sp. *hordei.* Physiol Mol Plant Pathol. 49: 201-11.

FRIEDMAN, J.R. and VOELTZ, G.K. (2011) The ER in 3D: a multifunctional dynamic membrane network. Trends Cell Biol. 21: 709-17.

GALLOIS, P., MAKISHIMA, T., HECHT, V., DESPRES, B., LAUDIÉ, M., NISHIMOTO, T. and COOKE, R. (1997) An *Arabidopsis thaliana* cDNA complementing a hamster apoptosis suppressor mutant. Plant J. 11: 1325-31.

GAO, M. and SHOWALTER, A.M. (1999) Yariv reagent treatment induces programmed cell death in *Arabidopsis* cell cultures and implicates arabinogalactan protein involvement. Plant J. 19: 321-32.

GIL, F. and GAY, J.L. (1977) Ultrastructural and physiological properties of host interfacial components of haustoria of *Erysiphe pisi* in vivo and in vitro. Physiol Plant Pathol. 10: 1–12.

GJETTING, T., CARVER, T.L., SKØT, L. and LYNGKJAER, M.F. (2004) Differential gene expression in individual papilla-resistant and powdery mildew-infected barley epidermal cells. Mol Plant Microbe Interact. 17: 729-38.

GLAWE, D.A. (2008) The powdery mildews: a review of the world's most familiar (yet poorly known) plant pathogens. Annu Rev Phytopathol. 46: 27-51.

GLAWISCHNIG, E. (2007) Camalexin. Phytochemistry. 68: 401-406.

GLAZEBROOK, J. (2001) Genes controlling expression of defense responses in *Arabidopsis.* Curr Opin Plant Biol. 4: 301-308.

GLAZEBROOK, J. (2005) Contrasting mechanisms of defense against biotrophic and necrotrophic pathogens. Annu Rev Phytopathol. 43: 205-27.

GODFREY, D., BÖHLENIUS, H., PEDERSEN, C., ZHANG, Z., EMMERSEN, J. and THORDAL-CHRISTENSEN, H. (2010) Powdery mildew fungal effector candidates share N-terminal Y/F/WxC-motif. BMC Genomics. 11: 317.

GÖLLNER, K., SCHWEIZER, P., BAI, Y. and PANSTRUGA, R. (2008) Natural genetic resources of *Arabidopsis thaliana* reveal a high prevalence and unexpected

phenotypic plasticity of RPW8-mediated powdery mildew resistance. New Phytol. 177: 725-42.

GOVRIN, E.M. and LEVINE, A. (2000) The hypersensitive response facilitates plant infection by the necrotrophic pathogen *Botrytis cinerea*. Curr Biol. 10: 751-57.

GRANT, M., BROWN, I., ADAMS, S., KNIGHT, M., AINSLIE, A. and MANSFIELD, J. (2000) The *RPM1* plant disease resistance gene facilitates a rapid and sustained increase in cytosolic calcium that is necessary for the oxidative burst and hypersensitive cell death. Plant J. 23: 441-50.

GRANT, S.R., FISHER, E.J., CHANG, J.H, MOLE, B.M. and DANGL, J.L. (2006) Subterfuge and manipulation: type III effector proteins of phytopathogenic bacteria. Annu Rev Microbiol. 60: 425-49.

GREEN, D.R. and KROEMER, G. (2004) The pathophysiology of mitochondrial cell death. Science. 305: 626-29.

GREEN, J.R., CARVER, T.L. and GURR, S.J. (2002) The formation and function of infection and feeding structures. The Powdery Mildews: A Comprehensive Treatise (Bélanger, R.R., Bushnell, W.R., Dik, A.J. and Carver, T.L. Eds.), St. Paul, Minnesota, pp. 66–82.

GUBSER, C., BERGMASCHI, D., HOLLINSHEAD, M., LU, X., VAN KUPPEVELD, F.J.M. and SMITH, G.L. (2007) A new inhibitor of apoptosis from vaccinia virus and eukaryotes. PLoS Pathog. 3: e17.

GUST, A.A., BRUNNER, F. and NÜRNBERGER, T. (2010) Biotechnological concepts for improving plant innate immunity. Curr Opin Biotechnol. 21: 204-10.

GUTIÉRREZ-NÁJERA, N., MUÑOZ-CLARES, R.A., PALACIOS-BAHENA, S., RAMÍREZ, J., SÁNCHEZ-NIETO, S., PLASENCIA, J. and GAVILANES-RUÍZ, M. (2005) Fumonisin B1, a sphingoid toxin, is a potent inhibitor of the plasma membrane H^+-ATPase. Planta. 221: 589-96.

HAHLBROCK, K., BEDNAREK, P., CIOLKOWSKI, I., HAMBERGER, B., HEISE, A., LIEDGENS, H., LOGEMANN, E., NÜRNBERGER, T., SCHMELZER, E., SOMSSICH, I.E. and TAN, J. (2003) Non-self recognition, transcriptional reprogramming, and secondary metabolite accumulation during plant/pathogen interactions. Proc Natl Acad Sci U S A. 100: 14569-76.

HALKIER, B.A. and DU, L.C. (1997) The biosynthesis of glucosinolates. Trends Plant Sci. 2: 425-31.

HALKIER, B.A., SIBBESEN, O., KOCH, B. and MØLLER, B.L. (1995) Characterization of cytochrome P450TYR, a multifunctional haem-thiolate N-hydroxylase involved in the biosynthesis of the cyanogenic glucoside dhurrin. Drug Metabol Drug Interact. 12: 285-97.

HALL, J.L. and WILLIAMS, L.E. (2000) Assimilate transport and partitioning in fungal biotrophic interactions. Aust J Plant Physiol. 27: 549-60.

HALTERMAN, D., ZHOU, F., WEI, F., WISE, R.P. and SCHULZE-LEFERT, P. (2001) The MLA6 coiled-coil, NBS-LRR protein confers AvrMla6-dependent resistance specificity to *Blumeria graminis* f. sp. *hordei* in barley and wheat. Plant J. 25: 335-48.

HALTERMAN, D.A. and WISE, R.P. (2004) A single-amino acid substitution in the sixth leucine-rich repeat of barley MLA6 and MLA13 alleviates dependence on RAR1 for disease resistance signaling. Plant J. 38: 215-26.

HAMMOND-KOSACK, K.E. and JONES, J.D.G. (1996) Resistance gene-dependent plant defense responses. Plant Cell. 8: 1773-91.

HAMMOND-KOSACK, K.E. and PARKER, J.E. (2003) Deciphering plant-pathogen communication: fresh perspectives for molecular resistance breeding. Curr Opin Biotechnol. 14: 177-93.

HANSEN, C.H., DU, L., NAUR, P., OLSEN, C.E., AXELSEN, K.B., HICK, A.J., PICKETT, J.A. and HALKIER, B.A. (2001) CYP83b1 is the oxime-metabolizing enzyme in the glucosinolate pathway in *Arabidopsis*. J Biol Chem. 276: 24790-96.

HANSJAKOB, A., BISCHOF, S., BRINGMANN, G., RIEDERER, M. and HILDEBRANDT, U. (2010) Very-long-chain aldehydes promote in vitro prepenetration processes of *Blumeria graminis* in a dose- and chain length-dependent manner. New Phytol. 188: 1039-54.

HARRISON, S.J., MOTT, E.K., PARSLEY, K., ASPINALL, S., GRAY, J.C. and COTTAGE, A. (2006) A rapid and robust method of identifying transformed *Arabidopsis* seedlings following floral dip transformation. Plant Methods. 2: 19.

HE, P., SHAN, L. and SHEEN, J. (2007) Elicitation and suppression of microbe-associated molecular pattern-triggered immunity in plant-microbe interactions. Cell Microbiol. 9: 1385-96.

HEATH, M.C. (2000a) Hypersensitive response-related death. Plant Mol Biol. 44: 321-34.

HEATH, M.C. (2000b) Nonhost resistance and nonspecific plant defenses. Curr Opin Plant Biol. 3: 315-19.

HEAZLEWOOD, J.L., TONTI-FILIPPINI, J.S., GOUT, A.M., DAY, D.A., WHELAN, J. and MILLAR, A.H. (2004) Experimental analysis of the *Arabidopsis* mitochondrial proteome highlights signaling and regulatory components, provides assessment of targeting prediction programs, and indicates plant-specific mitochondrial proteins. Plant Cell. 16: 241-56.

HEESE, A., HANN, D.R., GIMENEZ-IBANEZ, S., JONES, A.M.E., HE, K., LI, J., SCHROEDER, J.I., PECK, S.C. and RATHJEN, J.P. (2007) The receptor-like kinase SERK3/BAK1 is a central regulator of innate immunity in plants. Proc Natl Acad Sci U S A. 104: 12217-22.

HEMM, M.R., RUEGGER, M.O. and CHAPPLE, C. (2003) The *Arabidopsis ref2* mutant is defective in the gene encoding CYP83A1 and shows both phenylpropanoid and glycosinolate phenotypes. Plant Cell. 15: 179-94.

HEMRAJANI, C., BERGER, C.N., ROBINSON, K.S., MARCHÈS, O., MOUSNIER, A. and FRANKEL, G. (2010) NleH effectors interact with Bax inhibitor-1 to block apoptosis during enteropathogenic *Escherichia coli* infection. Proc Natl Acad Sci U S A. 107: 3129-34.

HIGAKI, T., KUTSUNA, N., OKUBO, E., SANO, T. and HASEZAWA, S. (2006) Actin microfilaments regulate vacuolar structures and dynamics: dual observation of actin microfilaments and vacuolar membrane in living tobacco BY-2 cells. Plant Cell Physiol. 47: 839-52.

HOEBERICHTS, F.A., VAECK, E., KIDDLE, G., COPPENS, E., VAN DE COTTE, B., ADAMANTIDIS, A., ORMENESE, S., FOYER, C.H., ZABEAU, M., INZÉ, D., PÉRILLEUX, C., VAN BREUSEGEM, F. and VUYLSTEKE, M.A. (2007) Temperature-sensitive mutation in the *Arabidopsis thaliana* phosphomannomutase gene disrupts protein glycosylation and triggers cell death. J Biol Chem. 283: 5708-18.

HÖFLE, C., HUESMANN, C., SCHULTHEISS, H., BÖRNKE, F., HENSEL, G., KUMLEHN, J. and HÜCKELHOVEN, R. (2011) A barley ROP GTPase ACTIVATING PROTEIN associates with microtubules and regulates entry of the barley powdery mildew fungus into leaf epidermal cells. Plant Cell. 23: 2422-39.

HÖFER, R., BRIESEN, I., BECK, M., PINOT, F., SCHREIBER, L. and FRANKE, R. (2008) The *Arabidopsis* cytochrome P450 CYP86A1 encodes a fatty acid omega-hydroxylase involved in suberin monomer biosynthesis. J Exp Bot. 59: 2347-60.

HOPKINS, R.J., VAN DAM, N.M. and VAN LOON, J.J. (2009) Role of glucosinolates in insect-plant relationships and multitrophic interactions. Annu Rev Entomol. 54: 57-83.

HOPPINS, S., LACKNER, L. and NUNNARI, J. (2007) The machines that divide and fuse mitochondria. Annu Rev Biochem. 76: 751-80.

HORTON, P., PARK, K.J., OBAYASHI, T., FUJITA, N., HARADA, H., ADAMS-COLLIER, C.J. and NAKAI, K. (2007) WoLF PSORT: protein localization predictor. Nucleic Acids Res. 35 (Web Server issue): W585-87.

HU, L., SMITH, T.F. and GOLDBERGER, G. (2009) LFG: a candidate apoptosis regulatory gene family. Apoptosis. 14: 1255-65.

HÜCKELHOVEN, R. (2004) BAX Inhibitor-1, an ancient cell death suppressor in animals and plants with prokaryotic relatives. Apoptosis. 9: 299-307.

HÜCKELHOVEN, R. (2005) Powdery mildew susceptibility and biotrophic infection strategies. FEMS Microbiol Lett. 245: 9-17.

HÜCKELHOVEN, R. (2007a) Cell wall-associated mechanisms of disease resistance and susceptibility. Annu Rev Phytopathol. 45: 101-27.

HÜCKELHOVEN, R. (2007b) Transport and secretion in plant-microbe interactions. Curr Opin Plant Biol. 10: 573-79.

HÜCKELHOVEN, R. and KOGEL, K.-H. (1998) Tissue-specific superoxide generation at interaction sites in resistant and susceptible near-isogenic barley lines attacked by the powdery mildew fungus (*Erysiphe graminis* f. sp. *hordei*). MPMI. 11: 292-300.

HÜCKELHOVEN, R. and PANSTRUGA, R. (2011) Cell biology of the plant-powdery mildew interaction. Curr Opin Plant Biol. 14: 738-46.

HÜCKELHOVEN, R., DECHERT, C. and KOGEL, K.-H. (2003) Overexpression of barley *BAX inhibitor 1* induces breakdown of *mlo*-mediated penetration resistance to *Blumeria graminis*. Proc Natl Acad Sci U S A. 100: 5555-60.

HÜCKELHOVEN, R., DECHERT, C., TRUJILLO, M. and KOGEL, K.-H. (2001) Differential expression of putative cell death regulator genes in near-isogenic, resistant and susceptible barley lines during interaction with the powdery mildew fungus. Plant Mol Biol. 47: 739-48.

HÜCKELHOVEN, R., FODOR, J., PREIS, C. and KOGEL, K.-H. (1999) Hypersensitive cell death and papilla formation in barley attacked by the powdery mildew fungus are associated with hydrogen peroxide but not with salicylic acid accumulation. Plant Physiol. 119: 1251-60.

HUMPHRY, M., REINSTÄDLER, A., IVANOV, S., BISSELING, T. and PANSTRUGA, R. (2011) Durable broad-spectrum powdery mildew resistance in pea er1 plants is

conferred by natural loss-of-function mutations in PsMLO1. Mol Plant Pathol. 12: 866-78.

HUNTER, S., APWEILER, R., ATTWOOD, T.K., BAIROCH, A., BATEMAN, A., BINNS, D., BORK, P., DAS, U., DAUGHERTY, L., DUQUENNE, L., FINN, R.D., GOUGH, J., HAFT, D., HULO, N., KAHN, D., KELLY, E., LAUGRAUD, A., LETUNIC, I., LONSDALE, D., LOPEZ, R., MADERA, M., MASLEN, J., MCANULLA, C., MCDOWALL, J., MISTRY, J., MITCHELL, A., MULDER, N,, NATALE. D,, ORENGO, C., QUINN, A.F., SELENGUT, J.D., SIGRIST, C.J., THIMMA, M., THOMAS, P.D., VALENTIN, F., WILSON, D., WU, C.H. and YEATS, C. (2009) InterPro: the integrative protein signature database. Nucleic Acids Res. 37: D211-15.

IHARA-OHORI, Y., NAGANO, M., MUTO, S., UCHIMIYA, H. and KAWAI-YAMADA, M. (2007) Cell death suppressor *Arabidopsis* Bax Inhibitor-1 is associated with Calmodulin binding and ion homeostasis. Plant Physiol. 143: 650-60.

IKONEN, E., FIEDLER, K., PARTON, R.G. and SIMONS, K. (1995) Prohibitin, an antiproliferative protein, is localized to mitochondria. FEBS Lett. 358: 273-77.

IMANI, J., BALTRUSCHAT, H., STEIN, E., JIA, G., VOGELSBERG, J., KOGEL, K.H. and HÜCKELHOVEN, R. (2006) Expression of barley BAX Inhibitor-1 in carrots confers resistance to *Botrytis cinerea*. Mol Plant Pathol. 7: 279-84.

INUMA, T., KHODAPARAST, S.A. and TAKAMATSU, S. (2007) Multilocus phylogenetic analyses within *Blumeria graminis*, a powdery mildew fungus of cereals. Mol Phylogenet Evol. 44: 741-51.

ISAYENKOV, S., ISNER, J.C. and MAATHUIS, F.J. (2011) Rice two-pore K+ channels are expressed in different types of vacuoles. Plant Cell. 23: 756-68.

IWASAWA, R., MAHUL-MELLIER, A.L., DATLER, C., PAZARENTZOS, E. and GRIMM, S. (2011) Fis1 and Bap31 bridge the mitochondria-ER interface to establish a platform for apoptosis induction. EMBO J. 30: 556-68.

JENSEN, J., JORGENSEN, J.H., JENSEN, H.P., GIESE, H. and DOLL, H. (1980) Linkage of the hordein loci Hor1 and Hor2 with the powdery mildew resistance loci Ml-k and Ml-a on barley chromosome 5. Theor Appl. Genet. 58: 27-31.

JIA, Y., MCADAMS, S.A., BRYAN, G.T., HERSHEY, H.P. and VALENT, B. (2000) Direct interaction of resistance gene and avirulence gene products confers rice blast resistance. EMBO J. 19: 4004-14.

JIANG, R.H., TRIPATHY, S., GOVERS, F. and TYLER, B.M. (2008) RXLR effector reservoir in two *Phytophthora* species is dominated by a single rapidly evolving superfamily with more than 700 members. Proc Natl Acad Sci U S A. 105: 4874-79.

JOHAL, G.S., HULBERT, S.H. and BRIGGS, S.P. (1995) Disease lesion mimics of maize: a model for cell death in plants. BioEssays. 17: 685-93.

JOHNSON, M.A., VON BESSER, K., ZHOU, Q., SMITH, E., AUX, G., PATTON, D., LEVIN, J.Z. and PREUSS, D. (2004) *Arabidopsis* hapless mutations define essential gametophytic functions. Genetics. 168: 971-82.

JONES, J.D. and DANGL, J.L. (2006) The plant immune system. Nature. 444: 323-29.

JØRGENSEN, J.H. (1992) Discovery, characterization and exploitation of *Mlo* powdery mildew resistance in barley. Euphytica. 63: 141-52.

JØRGENSEN, J.H. (1994) Genetics of powdery mildew resistance in barley. Crit Rev Plant Sci. 13: 97-119.

JØRGENSEN, K., RASMUSSEN, A.V., MORANT, M., NIELSEN, A.H., BJARNHOLT, N., ZAGROBELNY, M., BAK, S. and MØLLER, B.L. (2005) Metabolon formation and metabolic channeling in the biosynthesis of plant natural products. Curr Opin Plant Biol. 8: 280-91.

KAKU, H., NISHIZAWA, Y., ISHII-MINAMI, N., AKIMOTO-TOMIYAMA, C., DOHMAE, N., TAKIO, K., MINAMI, E. and SHIBUYA, N. (2006) Plant cells recognize chitin fragments for defense signaling through a plasma membrane receptor. Proc Natl Acad Sci U S A. 103: 11086-91.

KALE, S.D., GU, B., CAPELLUTO, D.G., DOU, D., FELDMAN, E., RUMORE, A., ARREDONDO, F.D., HANLON, R., FUDAL, I., ROUXEL, T., LAWRENCE. C.B., SHAN, W. and TYLER, B.M. (2010) External lipid PI3P mediates entry of eukaryotic pathogen effectors into plant and animal host cells. Cell. 142: 284-95.

KAMOUN, S. (2006) A catalogue of the effector secretome of plant pathogenic oomycetes. Annu Rev Phytopathol. 44: 41-60.

KANG, J.S., FRANK, J., KANG, C.H., KAJIURA, H., VIKRAM, M., UEDA, A., KIM, S, BAHK, J.D., TRIPLETT, B., FUJIYAMA, K., LEE, S.Y., VON SCHAEWEN, A. and KOIWA, H. (2008) Salt tolerance of *Arabidopsis thaliana* requires maturation of N-glycosylated proteins in the Golgi apparatus. Proc Natl Acad Sci U S A. 105: 5933-38.

KAWAI, M., PANB, L., REED, J.C. and UCHIMIYA, H. (1999) Evolutionally conserved plant homologue of the *Bax Inhibitor-1* (*BI-1*) gene capable of suppressing Bax-induced cell death in yeast. FEBS Lett. 464: 143-47.

KAWAI-YAMADA, M., HORI, Z., OGAWA, T., IHARA-OHORI, Y., TAMURA, K., NAGANO, M., ISHIKAWA, T. and UCHIMIYA, H. (2009) Loss of calmodulin binding to Bax inhibitor-1 affects *Pseudomonas*-mediated hypersensitive response-associated cell death in *Arabidopsis thaliana*. J Biol Chem. 284: 27998-28003.

KAWAI-YAMADA, M., JIN, L., YOSHINAGA, K., HIRATA, A. and UCHIMIYA, H. (2001) Mammalian Bax-induced plant cell death can be down-regulated by overexpression of *Arabidopsis Bax Inhibitor-1* (*AtBI-1*). Proc Natl Acad Sci U S A. 98: 12295-300.

KAWAI-YAMADA, M., OHORI, Y. and UCHIMIYA, H. (2004) Dissection of *Arabidopsis* Bax inhibitor-1 suppressing Bax-, hydrogen peroxide-, and salicylic acid-induced cell death. Plant Cell. 16: 21-32.

KAY, S., HAHN, S., MAROIS, E., HAUSE, G. and BONAS, U. (2007) A bacterial effector acts as a plant transcription factor and induces a cell size regulator. Science. 318: 648-51.

KEINATH, N.F., KIERSZNIOWSKA, S., LOREK, J., BOURDAIS, G., KESSLER, S.A., SHIMOSATO-ASANO, H., GROSSNIKLAUS, U., SCHULZE, W.X., ROBATZEK, S. and PANSTRUGA, R. (2010) PAMP (pathogen-associated molecular pattern)-induced changes in plasma membrane compartmentalization reveal novel components of plant immunity. J Biol Chem. 285: 39140-49.

KELLEHER, D.J. and GILMORE, R. (2006) An evolving view of the eukaryotic oligosaccharyltransferase. Glycobiology. 16: 47R-62R.

KESSLER, S.A., SHIMOSATO-ASANO, H., KEINATH, N.F., WUEST, S.E., INGRAM, G., PANSTRUGA, R. and GROSSNIKLAUS, U. (2010) Conserved molecular components for pollen tube reception and fungal invasion. Science. 330: 968-71.

KIM, H.R., LEE, G.H., CHO, E.Y., CHAE, S.W., AHN, T. and CHAE, H.J. (2009) Bax inhibitor 1 regulates ER-stress-induced ROS accumulation through the regulation of cytochrome P450 2E1. J Cell Sci. 122: 1126-33.

KIM, H.R., LEE, G.H., HA, K.C., AHN, T., MOON, J.-Y., LEE, B.J., CHO, S.G., KIM, S., SEO, Y.R., SHIN, Y.J., CHAE, S.W., REED, J.C. and CHAE, H.-J. (2008). Bax inhibitor-1 (BI-1) is a pH-dependent regulator of Ca^{2+} channel activity in the endoplasmic reticulum. J Biol Chem. 283: 15946-55.

KIM, M.C., LEE, S.H., KIM, J.K., CHUN, H.J., CHOI, M.S., CHUNG, W.S., MOON, B.C., KANG, C.H., PARK, C.Y., YOO, J.H., KANG, Y.H., KOO, S.C., KOO, Y.D., JUNG, J.C., KIM, S.T., SCHULZE-LEFERT, P., LEE, S.Y. and CHO, M.J. (2002a) Mlo, a modulator of plant defence and cell death, is a novel calmodulin-binding protein. Isolation and characterization of a rice Mlo homologue. J Biol Chem. 277: 19304-14.

KIM, M.C., PANSTRUGA, R., ELLIOTT, C., MÜLLER, J., DEVOTO, A., YOON, H.W., PARK, H.C., CHO, M.J. and SCHULZE-LEFERT, P. (2002b) Calmodulin interacts with MLO protein to regulate defence against mildew in barley. Nature. 416: 447-51.

KIM, T.H., BÖHMER, M., HU, H., NISHIMURA, N. and SCHROEDER, J.I. (2010) Guard cell signal transduction network: advances in understanding abscisic acid, CO_2, and Ca^{2+} signaling. Annu Rev Plant Biol. 61: 561-91.

KNAUER, R. and LEHLE, L. (1999) The oligosaccharyltransferase complex from yeast. Biochim Biophys Acta. 1426: 259-73.

KOGA, H., BUSHNELL, W.R. and ZEYEN, R.J. (1990) Specificityof cell type and timing of events associated with papilla formation and the hypersensitive reaction in leaves of Hordeum vulgare attached by Erysiphe graminis f.sp. hordei. Can J Bot. 68: 2344-52.

KOIWA, H., LI, F., McCULLY, M.G., MENDOZA, I., KOIZUMI, N., MANABE, Y., NAKAGAWA, Y., ZHU, J., RUS, A., PARDO, J.M., BRESSAN, R.A. and HASEGAWA, P.M. (2003) The STT3a subunit isoform of the Arabidopsis oligosaccharyltransferase controls adaptive responses to salt/osmotic stress. Plant Cell. 15: 2273-84.

KØLSTER, P., MUNK, L., STØLEN, O. and LØHDE, J. (1986) Near-isogenic barley lines with genes for resistance to powdery mildew. Crop Sci. 26: 903-907.

KOMBRINK, A., SÁNCHEZ-VALLET, A. and THOMMA, B.P. (2011) The role of chitin detection in plant-pathogen interactions. Microbes Infect. 13: 1168-76.

KORNMANN, B., CURRIE, E., COLLINS, S.R., SCHULDINER, M., NUNNARI, J., WEISSMAN, J.S. and WALTER, P. (2009) An ER-mitochondria tethering complex revealed by a synthetic biology screen. Science. 325: 477-81.

KRISHNA, P. (2003) Brassinosteroid-mediated stress responses. J Plant Growth Regul. 22: 289-97.

KROL, E., MENTZEL, T., CHINCHILLA, D., BOLLER, T., FELIX, G., KEMMERLING, B., POSTEL, S., ARENTS, M., JEWORUTZKI, E., AL-RASHEID, K.A., BECKER, D. and HEDRICH, R. (2010) Perception of the Arabidopsis danger signal peptide 1 involves the pattern recognition receptor AtPEPR1 and its close homologue AtPEPR2. J Biol Chem. 285: 13471-79.

KRUGER, N.J. (1994) The Bradford method for protein quantitation. Methods Mol Biol. 32: 9-15.

KULIKOV, A.V., SHILOV, E.S., MUFAZALOV, I.A., GOGVADZE, V., NEDOSPASOV, S.A. and ZHIVOTOVSKY, B. (2011) Cytochrome c: the Achilles' heel in apoptosis. Cell Mol Life Sci. doi: 10.1007/s00018-011-0895-z.

KUNOH, H., ITOH, O., KOHNO, M. and ISHIZAKI, H. (1979) Are primary germ tubes of conidia unique to *Erysiphe graminis*? Ann Phytopathol Soc Jpn. 45: 675-82.

KWAAITAAL, M., KEINATH, N.F., PAJONK, S., BISKUP, C. and PANSTRUGA, R. (2010) Combined bimolecular fluorescence complementation and Forster resonance energy transfer reveals ternary SNARE complex formation in living plant cells. Plant Physiol. 152: 1135-47.

LAEMMLI, U.K. (1970) Cleaveage of structural proteins during assembly of the head of bacteriophage T4. Nature. *227*: 680-85.

LAM, E., KATO, N. and LAWTON, M. (2001) Programmed cell death, mitochondria and the plant hypersensitive response. Nature. 411: 848-53.

LAMB, C. and DIXON, R.A. (1997) The oxidative burst in plant disease resistance. Annu Rev Plant Biol. 48: 251-75.

LEE, G.H., KIM, D.S., KIM, H.T., LEE, J.W., CHUNG, C.H., AHN, T., LIM, J.M., KIM, I.K., CHAE, H.J. and KIM, H.R. (2011) Enhanced lysosomal activity is involved in Bax inhibitor-1-induced regulation of the endoplasmic reticulum (ER) stress response and cell death against ER stress: involvement of vacuolar H^+-ATPase (V-ATPase). J Biol Chem. 286: 24743-53.

LEE, G.H., KIM, H.R. and CHAE, H.J. (2012) Bax inhibitor-1 regulates the expression of P450 2E1 through enhanced lysosome activity. Int J Biochem Cell Biol. doi:10.1016/j.biocel.2011.12.017.

LEROUXEL, O., MOUILLE, G., ANDÈME-ONZIGHI, C., BRUYANT, M.P., SÉVENO, M., LOUTELIER-BOURHIS, C., DRIOUICH, A., HÖFTE, H. and LEROUGE, P. (2005) Mutants in DEFECTIVE GLYCOSYLATION, an *Arabidopsis* homolog of an oligosaccharyltransferase complex subunit, show protein underglycosylation and defects in cell differentiation and growth. Plant J. 42: 455-68.

LEVINE, A., PENNELL, R.I., ALVAREZ, M.E., PALMER, R. and LAMB, C. (1996) Calcium-mediated apoptosis in a plant hypersensitive disease resistance response. Curr Biol. 6: 427-37.

L'HARIDON, F., BESSON-BARD, A., BINDA, M., SERRANO, M., ABOU-MANSOUR, E., BALET, F., SCHOONBEEK, H.J., HESS, S., MIR, R., LÉON, J., LAMOTTE, O. and MÉTRAUX, J.P. (2011) A permeable cuticle is associated with the release of reactive oxygen species and induction of innate immunity. PLoS Pathog. 7: e1002148.

LI-BEISSON, Y., POLLARD, M., SAUVEPLANE, V., PINOT, F., OHLROGGE, J. and BEISSON, F. (2009) Nanoridges that characterize the surface morphology of flowers require the synthesis of cutin polyester. Proc Natl Acad Sci U S A. 106: 22008-13.

LIPKA, U, FUCHS, R. and LIPKA, V. (2008): *Arabidopsis* non-host resistance to powdery mildews. Curr Opin Plant Biol. 11: 404-11.

LIPKA, V., DITTGEN, J., BEDNAREK, P., BHAT, R., WIERMER, M., STEIN, M., LANDTAG, J., BRANDT, W., ROSAHL, S., SCHEEL, D., LLORENTE, F., MOLINA, A., PARKER, J., SOMERVILLE, S. and SCHULZE-LEFERT, P. (2005) Pre- and postinvasion defenses both contribute to nonhost resistance in *Arabidopsis*. Science. 310: 1180-83.

Liu, J., Elmore, J.M., Fuglsang, A.T., Palmgren, M.G., Staskawicz, B.J. and Coaker, G. (2009) RIN4 functions with plasma membrane H^+-ATPases to regulate stomatal apertures during pathogen attack. PLoS Biol. 7: e1000139.

Liu, J.X. and Howell, S.H. (2010) Endoplasmic reticulum protein quality control and its relationship to environmental stress responses in plants. Plant Cell. 22: 2930-42.

Liu, Y., Schiff, M., Czymmek, K., Tallóczy, Z., Levine, B. and Dinesh-Kumar, S.P. (2005) Autophagy regulates programmed cell death during the plant innate immune response. Cell. 121: 567-77.

Lynch, D.V. (1999) Enzymes of sphingolipid metabolism in plants. Methods Enzymol. 311: 130-49.

Lyngkjær, M.F. and Carver, T.L. (2000) Conditioning of cellular defence responses to powdery mildew in cereal leaves by prior attack. Mol Plant Pathol. 1: 41-49.

Mattson, M.P., Kumar, K.N., Wang, H., Cheng, B. and Michaelis, E.K. (1993) Basic FGF regulates the expression of a functional 71 kDa NMDA receptor protein that mediates calcium influx and neurotoxicity in hippocampal neurons. J Neurosci. 13: 4575-88.

Merkle, T. (2003) Nucleo-cytoplasmic partitioning of proteins in plants: implications for the regulation of environmental and developmental signalling. Curr Genet. 44: 231-60.

Micali, C., Göllner, K., Humphry, M., Consonni, C. and Panstruga, R. (2008) The powdery mildew disease of *Arabidopsis*: A paradigm for the interaction between plants and biotrophic fungi. The Arabidopsis book. 6: e0115.

Millar, A.H., Sweetlove, L.J., Giegé, P. and Leaver, C.J. (2001) Analysis of the *Arabidopsis* mitochondrial proteome. Plant Physiol. 127: 1711-27.

Miya, A., Albert, P., Shinya, T., Desaki, Y., Ichimura, K., Shirasu, K., Narusaka, Y., Kawakami, N., Kaku, H. and Shibuya, N. (2007). CERK1, a LysM receptor kinase, is essential for chitin elicitor signaling in *Arabidopsis*. Proc Natl Acad Sci U S A. 104: 19613-18.

Møller, B.L. (2010) Plant science. Dynamic metabolons. Science. 330: 1328-29.

Morales, A.P., Carvalho, A.C., Monteforte, P.T., Hirata, H., Han, S.W., Hsu, Y.T. and Smaili, S.S. (2011) Endoplasmic reticulum calcium release engages Bax translocation in cortical astrocytes. Neurochem Res. 36: 829-38.

Mucyn, T.S., Clemente, A., Andriotis, V.M., Balmuth, A.L., Oldroyd, G.E., Staskawicz, B.J. and Rathjen, J.P. (2006) The tomato NBARC-LRR protein Prf interacts with Pto kinase *in vivo* to regulate specific plant immunity. Plant Cell. 18: 2792-806.

Mur, L.A., Kenton, P., Lloyd, A.J., Ougham, H. and Prats, E. (2008) The hypersensitive response; the centenary is upon us but how much do we know? J Exp Bot. 59: 501-20.

Nafisi, M., Sønderby, I.E., Hansen, B.G., Geu-Flores, F., Nour-Eldin, H.H., Nørholm, M.H.H., Jensen, N.B., Li, J. and Halkier, B.A. (2006) Cytochromes P450 in the biosynthesis of glucosinolates and indole alkaloids. Phytochem Rev. 5: 331-46.

Nagano, M., Ihara-Ohori, Y., Imai, H., Inada, N., Fujimoto, M., Tsutsumi, N., Uchimiya, H. and Kawai-Yamada, M. (2009) Functional association of cell

death suppressor, *Arabidopsis* Bax inhibitor-1, with fatty acid 2-hydroxylation through cytochrome b. Plant J. 58: 122-34.

NAKASHITA, H., YASUDA, M., NITTA, T., ASAMI, T., FUJIOKA, S., ARAI, Y., SEIKIMATA, K., TAKATSUTO, S., YAMAGUCHI, I. and YOSHIDA, S. (2003) Brassinosteroid functions in a broad range of disease resistance in tobacco and rice. Plant J. 33: 887-98.

NAM, K.H. and LI, J. (2002) BRI1/BAK1, a receptor kinase pair mediating brassinosteroid signaling. Cell. 110: 203-12.

NAUR, P., PETERSEN, B.L., MIKKELSEN, M.D., BAK, S., RASMUSSEN, H., OLSEN, C.E. and HALKIER, B.A. (2003) CYP83A1 and CYP83B1, two nonredundant cytochrome P450 enzymes metabolizing oximes in the biosynthesis of glucosinolates in *Arabidopsis*. Plant Physiol. 133: 63-72.

NIELSEN, J.A., CHAMBERS, M.A., ROMM, E., LEE, L.Y.-H., BERNDT, J.A. and HUDSON, L.D. (2011) Mouse transmembrane BAX inhibitor Motif 3 (Tmbim3) encodes a 38 kDa transmembrane protein expressed in the central nervous system. Mol Cell Biochem. 357: 73-81.

NIELSEN, J.S. and MØLLER, B.L. (2000) Cloning and expression of cytochrome P450 enzymes catalyzing the conversion of tyrosine to *p*-hydroxyphenylacetaldoxime in the biosynthesis of cyanogenic glucosides in *Triglochin maritima*. Plant Physiol. 122: 1311-21.

NIJTMANS, L.G., DE JONG, L., ARTAL SANZ, M., COATES, P.J., BERDEN, J.A., BACK, J.W., MUIJSERS, A.O., VAN DER SPEK, H. and GRIVELL, L.A. (2000) Prohibitins act as a membrane-bound chaperone for the stabilization of mitochondrial proteins. EMBO J. 19: 2444-51.

NÜRNBERGER, T., BRUNNER, F., KEMMERLING, B. and PIATER, L. (2004) Innate immunity in plants and animals: striking similarities and obvious differences. Immunol Rev. 198: 249-66.

O'CONNELL, R.J. and PANSTRUGA, R. (2006) Tête à tête inside a plant cell: establishing compatibility between plants and biotrophic fungi and oomycetes. New Phytol. 171: 699-718.

OERKE, E.-C. and DEHNE, H.-W. (2004) Safeguarding production-losses in major crops and the role of crop protection. Crop Protection. 23: 275-85.

OPALSKI, K.S., SCHULTHEISS, H., KOGEL, K.-H. and HÜCKELHOVEN, R. (2005) The receptor-like MLO protein and the RAC/ROP family G-protein RACB modulate actin reorganization in barley attacked by the biotrophic powdery mildew fungus *Blumeria graminis* f.sp*. hordei*. Plant J. 41: 291-303.

PAJONK, S., KWON, C., CLEMENS, N., PANSTRUGA, R. and SCHULZE-LEFERT, P. (2008) Activity determinants and functional specialization of *Arabidopsis* PEN1 syntaxin in innate immunity. J Biol Chem. 283: 26974-84.

PANSTRUGA, R. (2003) Establishing compatibility between plants and obligate biotrophic pathogens. Curr Opin Plant Biol. 6: 320-26.

PANSTRUGA, R. (2005) Serpentine plant MLO proteins as entry portals for powdery mildew fungi. Biochem Soc Trans. 33: 389-92.

PECENKOVÁ, T., HÁLA, M., KULICH, I., KOCOURKOVÁ, D., DRDOVÁ, E., FENDRYCH, M., TOUPALOVÁ, H. and ZÁRSKY, V. (2011) The role for the exocyst complex subunits Exo70B2 and Exo70H1 in the plant-pathogen interaction. J Exp Bot. 62: 2107-16.

PERFECT, S.E. and GREEN, J.R. (2008) Infection structures of biotrophic and hemibiotrophic fungal plant pathogens. Mol Plant Pathol. 2: 101-108.

PETUTSCHNIG, E.K., JONES, A.M., SERAZETDINOVA, L., LIPKA, U. and LIPKA, V. (2010) The lysin motif receptor-like kinase (LysM-RLK) CERK1 is a major chitin-binding protein in *Arabidopsis thaliana* and subject to chitin-induced phosphorylation. J Biol Chem. 285: 28902-11.

PIFFANELLI, P., ZHOU, F., CASAIS, C., ORME, J., JAROSCH, B., SCHAFFRATH, U., COLLINS, N.C., PANSTRUGA, R. and SCHULZE-LEFERT, P. (2002) The barley MLO modulator of defense and cell death is responsive to biotic and abiotic stress stimuli. Plant Physiol. 129: 1076-85.

POULTON, J.E. and MØLLER, B.L. (1993) Glucosinolates. Methods in Plant Biochemistry (Lea, P.J. Ed.), vol. 9, Academic Press, London, pp. 209-237.

PRÖLS, R. and ROITSCH, T. (2009) Extracellular invertase LIN6 of tomato: a pivotal enzyme for integration of metabolic, hormonal, and stress signals is regulated by a diurnal rhythm. J Exp Bot. 60: 1555-67.

PRYCE-JONES, E., CARVER, T. and GURR, S.J. (1999) The roles of cellulose enzymes and mechanical force in host penetration by *Erysiphe graminis* f.sp. *hordei*. Physiol Mol Plant Pathol. 55: 175-82.

PSHENICHNAYA, L.A., KHRIPACH, V.A., VOLYNETZ, A.P., PROKKHORCHIK, R.A., MANZHELESOVA, N.E. and MOROZIK, G.V. (1997) Brassinosteroids and resistance of barley plants to leaf diseases. Problems of Experimental Botany (Parfenov, V.I. Ed.), Byelorussian Science, Minsk, pp. 210-17.

REIMERS, K., CHOI, C.Y.U., MAU-THEK, E. and VOGT, P.M. (2006) Sequence analysis shows that Lifeguard belongs to a new evolutionarily conserved cytoprotective family. Int J Mol Med. 18: 729-34.

REINTANZ, B., LEHNEN, M., REICHELT, M., GERSHENZON, J., KOWALCZYK, M., SANDBERG, G., GODDE, M., UHL, R. and PALME, K. (2001) Bus, a Bushy *Arabidopsis cyp79f1* knockout mutant with abolished synthesis of short-chain aliphatic glucosinolates. Plant Cell. 13: 351-67.

REISEN, D., MARTY, F. and LEBORGE-CASTEL, N. (2005) New insights into tonoplast architecture of plant vacuoles and vacuolar dynamics during osmotic stress. BMC Plant Biology. 5: 1-13.

REUBER T.L., PLOTNIKOVA, J.M., DEWDNEY, J., ROGERS, E.E., WOOD, W. and AUSUBEL, F.M. (1998) Correlation of defense gene induction defects with powdery mildew susceptibility in *Arabidopsis* enhanced disease susceptibility mutants. Plant J. 16: 473-85.

RIDOUT, C.J., SKAMNIOTI, P., PORRITT, O., SACRISTAN, S., JONES, J.D. and BROWN, J.K. (2006) Multiple avirulence paralogues in cereal powdery mildew fungi may contribute to parasite fitness and defeat of plant resistance. Plant Cell. 18: 2402-14.

ROJAS-RIVERA, D., ARMISÉN, R., COLOMBO, A., MARTÍNEZ, G., EGUIGUREN, A.L., DÍAZ, A., KIVILUOTO, S., RODRÍGUEZ, D., PATRON, M., RIZZUTO, R., BULTYNCK, G., CONCHA, M.L., SIERRALTA, J., STUTZIN, A. and HETZ, C. (2012) TMBIM3/GRINA is a novel unfolded protein response (UPR) target gene that controls apoptosis through the modulation of ER calcium homeostasis. Cell Death Differ. doi: 10.1038/cdd.2011.189.

ROONEY, H.C., VAN'T KLOOSTER, J.W., VAN DER HOORN, R.A., JOOSTEN, M.H., JONES, J.D. and DE WIT, P.J. (2005) *Cladosporium* Avr2 inhibits tomato Rcr3 protease required for *Cf-2*-dependent disease resistance. Science. 308: 1783-86.

ROSEBROCK, T.R., ZENG, L., BRADY, J.J., ABRAMOVITCH, R.B., XIAO, F. and MARTIN, G.B. (2007) A bacterial E3 ubiquitin ligase targets a host protein kinase to disrupt plant immunity. Nature. 448: 370-74.

ROSSO, M.G., LI, Y., STRIZHOV, N., REISS, B., DEKKER, K. and WEISSHAAR, B. (2003) An *Arabidopsis thaliana* T-DNA mutagenized population (GABI-Kat) for flanking sequence tag-based reverse genetics. Plant Mol Biol. 53: 247-59.

ROTHBAUER, U., ZOLGHADR, K., MUYLDERMANS, S., SCHEPERS, A. CARDOSO, C.M. and LEONHARDT, H. (2008) A versatile nanotrap for biochemical and functional studies with fluorescent fusion proteins. Mol Cell Proteomics. 7: 282-89.

ROUX, M., SCHWESSINGER, B., ALBRECHT, C., CHINCHILLA, D., JONES, A., HOLTON, N., MALINOVSKY, F.G., TÖR, M., DE VRIES, S. and ZIPFEL, C. (2011) The *Arabidopsis* leucine-rich repeat receptor-like kinases BAK1/SERK3 and BKK1/SERK4 are required for innate immunity to hemibiotrophic and biotrophic pathogens. Plant Cell. 23: 2440-55.

RUEGGER, M. and CHAPPLE, C. (2001) Mutations that reduce sinapoylmalate accumulation in *Arabidopsis thaliana* define loci with diverse roles in phenylpropanoid metabolism. Genetics. 159: 1741-49.

SAGI, M. and FLUHR, R. (2001) Superoxide production by plant homologues of the gp91(phox) NADPH oxidase. Modulation of activity by calcium and by tobacco mosaic virus infection. Plant Physiol. 126: 1281-90.

SAKURADA, K., IKEGAYA, H., OHTA, H., FUKUSHIMA, H., AKUTSU, T. and WATANABE, K. (2009) Effects of oximes on mitochondrial oxidase activity. Toxicol Lett. 189: 110-14.

SANCHEZ, P., DE TORRES ZABALA, M. and GRANT, M. (2000) AtBI-1, a plant homologue of Bax inhibitor-1, suppresses Bax-induced cell death in yeast and is rapidly upregulated during wounding and pathogen challenge. Plant J. 21: 393-99.

SCHULER, M.A. and WERCK-REICHHART, D. (2003) Functional genomics of P450s. Annu Rev Plant Biol. 54: 629-67.

SCHULTHEISS, H., DECHERT, C., KOGEL, K.-H. and HÜCKELHOVEN, R. (2003) Functional analysis of barley RAC/ROP G-protein family members in susceptibility to the powdery mildew fungus. Plant J. 36: 589-601.

SCHULTHEISS, H., DECHERT, C., KOGEL, K.H. and HÜCKELHOVEN, R. (2002) A small GTP-binding host protein is required for entry of powdery mildew fungus into epidermal cells of barley. Plant Physiol. 128: 1447-54.

SCHULTHEISS, H., PREUSS, J., PIRCHER, T., EICHMANN, R. and HÜCKELHOVEN, R. (2008) Barley RIC171 interacts with RACB in planta and supports entry of the powdery mildew fungus. Cell Microbiol. 10: 1815-26.

SCHULTZ, C., GILSON, P., OXLEY, D., YOUL, J. and BACIC, A. (1998) GPI-anchors on arabinogalactan-proteins: implications for signalling in plants. Trends Plant Sci. 3: 426-31.

SCHULZE GRONOVER, C., KASULKE, D., TUDZYNSKI, P. and TUDZYNSKI, B. (2001) The role of G protein alpha subunits in the infection process of the gray mold fungus *Botrytis cinerea*. Mol Plant Microbe Interact. 14: 1293-302.

SCHULZE-LEFERT, P. (2004): Knocking on the heaven's wall: pathogenesis of and resistance to biotrophic fungi at the cell wall. Curr Opin Plant Biol. 7: 377-83.

SCHWEIZER, P., POKORNY, J., ABDERHALDEN, O. and DUDLER, R. (1999) A transient assay system for the functional assessment of defense-related genes in wheat. Mol Plant Microbe Interact. 12: 647-54.

SHABAB, M., SHINDO, T., GU, C., KASCHANI, F., PANSURIYA, T., CHINTHA, R., HARZEN, A., COLBY, T., KAMOUN, S. and VAN DER HOORN, R. A. (2008) Fungal effector protein AVR2 targets diversifying defense-related cys proteases of tomato. Plant Cell. 20: 1169-83.

SHAN, L., HE, P., LI, J., HEESE, A., PECK, S.C., NÜRNBERGER, T., MARTIN, G.B. and SHEEN, J. (2008) Bacterial effectors target the common signaling partner BAK1 to disrupt multiple MAMP receptor-signaling complexes and impede plant immunity. Cell Host Microbe. 4: 17-27.

SHAO, F., GOLSTEIN, C., ADE, J., STOUTEMYER, M., DIXON, J.E. and INNES, R.W. (2003) Cleavage of *Arabidopsis* PBS1 by a bacterial type III effector. Science. 301: 1230-33.

SHEN, Q.H., SAIJO, Y., MAUCH, S., BISKUP, C., BIERI, S., KELLER, B., SEKI, H., ULKER, B., SOMSSICH, I.E. and SCHULZE-LEFERT, P. (2007) Nuclear activity of MLA immune receptors links isolate-specific and basal disease-resistance responses. Science. 315: 1098-103.

SHEN, Q.H., ZHOU, F., BIERI, S., HAIZEL, T., SHIRASU, K. and SCHULZE-LEFERT, P. (2003) Recognition specificity and RAR1/SGT1 dependence in barley Mla disease resistance genes to the powdery mildew fungus. Plant Cell. 15: 732-44.

SHIMIZU, T., NAKANO, T., TAKAMIZAWA, D., DESAKI, Y., ISHII-MINAMI, N., NISHIZAWA, Y., MINAMI, E., OKADA, K., YAMANE, H., KAKU, H. and SHIBUYA, N. (2010) Two LysM receptor molecules, CEBiP and OsCERK1, cooperatively regulate chitin elicitor signaling in rice. Plant J. 64: 204-14.

SHIMMEN, T. and YOKOTA, E. (2004) Cytoplasmic streaming in plants. Curr Opin Cell Biol.16: 68-72.

SHIRASU, K. and SCHULZE-LEFERT, P. (2003) Complex formation, promiscuity and multi-functionality: protein interactions in disease-resistance pathways. Trends Plant Sci. 8: 252-58.

SHIRASU, K., NIELSEN, K., PIFFANELLI, P., OLIVER, R. and SCHULZE-LEFERT, P. (1999) Cell-autonomous complementation of *mlo* resistance using a biolistic transient expression system. Plant J. 17: 293-99.

SHUKLA, S., FUJITA, K.I., XIAO, Q., LIAO, Z., GARFIELD, S. and SRINIVASULA, S.M. (2010) A shear stress responsive gene product PP1201 protects against Fas-mediated apoptosis by reducing Fas expression on the cell surface. Apoptosis 16: 1-12.

SIMINSZKY, B., CORBIN, F.T., WARD, E.R., FLEISCHMANN, T.J. and DEWEY, R.E. (1999) Expression of a soybean cytochrome P450 monooxygenase cDNA in yeast and tobacco enhances the metabolism of phenylurea herbicides. Proc Natl Acad Sci U S A. 96: 1750-55.

SNEDDEN, W.A. and FROMM, H. (1997) Characterization of the plant homologue of prohibitin, a gene associated with antiproliferative activity in mammalian cells. Plant Mol Biol. 33: 753-56.

SOMIA, N.V., SCHMITT, M.J., VETTER, D.E., VAN ANTWERP, D., HEINEMANN, S.F. and VERMA, I.M. (1999) LFG: an anti-apoptotic gene that provides protection from Fas-mediated cell death. Proc Natl Acad Sci U S A. 96: 12667-72.

SONG, J., WIN, J., TIAN, M., SCHORNACK, S., KASCHANI, F., ILYAS, M., VAN DER HOORN, R.A. and KAMOUN, S. (2009) Apoplastic effectors secreted by two unrelated eukaryotic plant pathogens target the tomato defense protease Rcr3. Proc Natl Acad Sci U S A. 106: 1654-59.

SPANU, P.D., ABBOTT, J.C., AMSELEM, J., BURGIS, T.A., SOANES, D.M., STÜBER, K., VER LOREN VAN THEMAAT, E., BROWN, J.K., BUTCHER, S.A., GURR, S.J., LEBRUN, M.H., RIDOUT, C.J., SCHULZE-LEFERT, P., TALBOT, N.J., AHMADINEJAD, N., AMETZ, C., BARTON, G.R., BENJDIA, M., BIDZINSKI, P., BINDSCHEDLER, L.V., BOTH, M., BREWER, M.T., CADLE-DAVIDSON, L., CADLE-DAVIDSON, M.M., COLLEMARE, J., CRAMER, R., FRENKEL, O., GODFREY, D., HARRIMAN, J., HOEDE, C., KING, B.C., KLAGES, S., KLEEMANN, J., KNOLL, D., KOTI, P.S., KREPLAK, J., LÓPEZ-RUIZ, F.J., LU, X., MAEKAWA, T., MAHANIL, S., MICALI, C., MILGROOM, M.G., MONTANA, G., NOIR, S., O'CONNELL, R.J., OBERHAENSLI, S., PARLANGE, F., PEDERSEN, C., QUESNEVILLE, H., REINHARDT, R., ROTT, M., SACRISTÁN, S., SCHMIDT, S.M., SCHÖN M., SKAMNIOTI, P., SOMMER, H., STEPHENS, A., TAKAHARA, H., THORDAL-CHRISTENSEN, H., VIGOUROUX, M., WESSLING, R., WICKER, T. and PANSTRUGA, R. (2010) Genome expansion and gene loss in powdery mildew fungi reveal tradeoffs in extreme parasitism. Science. 330: 1543-46.

SPASSIEVA, S.D., MARKHAM, J.E. and HILLE, J. (2002) The plant disease resistance gene Asc-1 prevents disruption of sphingolipid metabolism during AAL toxin-induced programmed cell death. Plant J. 32: 561-72.

STAEHELIN, L.A. (1997) The plant ER: a dynamic organelle composed of a large number of discrete functional domains. Plant J. 11: 1151-65.

STAKMAN, E.C. (1915) Relation between *Puccina graminis* and plants highly resistant to its attack. J Agric Res. 4: 193-99.

STEIN, M., DITTGEN, J., SÁNCHEZ-RODRÍGUEZ, C., HOU, B.H., MOLINA, A., SCHULZE-LEFERT, P., LIPKA, V. and SOMERVILLE, S. (2006) *Arabidopsis* PEN3/PDR8, an ATP binding cassette transporter, contributes to nonhost resistance to inappropriate pathogens that enter by direct penetration. Plant Cell. 18: 731-46.

STERGIOPOULOS, I. and DE WIT, P.J. (2009) Fungal effector proteins. Annu Rev Phytopathol. 47: 233-63.

STERGIOPOULOS, I., VAN DEN BURG, H.A., OKMEN, B., BEENEN, H.G., VAN LIERE, S., KEMA, G.H. and DE WIT, P.J. (2010) Tomato Cf resistance proteins mediate recognition of cognate homologous effectors from fungi pathogenic on dicots and monocots. Proc Natl Acad Sci U S A. 107: 7610-15.

STOLZENBURG, M.C., AIST, J.R. and ISRAEL, H.W. (1984) The role of papillae in resistance to powdery mildew conditioned by the *mlo* gene in barley. I Correlative evidence. Physiol Plant Pathol. 25: 337-46.

TAKAHASHI, A., KAWASAKI, T., WONG, H.L., SUHARSONO, U., HIRANO, H. and SHIMAMOTO, K. (2003) Hyperphosphorylation of a mitochondrial protein, prohibitin, is induced by calyculin A in a rice lesion-mimic mutant *cdr1*. Plant Physiol. 132: 1861-69.

TANAKA, S., ICHIKAWA, A., YAMADA, K., TSUJI, G., NISHIUCHI, T., MORI, M., KOGA, H., NISHIZAWA, Y., O'CONNELL, R. and KUBO, Y. (2010) HvCEBiP, a gene

homologues to rice chitin receptor CEBiP, contributes to basal resistance of barley to *Magnaporthe oryzae*. BMC Plant Biol. 10: 228.

TATSUTA, T., MODEL, K. and LANGER, T. (2005) Formation of membrane-bound ring complexes by prohibitins in mitochondria. Mol Biol Cell. 16: 248-59.

THOMMA, B.P., VAN ESSE, H.P., CROUS, P.W. and DE WIT, P.J. (2005) *Cladosporium fulvum* (syn. *Passalora fulva*), a highly specialized plant pathogen as a model for functional studies on plant pathogenic *Mycosphaerellaceae*. Mol Plant Pathol. 64: 379-93.

THORDAL-CHRISTENSEN, H., ZHANG, Z., WIE, Y. and COLLINGE, D.B. (1997) Subcellular localization of H_2O_2 in plants. H_2O_2 accumulation in papillae and hypersensitive response during the barley-powdery mildew interaction. Plant J. 11: 1187-94.

TRUERNIT, E., BAUBY, H., DUBREUCQ, B., GRANDJEAN, O., RUNIONS, J., BARTHELEMY, J. and PALAUQUI, J.C. (2008) High-resolution whole-mount imaging of three-dimensional tissue organization and gene expression enables the study of phloem development and structure in *Arabidopsis*. Plant Cell. 20: 1494-503.

UEDA, H., YOKOTA, E., KUTSUNA, N., SHIMADA, T., TAMURA, K., SHIMMEN, T., HASEZAWA, S., DOLJA, V.V. and HARA-NISHIMURA, I. (2010) Myosin-dependent endoplasmic reticulum motility and F-actin organization in plant cells. Proc Natl Acad Sci U S A. 107: 6894-99.

VAN AKEN, O., PECENKOVA, T., VAN DE COTTE, B., DE RYCKE, R., EECKHOUT, D., FROMM, H., DE JAEGER, G., WITTERS, E., BEEMSTER, G.B., INZE, D. and VAN BREUSEGEM, F. (2007) Mitochondrial type-I prohibitins of *Arabidopsis thaliana* are required for supporting proficient meristem development. Plant J. 5: 850-64.

VAN AKEN, O., WHELAN, J. and VAN BREUSEGEM, F. (2010) Prohibitins: mitochondrial partners in development and stress response. Trends Plant Sci. 15: 275-82.

VAN DEN BURG, H.A., HARRISON, S.J., JOOSTEN, M.H., VERVOORT, J. and DE WIT, P.J. (2006) *Cladosporium fulvum* Avr4 protects fungal cell walls against hydrolysis by plant chitinases accumulating during infection. Mol Plant Microbe Interact. 19: 1420-30.

VAN DER LINDE, K., KASTNER, C., KUMLEHN, J., KAHMANN, R. and DOEHLEMANN, G. (2011) Systemic virus-induced gene silencing allows functional characterization of maize genes during biotrophic interaction with *Ustilago maydis*. New Phytol. 189: 471-83.

VAN ESSE, H.P., VAN'T KLOOSTER, J.W., BOLTON, M.D., YADETA, K.A., VAN BAARLEN, P., BOEREN, S., VERVOORT, J., DE WIT, P.J. and THOMMA, B.P. (2008) The *Cladosporium fulvum* virulence protein Avr2 inhibits host proteases required for basal defense. Plant Cell. 10: 1948-63.

VOGEL, J. and SOMERVILLE, S. (2002) Powdery mildew of *Arabidopsis*: a model for host-parasite interactions. The Powdery Mildews: A Comprehensive Treatise. (Bélanger, R.R., Bushnell, W.R., Dik, A.J. and Carver, T.L. Eds.), St. Paul, Minnesota, pp. 161-68.

WALENSKY, L.D. and GAVATHIOTIS, E. (2011) BAX unleashed: the biochemical transformation of an inactive cytosolic monomer into a toxic mitochondrial pore. Trends Biochem Sci. 36: 642-52.

WALTER, L., DIRKS, B., ROTHERMEL, E., HEYENS, M., SZPIRER, C., LEVAN, G. and GUNTHER, E. (1994) A novel, conserved gene of the rat that is developmentally regulated in the testis. Mamm Genome. 5: 216-21.

WANG, W., DEVOTO, A., TURNER, J.G. and XIAO, S. (2007) Expression of the membrane-associated resistance protein RPW8 enhances basal defense against biotrophic pathogens. Mol Plant Microbe Interact. 20: 966-76.

WANG, W., WEN, Y., BERKEY, R. and XIAO, S. (2009) Specific targeting of the *Arabidopsis* resistance protein RPW8.2 to the interfacial membrane encasing the fungal Haustorium renders broad-spectrum resistance to powdery mildew. Plant Cell. 21: 2898-913.

WATANABE, N. and LAM, E. (2006) *Arabidopsis* Bax inhibitor-1 functions as an attenuator of biotic and abiotic types of cell death. Plant J. 45: 884-94.

WATANABE, N. and LAM, E. (2008) BAX INHIBITOR-1 modulates endoplasmic reticulum stress-mediated programmed cell death in *Arabidopsis*. J Biol Chem. 283: 3200-10.

WEI, F., GOBELMAN-WERNER, K., MORROLL, S.M., KURTH, J., MAO, L., WING, R., LEISTER, D., SCHULZE-LEFERT, P. and WISE, R.P. (1999) The Mla (powdery mildew) resistance cluster is associated with three NBS-LRR gene families and suppressed recombination within a 240-kb DNA interval on chromosome 5S (1HS) of barley. Genetics. 153: 1929-48.

WEIGEL D. and GLAZEBROOK J. (2006) Transformation of *Agrobacterium* using the freeze-thaw method. Cold Spring Harb Protoc. doi: 10.1101/pdb.prot4666.

WELLESEN, K., DURST, F., PINOT, F., BENVENISTE, I., NETTESHEIM, K., WISMAN, E., STEINER-LANGE, S., SAEDLER, H. and YEPHREMOV, A. (2001) Functional analysis of the LACERATA gene of *Arabidopsis* provides evidence for different roles of fatty acid omega-hydroxylation in development. Proc Natl Acad Sci U S A. 98: 9694-99.

WESTPHALEN, B.C., WESSIG, J., LEYPOLDT, F., ARNOLD, S. and METHNER, A. (2005) BI-1 protects cells from oxygen glucose deprivation by reducing the calcium content of the endoplasmic reticulum. Cell Death Differ. 12: 304-306.

WHISSON, S.C., BOEVINK, P.C., MOLELEKI, L., AVROVA, A.O., MORALES, J.G., GILROY, E.M., ARMSTRONG, M.R., GROUFFAUD, S., VAN WEST, P., CHAPMAN, S., HEIN, I., TOTH, I.K., PRITCHARD, L. and BIRCH, P.R. (2007) A translocation signal for delivery of oomycete effector proteins into host plant cells. Nature. 450: 115-18.

WOLTER, M., HOLLRICHER, K., SALAMINI, F. and SCHULZE-LEFERT, P. (1993) The mlo resistance alleles to powdery mildew infection in barley trigger a developmentally controlled defence mimic phenotype. Mol Gen Genet. 239: 122-28.

WRIGHT, A.J., THOMAS, B.J. and CARVER, T.L. (2002a) Early adhesion of *Blumeria graminis* to plant and artificial surfaces demonstrated by centrifugation. Physiol Mol Plant Pathol. 61: 217-26.

WRIGHT, A.J., THOMAS, B.J., KUNOH, H., NICHOLSON, R.L. and CARVER, T.L. (2002b) Influences of substrata and interface geometry on the release of extracellular material by *Blumeria graminis* conidia. Physiol Mol Plant Pathol. 61: 163-78.

XIAO, F., GOODWIN, S.M., XIAO, Y., SUN, Z., BAKER, D., TANG, X., JENKS, M.A. and ZHOU, J.M. (2004) *Arabidopsis* CYP86A2 represses *Pseudomonas syringae* type III genes and is required for cuticle development. EMBO J. 23: 2903-13.

XIAO, S., CALIS, O., PATRICK, E., ZHANG, G., CHAROENWATTANA, P., MUSKETT, P., PARKER, J.E. and TURNER, J.G. (2005) The atypical resistance gene, *RPW8*, recruits components of basal defence for powdery mildew resistance in *Arabidopsis.* Plant J. 42: 95-110.

XIAO, S., ELLWOOD, S., CALIS, O., PATRICK, E., LI, T., COLEMAN, M. and TURNER, J.G. (2001) Broad-spectrum mildew resistance in *Arabidopsis thaliana* mediated by RPW8. Science. 291: 118-20.

XU, C., XU, W., PALMER, A.E. and REED, J.C. (2008) BI-1 regulates endoplasmic reticulum Ca^{2+} homeostasis downstream of Bcl-2 family proteins. J Biol Chem. 283: 11477-84.

XU, Q. and REED, J.C. (1998) Bax Inhibitor-1, a mammalian apoptosis suppressor identified by functional screening in yeast. Mol Cell. 1: 337-46.

YAMAGAMI, A., NAKAZAWA, M., MATSUI, M., TUJIMOTO, M., SAKUTA, M., ASAMI, T. and NAKANO, T. (2009) Chemical genetics reveal the novel transmembrane protein BIL4, which mediates plant cell elongation in brassinosteroid signaling. Biosci Biotechnol Biochem. 73: 415-21.

YAMAGUCHI, Y., HUFFAKER, A., BRYAN, A.C., TAX, F.E. and RYAN, C.A. (2010) PEPR2 is a second receptor for the Pep1 and Pep2 peptides and contributes to defense responses in *Arabidopsis.* Plant Cell 22*:* 508-22*.*

YAMAGUCHI, Y., PEARCE, G. and RYAN, C.A. (2006) The cell surface leucine-rich repeat receptor for AtPep1, an endogenous peptide elicitor in *Arabidopsis*, is functional in transgenic tobacco cells. Proc Natl Acad Sci U S A. 103: 10104-109.

YANG, Y., LI, R. and QI, M. (2000) In vivo analysis of plant promoters and transcription factors by agro infiltration of tobacco leaves. Plant J. 22: 543-51.

YANG, Y.D., ELAMAWI, R., BUBECK, J., PEPPERKOK, R., RITZENTHALER, C. and ROBINSON, D.G. (2005) Dynamics of COPII vesicles and the Golgi apparatus in cultured *Nicotiana tabacum* BY-2 cells provides evidence for transient association of Golgi stacks with endoplasmic reticulum exit sites. Plant Cell. 17: 1513-31.

ZEYEN, R.J., CARVER, T.L.W. and LYNGKJÆR, M.F. (2002) Epidermal cell papillae. The Powdery Mildews: a Comprehensive Treatise (Bélanger, R.R., Bushnell, W.R., Dik, A.J. and Carver, T.L. Eds.), St. Paul, Minnesota, pp. 107-25.

ZHANG, J., SHAO, F., LI, Y., CUI, H., CHEN, L., LI, H., ZOU, Y., LONG, C., LAN, L., CHAI, J., CHEN, S., TANG, X. and ZHOU, J.M. (2007) A *Pseudomonas syringae* effector inactivates MAPKs to suppress PAMP-induced immunity in plants. Cell Host Microbe. 1: 175-85.

ZHOU, F., ANDERSEN, C.H., BURHENNE, K., FISCHER, P.H., COLLINGE, D.B. and THORDAL-CHRISTENSEN, H. (2000) Proton extrusion is an essential signalling component in the HR of epidermal single cells in the barley-powdery mildew interaction. Plant J. 23: 245-54.

ZIMMERMANN, P., HIRSCH-HOFFMANN, M., HENNIG, L. and GRUISSEM, W. (2004) GENEVESTIGATOR. *Arabidopsis* microarray database and analysis toolbox. Plant Physiol. 136: 2621-32.

ZIPFEL, C., KUNZE, G., CHINCHILLA, D., CANIARD, A., JONES, J.D. , BOLLER, T. and FELIX, G. (2006) Perception of the bacterial PAMP Ef-Tu by the receptor Efr restricts *Agrobacterium*-mediated transformation. Cell. 125: 749-60.

ZOU, Y., AGGARWAL, M., ZHENG, W.G., WU, H.M. and CHEUNG, A.Y. (2011) Receptor-like kinases as surface regulators for RAC/ROP mediated pollen tube growth and interaction with the pistil. AoB Plants. doi:10.1093/aobpla/plr017.

ZUREK, D.M., RAYLE, D.L., MCMORRIS, T.C. and CLOUSE, S.D. (1994) Investigation of gene expression, growth kinetics, and wall extensibility during brassinosteroid-regulated stem elongation. Plant Physiol. 104: 505-13.
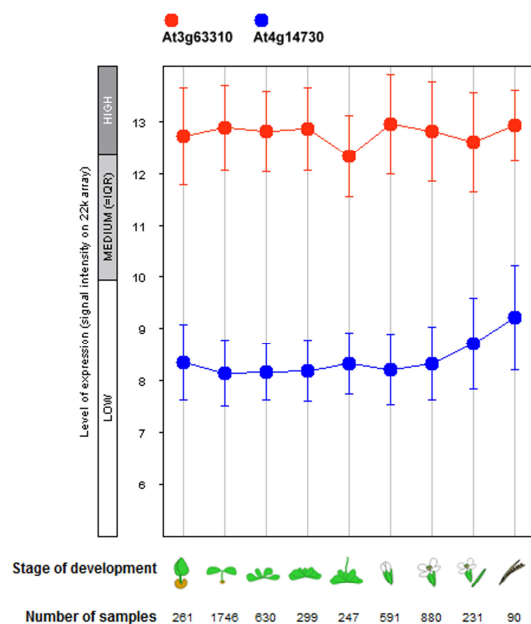
7   Supplement
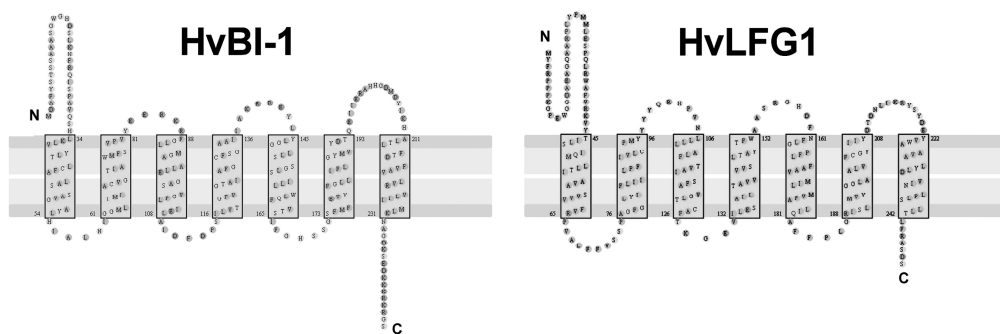
Supplementary figure 1: Prediction of transmembrane domain topology of HvBI-1 and HvLFG1. Marked boxes represent predicted transmembrane domains according to ConPred II (http://bioinfo.si.hirosaki-u.ac.jp/~ConPred2/, ARAI, M., MITSUKE, H., IKEDA, M., XIA, J.X., KIKUCHI, T., SATAKE, M. and SHIMIZU, T. (2004) ConPred II: a consensus prediction method for obtaining transmembrane topology models with high reliability. Nucleic Acids Res. 32 (Web Server issue): W390-93).
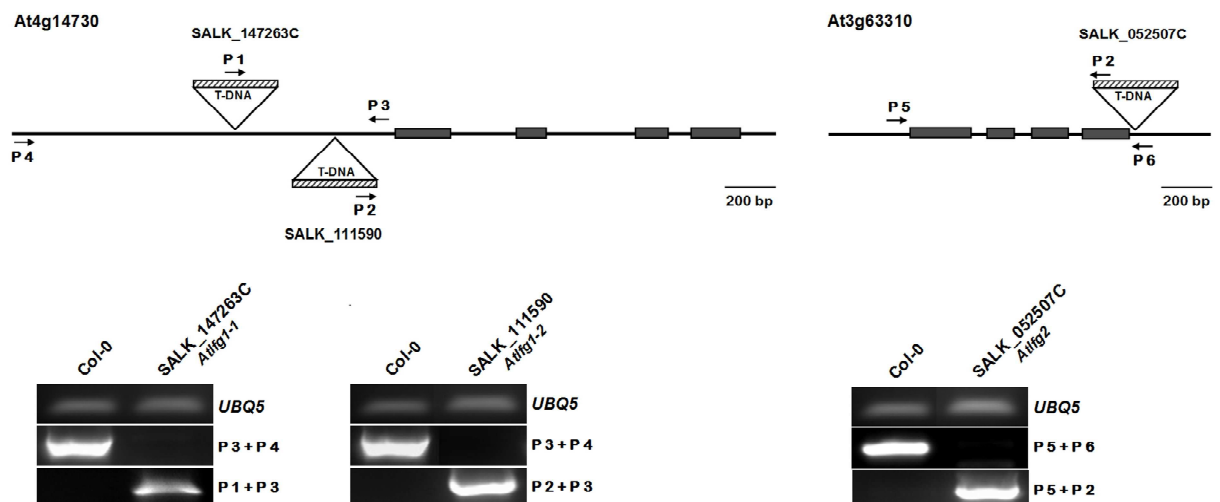

Supplementary figure 2: Characterization of *AtLFG* T-DNA insertion lines. Gene models of *AtLFG1* (At4g14730) and *AtLFG2* (At3g63310) are displayed, revealing information about T-DNA and primer positions. Genomic DNA was extracted from *Arabidopsis* Col-0, *AtLFG1* T-DNA insertion lines SALK_147263C and SALK_111590, and *AtLFG2* T-DNA insertion line SALK_052507C by following a protocol developed by EDWARDS et al. (EDWARDS, K., JOHNSTONE, C. and THOMPSON, C. (1991) A simple and rapid method for preparation of plant genomic DNA for PCR analysis. Nucleic Acids Res. 19: 1349). Standard PCR reactions were conducted using following primers: P1 5'-GTTTTCCCAGTCACGAC-3', P2 5'-ATTTTGCCGATTTCGGAAC-3', P3 5'-TTTTGTTGTTGAAATCGC-3', P4 5'-GTCTTATAATATTAAGGAAT-3', P5 5'-GGATCCCACCGGCGTTGACAAA-3', and P6 5'-TGGCACAGTCTTAAGAGCAA-3'. *UBIQUITIN 5* (*UBQ5*) was amplified using primers 5'-CCAAGCCGAAGAAGATCAAG-3' and 5'-ACTCCTTCCTCAAACGCTGA-3' to confirm equal genomic DNA loading. In Col-0 a 1,476 bp-long promoter fragment of *AtLFG1* was amplified using P4 + P3. Specific T-DNA positions in SALK_147263C and SALK_111590 were confirmed using the primer combination P1 + P3 and P2 + P3, respectively. Primer combination P5 + P6 was used to amplify the 1,025 bp-long genomic fragment sequence of *AtLFG2*. T-DNA position in the SALK line 052507C was confirmed using the primers P5 + P2.

Supplementary figure 3: Development-dependent expression profiles of *AtLFG1* and *AtLFG2*. Expression levels of *AtLFG1* (At4g14730, blue marks) and *AtLFG2* (At3g63310, red marks) were analyzed via Genevestigator.

Supplementary figure 4: *E. cruciferarum* symptoms on Col-0, *Atlfg1-1*, *Atlfg1-2*, and *Atlfg2*. About 5-weeks old-Col-0, *Atlfg1-1*, *Atlfg1-2*, and *Atlfg2* plants were inoculated with 3-5 *E. cruciferarum* spores per mm^2 and photographed 9 dai.
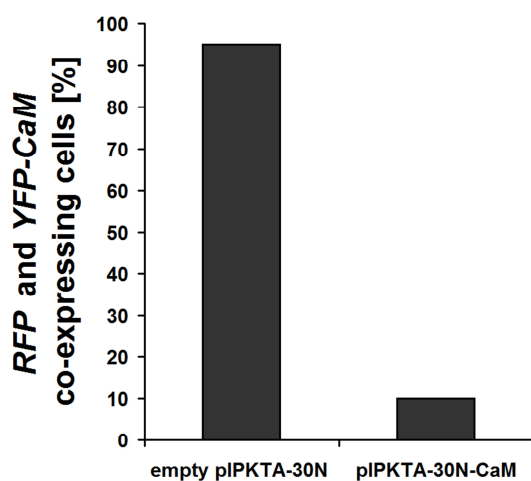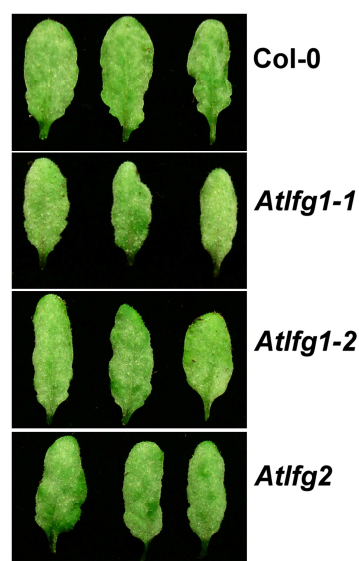
Supplementary figure 5: Transient knock-down of *YFP-CaM* expression. Barley cv. Ingrid cells were transiently co-bombarded with tungsten particles, coated with 1 µg per shot pIPKTA30N-CaM or empty RNAi vector pIPKTA30N together with 1 µg pGY-1-YPF-CaM (YFP-CaM under control of CaMV 35S promoter, provided by R. Panstruga, MPI, Köln) and 0.8 µg pGY-1-RFP, as transformation marker. Two days after bombardment, *RFP* expressing cells were analysed concerning an additional *YFP-CaM* expression. I conducted this experiment only once, whereby 100 cells per variant were inspected.

Supplementary table 1: Proteins co-immunoprecipitated with AtBI-1-GFP and identified by LC-MS/MS. The Mascot search result files were analyzed using Scaffold version 2.6.2 (Proteome Software Inc., Portland, OR, see chapter 2.3.3).Threshold parameters were set as follows: protein probability, 80 %; minimum number of peptides, 1; peptide probability, 80 %, yielding a false-discovery rate of 8.8% on protein level and 7.0% on the peptide-spectrum match level. Listed are all 95 proteins, which were only co-immunoprecipitated with AtBI-1-GFP and not in the control. Proteins are described according to NCBI (state February 16, 2007). Selected proteins for further analysis and BI-1 are highlighted in bold letters.

protein description	gi number	# peptides$_1$	cc$_2$
photosystem II 47 kDa protein [Arabidopsis thaliana]	gi|7525059	7	2
mitochondrial F1 ATP synthase beta subunit [Arabidopsis thaliana]	gi|17939849	6	3
AAC1 (ADP/ATP CARRIER 1); ATP:ADP antiporter/ binding [Arabidopsis thaliana]	gi|15231937	6	3
photosystem I P700 apoprotein A2 [Solanum tuberosum]	gi|108773129	6	2
ATP synthase CF0 B chain [Arabidopsis thaliana]	gi|7525019	6	3
ATP synthase subunit alpha, mitochondrial	gi|14916970	6	3
photosystem II D2 protein [Tofieldia glutinosa]	gi|37721035	5	2
AT5g01530/F7A7_50 [Arabidopsis thaliana]	gi|15081739	5	1
NPQ4 (NONPHOTOCHEMICAL QUENCHING) [Arabidopsis thaliana]	gi|15219418	5	2
photosystem II protein D1 [Eucalyptus globulus subsp. globulus] protein D1 [Populus alba]	gi|108802623	5	2
LHCB6; chlorophyll binding [Arabidopsis thaliana]	gi|15218330	4	2
photosystem II CP43 chlorophyll apoprotein [Eucalyptus globulus subsp. globulus]	gi|108802639	4	2
dolichyl-diphosphooligosaccharide-protein glycotransferase [Arabidopsis thaliana]$_a$	**gi|22328844**	**4**	**4**
putative mitochondrial processing peptidase [Arabidopsis thaliana]	gi|110740617	4	3
cytochrome b559 alpha chain [Spinacia oleracea]	gi|11497544	4	2
AT3g54890 [Arabidopsis thaliana]	gi|13265501	4	1
unknown protein [Arabidopsis thaliana]	gi|15235490	4	1
Lumen-Side Domain Of Reduced Cytochrome F At -35 Degrees Celsius	gi|1942179	4	2
oxoglutarate:malate antiporter [Arabidopsis thaliana]	gi|15237659	4	2
AT4g28750 [Arabidopsis thaliana]	gi|11692884	3	1
hydrolase, acting on acid anhydrides, catalyzing transmembrane movement of substances [Arabidopsis thaliana]	gi|15236722	3	4
hypothetical protein [Arabidopsis thaliana]	gi|110741046	3	1
VHA-A; ATP-binding / hydrogen-transporting ATP synthase, rotational mechanism / hydrogen-transporting ATPase, rotational mechanism [Arabidopsis thaliana]	**gi|15219234**	**3**	**3**
subunit VII of photosystem I [Zygnema circumcarinatum]	gi|108796706	3	2
LHCA2; chlorophyll binding [Arabidopsis thaliana]	gi|15233120	3	2
unknown protein [Arabidopsis thaliana]	gi|18400540	3	1
ATPC1 [Arabidopsis thaliana]	gi|18412632	3	2
unknown protein [Arabidopsis thaliana]	gi|15235503	3	1
binding / oxidative phosphorylation uncoupler [Arabidopsis thaliana]	gi|15241167	3	3

Supplementary table 1 (continued from previous page.)

protein description	gi number	# peptide$_1$	cc$_2$
putative dolichyl-di-phosphooligosaccharide-protein glycotransferase [Arabidopsis thaliana]	gi|14334506	3	4
PSBO-1 (OXYGEN-EVOLVING ENHANCER 33) [Arabidopsis thaliana]	gi|15240013	3	2
transportin [Arabidopsis thaliana]	**gi|23954104**	**3**	**5**
protein translocase/ protein transporter [Arabidopsis thaliana]	gi|15226998	2	2
unknown protein [Arabidopsis thaliana]	gi|18405061	2	1
hydrogen-transporting ATP synthase, rotational mechanism / hydrogen-transporting ATPase, rotational mechanism [Arabidopsis thaliana]	gi|15233985	2	3
PETC (PHOTOSYNTHETIC ELECTRON TRANSFER C) [Arabidopsis thaliana]	gi|15236275	2	2
unknown protein [Arabidopsis thaliana]	gi|18401511	2	1
cytochrome b6/f complex subunit IV [Eucalyptus globulus subsp. globulus]	gi|108802671	2	2
catalytic [Arabidopsis thaliana]	gi|30683676	2	1
Os04g0682800 [Oryza sativa (japonica cultivar-group)]	gi|115461398	2	1
unknown protein [Arabidopsis thaliana]	gi|15222757	2	1
LHCB2.2; chlorophyll binding [Arabidopsis thaliana]	gi|15224465	2	2
EMB1467; NADH dehydrogenase (ubiquinone)/ NADH dehydrogenase/ electron transporter/ iron ion binding / oxidoreductase [Arabidopsis thaliana]	gi|18421656	2	3
unknown protein [Arabidopsis thaliana]$_b$	**gi|18417787**	**2**	**1**
ATP synthase epsilon chain (ATP synthase F1 sector epsilon subunit)	gi|114591	2	3
LHCB4.2 [Arabidopsis thaliana]	gi|15231990	1	2
unknown protein [Arabidopsis thaliana]	gi|18407583	1	1
3-oxo-5-alpha-steroid 4-dehydrogenase [Arabidopsis thaliana]	gi|15237245	1	4
NAD(P)H-quinone oxidoreductase subunit 1, chloroplast (NAD(P)H dehydrogenase subunit 1) (NDH subunit 1) (NADH-plastoquinone oxidoreductase subunit 1)	gi|108860828	1	3
rhodopsin-like receptor [Arabidopsis thaliana]	gi|18398254	1	4
importin-alpha export receptor/ protein transporter [Arabidopsis thaliana]	gi|15226001	1	5
unknown protein [Arabidopsis thaliana]	gi|15225331	1	1
binding / transporter [Arabidopsis thaliana]	gi|15241291	1	4
AHA1 (PLASMA MEMBRANE PROTON ATPASE); ATPase [Arabidopsis thaliana]	**gi|15224264**	**1**	**3**
hypothetical protein OsI_035878 [Oryza sativa (indica cultivar-group)]	gi|125535371	1	1
ATP synthase beta subunit [Dioscorea nipponica]	gi|17224707	1	3
photosystem I psaH protein [Arachis hypogaea]	gi|115187527	1	2
ATP synthase beta subunit [Drypetes littoralis]	gi|118917410	1	3
exportin1 (XPO1) like protein [Arabidopsis thaliana]	gi|110742088	1	5
delta tonoplast integral protein	gi|1145699	1	4
Os05g0519900 [Oryza sativa (japonica cultivar-group)]	gi|115464937	1	1
CF0 subunit IV of ATP synthase [Chara vulgaris]	gi|108773235	1	3

Supplementary table 1 (continued from previous page.)

| protein description	gi number	# peptide$_1$	cc$_2$
lipoxygenase AtLOX2 - Arabidopsis thaliana	gi|11255729	1	2
Os07g0205000 [Oryza sativa (japonica cultivar-group)]	gi|115471095	1	1
clathrin heavy chain, putative [Arabidopsis thaliana]	gi|12321552	1	4
H+-transporting two-sector ATPase, alpha/beta subunit, central region; H+-transporting two-sector ATPase, delta/epsilon subunit [Medicago truncatula]	gi|124360831	1	3
unknown protein [Arabidopsis thaliana]	gi|15231176	1	1
unknown protein [Arabidopsis thaliana]	gi|15237201	1	1
metalloendopeptidase [Arabidopsis thaliana]	gi|15239226	1	4
unknown protein [Arabidopsis thaliana]	gi|18406877	1	1
unknown protein [Arabidopsis thaliana]	gi|18409276	1	1
unknown protein [Arabidopsis thaliana]	gi|18411555	1	1
ATP synthase beta subunit [Didymeles perrieri]	gi|5001597	1	3
ATP synthase beta subunit [Cucurbita pepo]	gi|14718024	1	3
ADP-ribosylation factor, putative, expressed [Oryza sativa (japonica cultivar-group)]	gi|108711707	1	3
Os01g0790900 [Oryza sativa (japonica cultivar-group)]	gi|115440423	1	1
F2G19.31/F2G19.31 [Arabidopsis thaliana]	gi|14517542	1	1
Photosystem II reaction center protein L (PSII-L) (PSII 5 kDa protein)	gi|32469731	1	2
PSII D1 protein [Prunus campanulata]	gi|15529745	1	2
ATPHB2 (PROHIBITIN 2) [Arabidopsis thaliana]	**gi|15219569**	**1**	**4**
NADH dehydrogenase subunit 9 [Brassica napus]	gi|112253858	1	3
Os11g0604500 [Oryza sativa (japonica cultivar-group)]	gi|115486191	1	1
unknown protein [Arabidopsis thaliana]	gi|42566070	1	1
RING finger-like protein (ISS) [Ostreococcus tauri]	gi|116057992	1	4
unknown protein [Arabidopsis thaliana]	gi|15231430	1	1
unknown protein [Arabidopsis thaliana]	gi|18417271	1	1
Bax inhibitor 1 [Brassica napus]	**gi|14719274**	**1**	**4**
atp synthase, beta subunit [Paris tetraphylla]	gi|16943751	1	3
unknown protein [Arabidopsis thaliana]	gi|18410409	1	1
Os05g0157600 [Oryza sativa (japonica cultivar-group)]	gi|115462215	1	1
unknown protein [Arabidopsis thaliana]	gi|15237854	1	1
CYP83A1 (CYTOCHROME P450 83A1); oxygen binding [Arabidopsis thaliana]	**gi|15236349**	**1**	**4**
Os12g0515400 [Oryza sativa (japonica cultivar-group)]	gi|115488796	1	1
unknown protein; 55290-58984 [Arabidopsis thaliana]$_c$	**gi|12323255**	**1**	**1**
Os07g0562700 [Oryza sativa (japonica cultivar-group)]	gi|115472785	1	1

$_1$ number of identified peptides, $_2$ classification code (personal reannotation): 1 = unknown, 2 = chloroplast-associated, 3 = energy/metabolism, 4 = proteins with other functions, 5 = nuclear trafficking; $_a$ HAPLESS 6 (HAP6), $_b$ MYOSIN HEAVY CHAIN-RELATED (MYHC), $_c$ GLYCOSYLPHOSPHATIDYL INOSITOL TRANSAMIDASE SUBUNIT PIG-U (GPI).

Supplementary table 2: Predicted protein signatures and localization of selected putative AtBI-1-interacting proteins.

| protein	InterPro records (IPR)[1]	predicted localization[2]
AHA1	IPR000695 ATPase, P-type, H+ transporting proton pump IPR001757 ATPase, P-type, K/Mg/Cd/Cu/Zn/Na/Ca/Na/H-transporter IPR004014 ATPase, P-type cation-transporter, N-terminal IPR005834 Haloacid dehalogenase-like hydrolase IPR006534 ATPase, P-type, plasma-membrane proton-efflux IPR008250 ATPase, P-type, ATPase-associated domain IPR018303 ATPase, P-type phosphorylation site IPR023214 HAD-like domain IPR023298 ATPase, P-type, transmembrane domain IPR023299 ATPase, P-type, cytoplasmic domain N IPR023300 ATPase, P-type, cytoplasmic transduction domain A	M, N, Pl, PM, V
HAP6	IPR008814 Ribophorin II	CW,ER, M, Mit, Pl, PM, VM
VHA-A	IPR000194 ATPase, F1/V1/A1 complex, alpha/beta subunit, nucleotide-binding domain IPR000793 ATPase, F1/V1/A1 complex, alpha/beta subunit, C-terminal IPR004100 ATPase, F1/V1/A1 complex, alpha/beta subunit, N-terminal IPR005725 ATPase, V1 complex, subunit A IPR018118 ATPase, F1/A1 complex, alpha/beta subunit, N-terminal IPR020003 ATPase, alpha/beta subunit, nucleotide-binding domain, active site IPR022878 V-type ATP synthase catalytic subunit A/alpha IPR024034 ATPase, F1 complex beta subunit/V1 complex, C-terminal	Chlo, CW, M, Pl, PM, V, VM
MYHC	n.s.	ER, VM
TRN1	IPR000357 HEAT IPR001494 Importin-beta, N-terminal IPR011989 Armadillo-like helical IPR016024 Armadillo-type fold	Cyt, N, NP
PHB2	IPR000163 Prohibitin IPR001107 Band 7 protein	Chlo, CW, Mit, P, V, VM
CYP83A1	IPR001128 Cytochrome P450 IPR002401 Cytochrome P450, E-class, group I IPR017972 Cytochrome P450, conserved site	n.s.
GPI	IPR009600 GPI transamidase subunit PIG-U	PM

[1] Protein signature analysis was conducted using InterProScan (state August 31, 2011).

[2] Predicted protein localizations according to TAIR (state August 31, 2011) are listed in alphabetic order. Chlo: chloroplast, CW: cell wall, Cyt: cytosol, ER: endoplasmic reticulum, M: membrane, Mit: mitochondria, N: nucleus, NP: nuclear pore, P: plastid, Pl: plasmodesma, PM: plasma membrane, V: vacuole, VM: vacuolar membrane, n.s.: not specified.
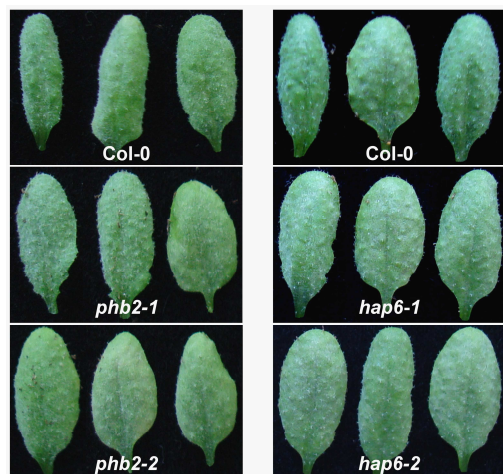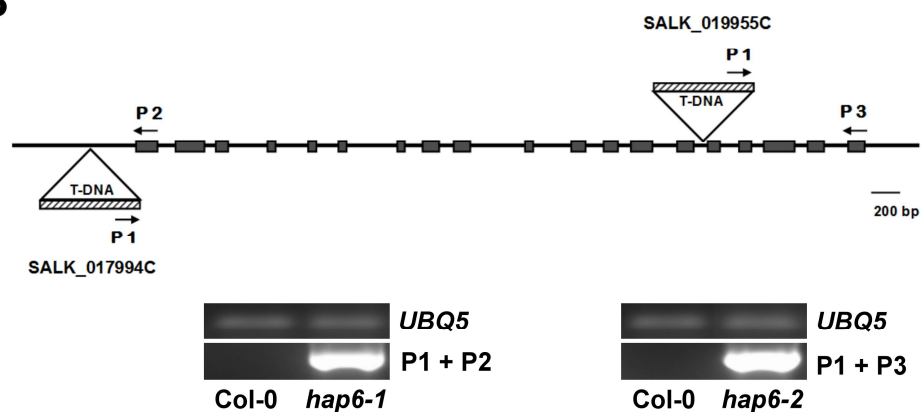
Supplementary figure 6: *E. crucifrarum* **symptoms on Col-0,** *phb2-1, phb2-2, hap6-1,* **and** *hap6-2.* 5-weeks-old Col-0, *phb2-1*, *phb2-2*, *hap6-1*, and *hap6-2* plants were inoculated with 3-5 *E. cruciferarum* spores per mm^2 and photographed 13 dai.
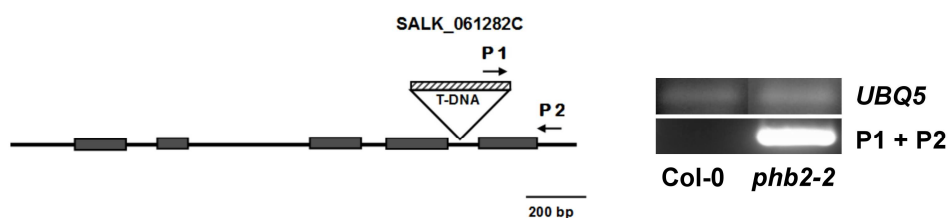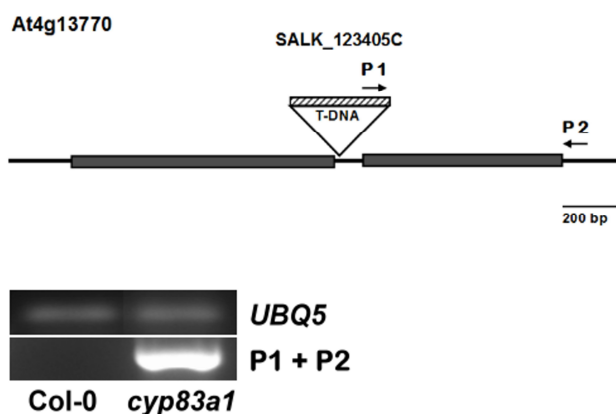

Supplementary figure 7: Confirmation of the T-DNA position in *phb2-2 (*SALK_061282C), *hap6-1* **(SALK_017994C), and** *hap6-2* **(SALK_019955C).** The gene models of **A** *PHB2* and **B** *HAP6* provide information about T-DNA and primer positions. Genomic DNA was extracted from Col-0, *phb2-2*, *hap6-1* and *hap6-2* as described by EDWARDS et al. (EDWARDS, K., JOHNSTONE, C. and THOMPSON, C. (1991) A simple and rapid method for preparation of plant genomic DNA for PCR analysis. Nucleic Acids Res. 19: 1349). Using standard PCR, *UBIQUITIN* (*UBQ5*) was amplified using primers 5'-CCAAGCCGAAGAAGATCAAG-3' and 5'-ACTCCTTCCTCAAACGCTGA-3' to confirm equal genomic DNA loading. **A** T-DNA position in *phb2-2* was confirmed using the primers P1 (5'-GTTTTCCCAGTCACGAC-3') and P2 (5'- GGATCCAAATCCTACCATCGCC-3'). **B** T-DNA confirmation in *hap6-1* and *hap6-1* was conducted using the primer pairs P1 (5'-ATTTTGCCGATTTCGGAAC-3')/P2 (5'-TCGACTGGTACGAAGACATCC-3') and P1/P3 (5'-CGAGCAGATTTCAACTT-3').

Supplementary figure 8: Confirmation of the T-DNA position in *cyp83a1* (SALK_123405C). A gene model of *CYP83A1* is displayed, revealing information on T-DNA and primer positions. Genomic DNA was extracted from Col-0 and *cyp83a1*, following a protocol developed by EDWARDS et al. (EDWARDS, K., JOHNSTONE, C. and THOMPSON, C. (1991) A simple and rapid method for preparation of plant genomic DNA for PCR analysis. Nucleic Acids Res. 19: 1349). *UBIQUITIN* (*UBQ5*) was amplified using primers 5'-CCAAGCCGAAGAAGATCAAG-3' and 5'-ACTCCTTCCTCAAACGCTGA-3' to confirm equal genomic DNA loading. T-DNA position in *cyp83a1* was confirmed using the primers P1 (5'-ATTTTGCCGATTTCGGAAC-3') and P2 (5'-CAGAATACACTGGAGGA-3').
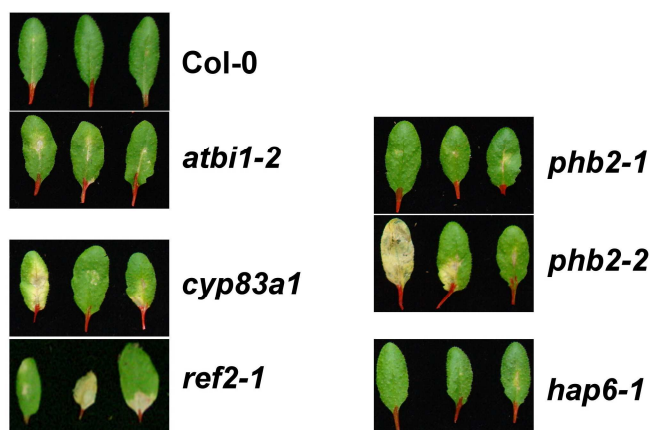
Supplementary figure 9: Typical symptoms of AAL toxin treated Col-0, *atbi1-2*, *cyp83a1*, *ref2-1*, *phb2-1*, *phb2-1*, and *hap6-1* leaves. 10 µl of a 100 mM AAL toxin solution were dropped on leaves of about 5-weeks-old Col-0, *atbi1-2*, *cyp83a1*, *ref2-1*, *phb2-1*, *phb2-1*, and *hap6-1* plants. Photographs were taken 9 days after treatment.

Supplementary table 3: Heat shock treatment of Col-0, *atbi1-2*, *cyp83a1*, *phb2-1*, *phb2-2*, *hap6-1*, and *VHA-A* T-DNA insertion line (SALK_089595C) seedlings.

Mutant line	Heat shock effect
atbi1-2	++
cyp83a1	+
phb2-1	++
phb2-2	++
hap6-1	-
VHA-A T-DNA insertion line (SALK_089595C)	+

8-days-old seedlings were grown on ½ MS media and set to 35℃ for 3 h, followed by a 3-day recovery phase and an additional heat stress at 45℃ for 2 h. Seedlings were evaluated 3 days after treatment.
This table shows the heat shock effect on the mutants compared to Col-0:
- = less affected seedlings
+ = enhanced number of discolored and in the growth restricted seedlings
++ = increased cell death symptoms.
The experiment was conducted only once.
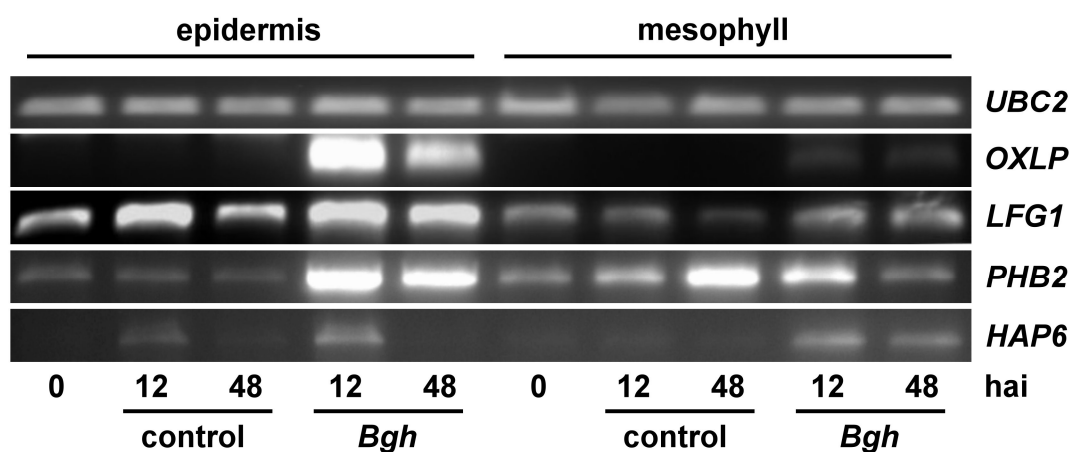
Supplementary figure 10: Tissue-specific gene expression of *LFG1, PHB2,* and *HAP6* in the interaction of barley with *Bgh*. Total RNA was isolated from *Bgh-* or mock-inoculated barley cv. Ingrid leaves that were harvested at 0, 12, and 48 hai. The abaxial epidermal peels and the remaining leaf tissue (mesophyll and adaxial epidermis) were collected, respectively. Gel photographs show ethidium bromide stained semi-quantitative RT-PCR products. Amplification of *UBIQUITIN CONJUGATING ENZYME 2* (*UBC2*) served as control for tissue-unspecific constitutive gene expression, and *OXALATE OXIDASE-LIKE PROTEIN* (*OXLP*) as control for epidermis-specific and pathogen-induced gene expression. Used primers and PCR conditions are listed in supplementary table 4. This experiment was conducted only once.

Supplementary table 4: Primers and PCR conditions for gene expression analyses displayed in supplementary figure 10.

| identity (accession no.)	5′ and 3′ primer sequences	product size (bp)	annealing temp. (℃)	cycle number
UBC2 (AY220735)	TCTCGTCCCTGAGATTGCCCACAT TTTCTCGGGACAGCAACACAATCTTCT	156	59	29
OXLP (X93171)	GGCCGACATGCATTCACCAG CATCTGATATTGCTGGGTCTG	506	57	35
LFG1$_a$	AAGGGGGAGGTGATCCT GGACAGGAGGAGGGGCTA	437	53	30
PHB2 (BAK00720)	GGATCCCGAGATGAACTTCAAGGG GCGTGACAGGAAACG	898	55	40
HAP6 (BAJ85530)	GGATCCCGTCTATGATAGGAGTCG TCCTTCGCATCTTCAC	1,477	55	40

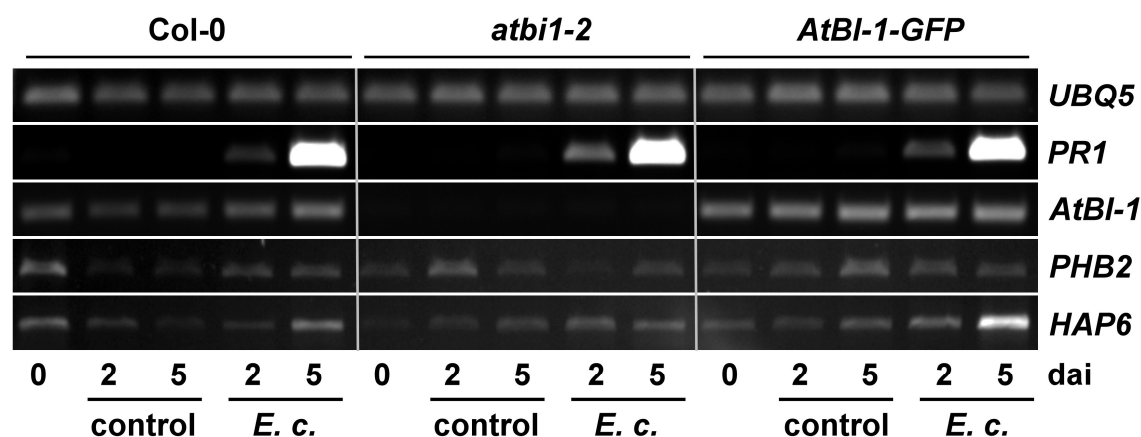$_a$ TIGR plant transcript assembly TA49291_4513.
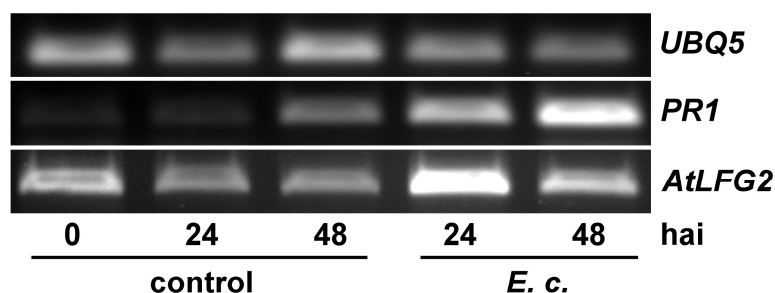
Supplementary figure 11: Gene expression of *AtLFG2* in the interaction of *Arabidopsis* with *E. cruciferarum*. Total RNA was isolated from *E. cruciferarum* (*E. c.*) - or non-inoculated *Arabidopsis* wild type Col-0 leaves that were harvested at 0, 24, and 48 hai. Gel photographs after ethidium bromide staining of semi-quantitative RT-PCR products are shown. Amplification of *UBIQUITIN 5* (*UBQ5)* and *PATHOGENESIS-RELATED GENE 1* (*PR1*) served as control for constitutive gene expression and pathogen-induced gene expression, respectively. Primers and PCR conditions are listed in supplementary table 5. Similar expression pattern were observed in an independent experiment.

Supplementary table 5: Primers and PCR conditions for gene expression analyses displayed in supplementary figure 11.

| identity (AGI code)	5′ and 3′ primer sequences	product size (bp)	annealing temp. (℃)	cycle number
UBQ5 (At3g62250)	CCAAGCCGAAGAAGATCAAG ACTCCTTCCTCAAACGCTGA	105	55	25
PR1 (At2g14610)	CTTCCCTCGAAAGCTCAAGA CGCTAGCCCAGGCTAAGTTT	199	60	30
AtLFG2 (At3g63310)	GGATCCCACCGGCGTTGACAAA TGGCACAGTCTTAAGAGCAA	800	55	30
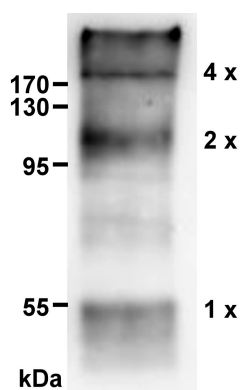
Supplementary figure 12: Oligomerization of AtBI-1-GFP. Microsomes were extracted from *AtBI-1-GFP*-expressing mutants following a protocol described by SANTONI (SANTONI, V. (2007) Plant plasma membrane protein extraction and solubilization for proteomic analysis. Methods Mol Biol. 355: 93-109). A 10% SDS gel was loaded with 5 µg microsomes and blotted on a nitrocellulose membrane. Immunoblotting was performed using anti-GFP.

Supplementary figure 13: Genotype-dependent gene expression of *PHB2* and *HAP6* in the interaction of *Arabidopsis* with *E. cruciferarum*. Total RNA was isolated from *E. cruciferarum* (*E. c.*) - or non-inoculated *Arabidopsis* wild type Col-0, *atbi1-2*, and constitutively *AtBI-1-GFP* expressing plants that were harvested at 0, 2, and 5 dai. Gel photographs after ethidium bromide staining of semi-quantitative RT-PCR products are shown. Amplification of *UBIQUITIN 5* (*UBQ5)* served as control for constitutive gene expression, and *AtBI-1* and *PATHOGENESIS-RELATED GENE 1* (*PR1*) as control for genotype- and pathogen-dependent gene expression. Primers and PCR conditions are listed in supplementary table 5. The experiment was repeated with similar results.

Supplementary table 5: Primers and PCR conditions for gene expression analyses by semi-quantitative RT-PCR displayed in supplementary figure 13.

identity (AGI code)	5′ and 3′ primer sequences	product size (bp)	annealing temp. (℃)	cycle number
UBQ5 (At3g62250)	CCAAGCCGAAGAAGATCAAG ACTCCTTCCTCAAACGCTGA	105	55	22
PR1 (At2g14610)	CTTCCCTCGAAAGCTCAAGA CGCTAGCCCAGGCTAAGTTT	199	60	25
AtBI-1 (At5g47120)	CAGAAGCTGGAGCTATGATTC GATAAGGATGCTTGGGT	366	52	30
PHB2 (At1g03860)	GGATCCAAATCCTACCATCGCC GTTGCTTCTTAGGCTCCA	909	52	26
HAP6 (At4g21150)	GGGATCCTCTTCGACTATACGGA GATTCAACGCTTCCAATG	1,364	51	33
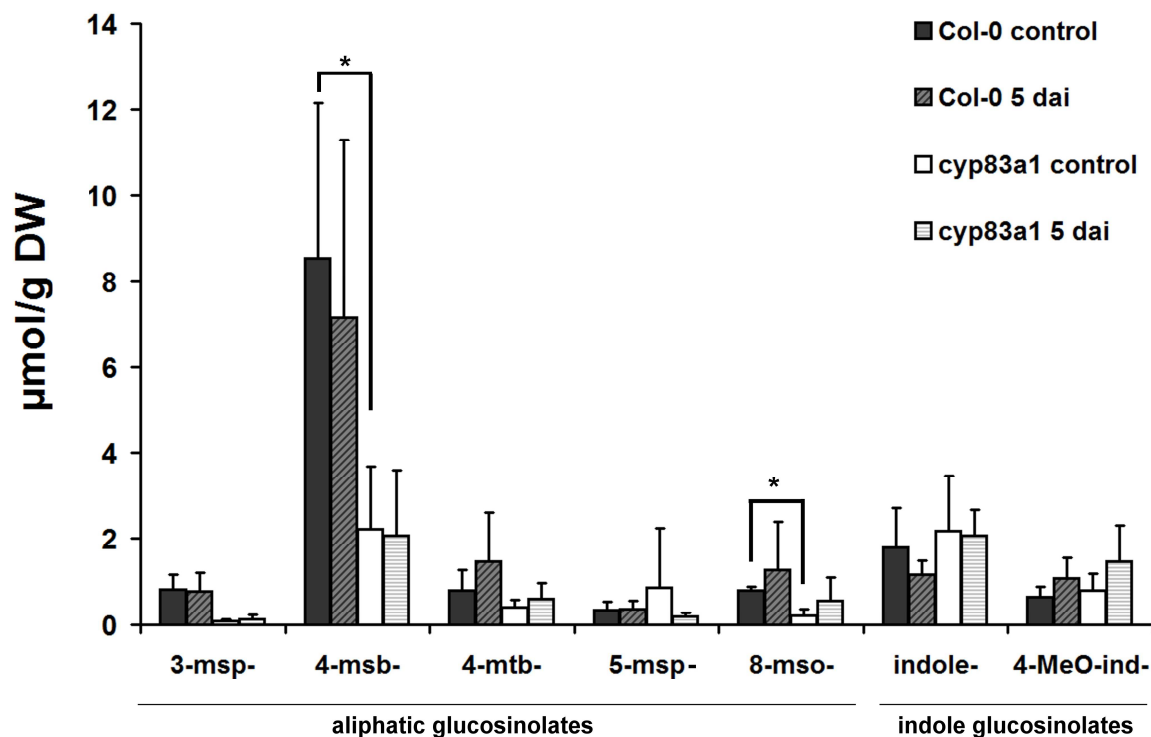
Supplementary figure 14: Glucosinolate content of wild type Col-0 and *cyp83a1*. 5-weeks-old *Arabidopsis* Col-0 and *cyp83a1* plants were inoculated with *E. cruciferarum* and harvested 5 dai, together with non-inoculated control plants. Measurement of 3-methylsulphinylpropyl (3-MSP)-, 4-methylsulphinylbutyl (4-MSB)-, 4-Methylthiobutyl (4-MTB)-, 5-methylsulphinylpentyl (5-MSP)-, 8-methylsulphinyloctyl (8-MSO)-, Indol-3-ylmethyl (indole)-, and 4-methoxy-indol-3-ylmethyl (4-MeO-ind)-glucosinolates was performed via HPLC (High-performance liquid chromatography, E. Glawischnig, TUM, Freising). Columns represent means of three independent experiments, bars represent standard errors, and * indicates significance at *P* < 0.05 according to Student's *t* test.

Danksagung

An dieser Stelle möchte ich mich bei all denen herzlich bedanken, mit deren Hilfe diese Arbeit erst ermöglicht wurde, und die mich die Zeit der Dissertation in schöner Erinnerung behalten lassen:

Zunächst gilt mein Dank Prof. Dr. R. Hückelhoven: Danke für die freundliche Aufnahme am Lehrstuhl, das in meine wissenschaftliche Arbeit gesetzte Vertrauen und die Überlassung des interessanten Themas.

Bei Prof. Dr. J. Durner bedanke ich mir für die Übernahme des Koreferats, und bei Prof. Dr. B. Küster für die Übernahme des Vorsitzes, sowie für die gute Zusammenarbeit mit seinem Lehrstuhl. In diesem Zusammenhang danke ich Hannes Hahne und Fiona Pachl für die LC-MS/MS-Analyse.

Ein riesiges Dankeschön geht an die wohl beste Betreuerin, die man sich wünschen kann. An Ruth Eichmann: Danke für einfach alles! Für die erstklassige fachliche Betreuung in jeglicher Hinsicht, für Deine stete Unterstützung, für die Zeit beim Kaffee und Spritz trinken, auf dem Sofa, beim Joggen, auf Konzerten, ….

Auch möchte ich meiner 2. (unfreiwilligen) Betreuerin, Erika Isono, vom Nachbarlehrstuhl danken: Danke für Deine kompetente Beratung und deine wertvollen Tipps zum Thema Proteinbiochemie.

Bei Erich Glawischnig bedanke ich mich für die Durchführung der HPLC Messungen.

Ein großes Dankeschön geht auch an die Studenten, die an diesem Projekt mitgewirkt haben: Danke Sebastian Pfeilmeier (Masterarbeit), Katharina Beckenbauer (Forschungspraktikum) und Anna Livić (Bacherlor Arbeit) für die gute Zusammenarbeit. Außerdem danke ich natürlich Angela Alkofer, Simon Selleneit und Franziska Kratzl für ihre tatkräftige Unterstützung.

Tina, Christina, Maya, Mathias, Melanie, Manti, Caro, Reinhard, Harry und allen anderen Kollegen danke ich für die gute Zusammenarbeit, Hilfsbereitschaft und freundliche Unterstützung im Laboralltag und darüber hinaus.

Ein ganz herzliches Dankeschön geht auch an meine Eltern, Brüder und den Paul, für die jahrelange Unterstützung während des Studiums und der Promotion.

Curriculum vitae

Persönliche Angaben

Name: Corina Weis

Geburtsdatum: 14. Mai 1982

Geburtsort: München

Familienstand: ledig

Schulausbildung

1988 - 1992   Besuch der Grundschule (Gotzmannschule) in München-Aubing

1992 - 1996   Besuch des Bertolt-Brecht Gymnasiums in München-Pasing

1996 - 2001   Besuch des Max-Planck Gymnasiums in München-Pasing

Studium und Beruf

10/2002   Beginn des Studiums der Gartenbauwissenschaften an der Technischen Universität München - Weihenstephan

04/2007 - 01/2008 Diplomarbeit bei Prof. Dr. R. Hückelhoven am Lehrstuhl für Phytopathologie der Technischen Universität München - Weihenstephan

01/2008   Erhalt des akademischen Grades einer Diplom-Agraringenieurin Univ.

seit 02/2008   Wissenschaftliche Mitarbeiterin am Lehrstuhl für Phytopathologie der Technischen Universität München - Weihenstephan